

UNIVERSITY OF NAPLES “FEDERICO II”

PhD Program

Molecular Pathology and Physiopathology



School of Molecular Medicine

XXVIII cycle

**Innovative therapeutic tools to prevent
BM-MSC recruitment and activity
into tumor microenvironment**

Candidate:

Dr. Raffaella Fontanella

Supervisor:

Dr. Antonella Zannetti, PhD

PhD Coordinator:

Prof. Vittorio Enrico Avvedimento

Naples 2016

**“Innovative
therapeutic tools to
prevent BM-MSK
recruitment and
activity into tumor
microenvironment”**

TABLE OF CONTENTS

LIST OF PUBLICATIONS	4
ABBREVIATIONS	5
ABSTRACT	7
1. BACKGROUND	8
1.1 Cancer	8
1.2 Tumor microenvironment	9
1.2.1 TME: Immune-mediated dormancy	10
1.2.2 TME: Cancer Associated Fibroblasts (CAFs)	11
1.2.3 TME: Hypoxia and angiogenesis	12
1.2.4 TME: EMT and metastasis development	13
1.2.5 TME: Cancer stem cells (CSCs)	14
1.2.6 TME: Mesenchymal stem cells (MSCs)	15
1.3 Targeting tumor microenvironment for therapy	17
1.4 CXCR4 and cancer	19
1.4.1 Development of a novel CXCR4 antagonist	21
1.4.2 CXCR4 as therapeutic target for osteosarcoma and hepatocellular carcinoma microenvironment	22
1.5 PDGFR β and cancer	24
1.5.1 Targeting PDGFR β : Gint4.T aptamer	26
1.5.2 Targeting Triple-Negative Breast Cancer microenvironment	29
2. AIM OF THE STUDY	31
3. MATERIALS AND METHODS	32
3.1 Cell lines and culture conditions	32
3.2 Isolation, culture and immunophenotypic characterization of human bone-marrow mesenchymal stem cells (BM-MSCs)	32
3.3 Aptamers and treatments	33
3.4 Cell viability assay	33
3.5 Cell lysate preparation and western blot analysis	34
3.6 RNA isolation and realtime-polymerase chain reaction (Real time-PCR)	35
3.7 RNA interference	35
3.8 Analysis of OS and HCC cell migration by wound healing assay	36
3.9 Analysis of BM-MSC migration using Boyden chamber	36
3.10 Tumor cell invasion assay	37

3.11 NIR fluorescent BM-MSC-labeling	37
3.12 <i>In vivo</i> BM-MSC tracking by Fluorescence Molecular Tomography	37
3.13 Statistical analysis	38
4. RESULTS	39
4.1 BM-MSCs promote tumor cell growth and increase p-AKT and p-ERK levels in human osteosarcoma (OS) and human hepatocellular carcinoma (HCC) cell lines	39
4.2 BM-MSCs increase CXCR4 mRNA and protein expression in OS and HCC cell lines	40
4.3 A novel CXCR4 antagonist, Peptide R, prevents BM-MSC-dependent wound healing in OS and HCC cells	41
4.4 A novel CXCR4 antagonist, Peptide R, prevents BM-MSC-dependent U2OS and SNU-398 cell invasion	45
4.5 Peptide R prevents BM-MSC-dependent ERK and AKT activation and Epithelial-Mesenchymal Transition in OS and HCC cell lines	49
4.6 BM-MSCs show high levels of PDGFR β mRNA and protein	51
4.7 Gint4.T aptamer inhibits PDGFR β -mediated signaling pathway in BM-MSCs	52
4.8 Gint4.T aptamer inhibits BM-MSC proliferation and migration	53
4.9 Gint4.T aptamer prevents BM-MSC migration towards triple negative breast cancer (TNBC) cells	54
4.10 <i>In vivo</i> tracking of BM-MSC recruitment into TNBC xenograft by Fluorescence Molecular Tomography	55
5. DISCUSSION	58
6. CONCLUSIONS	62
ACKNOWLEDGEMENTS	63
REFERENCES	65

LIST OF PUBLICATIONS

This dissertation is based upon the following publications:

1) **Fontanella R**, Pelagalli A, Nardelli A, D'Alterio C, Ieranò C, Cerchia L, Lucarelli E, Scala S, Zannetti A. A novel antagonist of CXCR4 prevents bone marrow-derived mesenchymal stem cell-mediated osteosarcoma and hepatocellular carcinoma cell migration and invasion. *Cancer Lett.* 2016; 370(1):100-7.

2) Iaboni M, Russo V, **Fontanella R**, Roscigno G, Fiore D, Donnarumma E, Esposito CL, Quintavalle C, Giangrande PH, de Franciscis V, Condorelli G. Aptamer-miRNA-212 conjugate sensitizes NSCLC cells to TRAIL. *Mol Ther Nucleic Acids* (2016) 5, e289; doi:10.1038/mtna.2016.5.

Abbreviations

BM-MSC, Bone marrow–derived mesenchymal stem cell

BM-MSC-CM, Bone marrow-derived mesenchymal stem cell conditioned medium

CAF, Cancer associated fibroblast

CXCL12, C-X-C motif chemokine 12

CXCR4, CXC receptor 4

DMEM, Dulbecco's modified Eagle's medium

EMT, Epithelial Mesenchymal Transition

ERK1/2, Extracellular signal-regulated kinase 1/2

FBS, Fetal bovine serum

FMT, Fluorescence Molecular Tomography

GBM, Glioblastoma multiforme

HCC, Hepatocellular carcinoma

HIF-1, Hypoxia-inducible factor-1

MSC, Mesenchymal stem cell

MTS, 3-(4,5-dimethylthiazol-2-yl)-5-(3-carboxymethoxy-phenyl)-2-(4-sulfophenyl)-2H tetrazolium

OS, Osteosarcoma

PCR, Polymerase chain reaction

PDGF, Platelet-derived growth factor

PDGFR β , PDGF receptor β

PI3K, Phosphatidylinositol-3-kinases

SELEX, Systematic Evolution of Ligands by Exponential enrichment

siRNA, Small interfering RNA

TAM, Tumor associated macrophage

TGF- β , Tumor growth factor β

TNBC, Triple negative breast cancer

TKI, Tyrosine kinase inhibitor

TME, Tumor microenvironment

VEGF, Vascular endothelial growth factor

ABSTRACT

Tumor progression is a multistep process in which cancer cells perform an intricate cross-talk with their surrounding stromal environment, generating a bidirectional communication that affects tumor survival, proliferation and aggressiveness. Among several cell types that constitute the tumor stroma, mesenchymal stem cells (MSCs) selectively migrate toward tumor microenvironment and contribute to the active formation of tumor-associated stroma, thus promoting cell survival, angiogenesis, invasion, evasion of immune system and metastasis.

In this thesis, I investigated the role of bone marrow-derived MSCs (BM-MSCs) in tumor processes, deepening the involvement of specific signaling pathways underlying their recruitment and activity into tumor microenvironment. In particular, innovative therapeutic tools have been tested to: 1) inhibit BM-MSC-mediated growth and aggressiveness of osteosarcoma (OS) and hepatocellular carcinoma (HCC) cell lines by targeting CXCR4; 2) interfere with BM-MSC recruitment by triple negative breast cancer (TNBC) cells through modulation of PDGFR β signaling.

For the first purpose, I tested a new CXCR4 inhibitor, Peptide R, which was recently developed as an anticancer agent to overcome the toxicity of the well-known CXCR4 antagonist AMD3100. I observed a reduction in BM-MSC-mediated OS and HCC migration and invasion and a parallel decrease in BM-MSC-dependent phosphorylation of ERK and AKT. Furthermore, Peptide R, targeting and inhibiting CXCR4, prevented Epithelial Mesenchymal Transition (EMT) of OS and HCC cells promoted by BM-MSCs.

For the second purpose, I used a novel aptamer-based PDGFR β inhibitor, named Gint4.T. Aptamers, thanks to their unique characteristics (low size, good target affinity, no immunogenicity, high stability), represent a new class of molecules with a great potential to rival monoclonal antibodies in both therapy and diagnosis. I observed that Gint4.T, binding PDGFR β , inhibited the phosphorylation of the receptor and its downstream signaling significantly preventing *in vitro* BM-MSC cell migration and blocking cell proliferation. Finally, I found that Gint4.T strongly reduced *in vitro* BM-MSC migration stimulated by two different Triple Negative Breast Cancer (TNBC) cell lines, suggesting that it could interfere with BM-MSC recruitment and their pro-tumorigenic activity within breast cancer microenvironment.

Therefore, this study represents an initial development of novel tumor microenvironment-targeting therapies that, in combination with conventional approaches-oriented to tumor cells, may offer more effective alternative to treat cancer patients by targeting BM-MSCs.

1. BACKGROUND

1.1 Cancer

Cancer is an intricate multistep process involving genetic and epigenetic alterations that result in the activation of oncogenic signals and/or inactivation of tumor suppressor pathways.

During cancer progression, cancer cells acquire a number of hallmarks that ensure their survival and proliferation and, therefore, tumor growth.

The ability of a cancer cell to undergo migration and invasion allow it to invade the surrounding stroma, enter the circulation and eventually metastasize to distant organs.

However, tumor growth involves tumor cells themselves, but also other cells, tissues, and molecules in the environment surrounding the tumor, the tumor microenvironment (TME). A tumor can influence its microenvironment by releasing extracellular signals, by promoting tumor angiogenesis and inducing the inflammatory response, whereas the stroma cells in the microenvironment can sustain tumor growth and promote metastasis development (Quail and Joyce 2013).

For this purpose, multi-targeted approaches, for both tumor cells and tumor microenvironment and/or the signaling pathways involved in their communication, may offer a more efficient way to treat cancer.

1.2 Tumor microenvironment

Cancer is not merely a mass of malignant cells, but a complex system to which many other cells are recruited and can be corrupted by the transformed cells. Interactions between malignant and non-transformed cells create the tumor microenvironment. In particular, interactions between tumor cells and the associated stroma generate a bidirectional communication that affects disease, beginning and progression, and patient prognosis (Hanahan and Coussens 2012).

The stroma consist of a class of cells, including fibroblasts/myofibroblasts, glial, epithelial, fat, immune, vascular, smooth muscle, and immune cells along with the extracellular matrix (ECM) and extracellular molecules. Though none of these cells is naturally malignant, they acquire an abnormal phenotype and altered functions due to the environment, interactions with each other, and directly or indirectly cross-talk with cancer cells.

The concomitant participation of various stromal components, including immune/inflammatory cells, carcinoma associated fibroblasts (CAFs), cancer stem cells (CSCs), as well as the activation of processes in which these factors are strongly involved (hypoxia, angiogenesis, epithelial-mesenchymal transition and metastasis), results in tumor microenvironment formation and progression (Hanahan and Coussens 2012) (Figure 1).

In particular, among several cell types, that constitute the tumor stroma, mesenchymal stem cells (MSCs) have been shown to selectively migrate toward tumor microenvironment and promote cancer progression and metastasis by supporting tumor stroma activity (Barcellos-de-Souza et al. 2013).

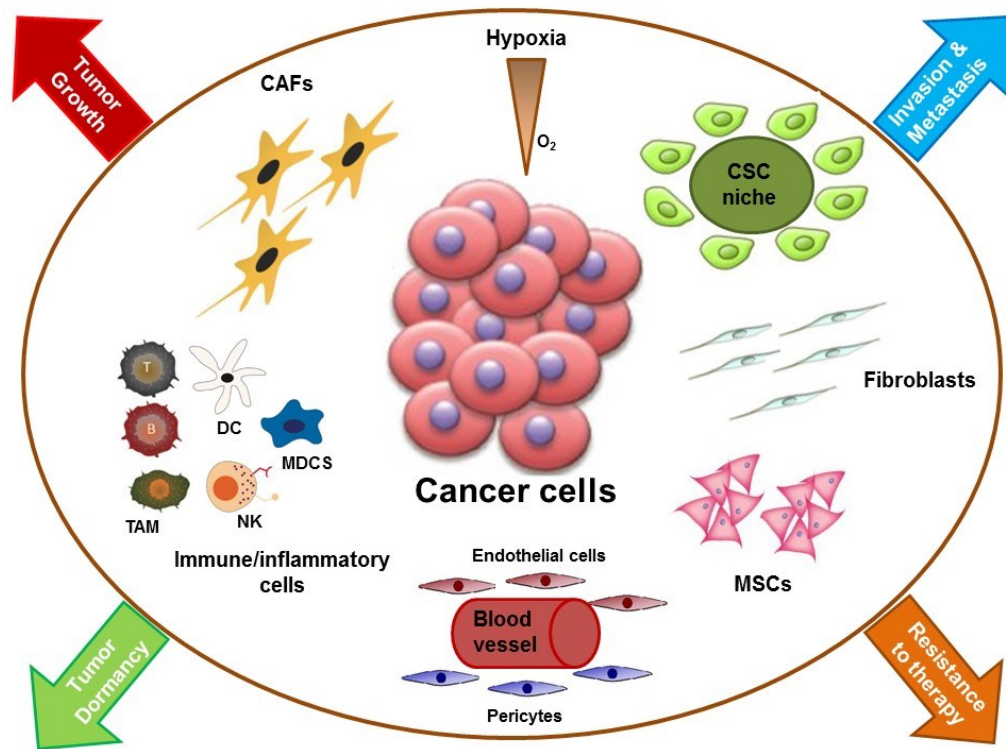


Figure 1. The primary tumor microenvironment. Cancer cells in primary tumor are surrounded by a complex microenvironment including multiple stromal cell types that converge to promote tumor growth and dormancy, invasion and metastasis development and resistance to therapy.

1.2.1 TME: Immune-mediated dormancy

The role played by the immune system in regulating tumor growth and propagation is crucial. Most of the immune cell populations in the tumor microenvironment interplay to prevent (or promote) the local growth of tumors and their spread:

- in the immune-suppressive microenvironment context, natural killer (NK) cells represent key cytotoxic tumoricidal lymphocytes, but also regulatory cells engaged in reciprocal interactions with dendritic cells, macrophages, T cells and endothelial cells (Vivier et al. 2008);
- dendritic cells (DCs) are the major antigen processing and presenting cells in the tumor milieu and usually act as the link between the innate and the adaptive immune systems (Banchereau and Steinman 1998);
- macrophages, often referred to as tumor associated macrophages (TAMs), interact with a wide range of growth factors, cytokines and

chemokines, which are thought to determine TAM functional role as tumoricidal/static (M1 polarization) or tumor promoters (M2 polarization) (Biswas and Mantovani 2010);

- myeloid-derived-suppressor cells (MDSCs) are a heterogeneous population of immune cells from the myeloid lineage that infiltrate the growing tumor and perform strong immunosuppressive activities (Talmadge and Gabrilovich 2013);
- the TH (T Helper) population, bearing CD3+ and CD4+ markers, performs a dual function, based on the subsets and the ratio of their populations. TH1 cells mediate a tumor suppressor inflammatory reaction, whereas TH2 can mediate a tumor promoter reaction (Coussens et al. 2013);
- B-lymphocytes mediating humoral immunity can promote cancer progression by altering the TH1/TH2 ratio to favor tumorigenesis (de Visser et al. 2005);
- cytotoxic T lymphocytes, bearing the CD8+ marker, can identify and destroy cancer cells through their major histocompatibility complex (MHC) recognition when recruited to the tumor milieu (Fridman et al. 2012);
- regulatory T cells (T regs) are crucial for peripheral tolerance as they maintain the homeostasis of innate cytotoxic lymphocytes, regulating the expansion and activation of T and B cells. They are intimately involved in immunological diseases and cancer (Zeng and Chi 2013).

The various components of the immune system seem to interplay with the stromal factors, regulating tumor growth and dissemination. It seems evident, therefore, that immune modulation should be a crucial component in the fight against cancer. The presence of suppressive factors in the tumor microenvironment, however, may explain the limited activity observed with previous immune-based anti-cancer therapies and why these therapies may be more effective in combination with agents that target immune modulators of the tumor microenvironment. Emerging clinical data suggest that cancer immunotherapy is likely to become a key part of the clinical management of cancer.

1.2.2 TME: Cancer Associated Fibroblasts (CAFs)

A specialized group of fibroblasts, named cancer associated fibroblasts (CAFs), is one of the most crucial components of the tumor microenvironment, which promotes the growth and invasion of cancer cells.

Compared to normal fibroblasts, CAFs are constantly activated, neither reverting back to a normal phenotype nor undergoing apoptosis. CAFs found in different cancers are highly heterogeneous, and they are potentially derived

from resident fibroblasts through genetic alterations, but also from epithelia, endothelia or mesenchymal cells (Xing et al. 2010).

In particular, recent evidence has suggested that MSCs selectively proliferate in tumor microenvironment and contribute to CAF formation (Mishra et al. 2008).

Several CAFs markers were identified including alpha-smooth muscle actin (alpha-SMA), fibroblast activation protein (FAP), desmin, and vimentin. Alpha-SMA has been known to play an essential role in the embryonic stem cell-derived cardiomyocyte differentiation. However, the expression of alpha-SMA in the tumor stroma increases fibroblast contractile ability and contributes to alterations in cytoskeletal organization (Rønnov-Jessen and Petersen 1996). Conversely, fibroblast activation protein (FAP) expression is not detected in normal fibroblasts, but its expression has been associated with an overall poorer prognosis in several cancer types, including colon, ovarian, pancreatic, and hepatocellular carcinoma (Brennen et al. 2012).

For this reason, it is becoming clear that the crosstalk between tumor stromal cells and CAFs plays a key role in the progression of cancer, and understanding this mutual relationship would eventually offer a novel way to treat cancer patients by targeting CAFs.

1.2.3 TME: Hypoxia and angiogenesis

Hypoxia is a concomitant microenvironmental factor, considered as a negative prognostic indicator associated with a significantly increased risk of metastasis and mortality in many human cancers (Kim et al. 2009).

Intratumoral hypoxia contributes to cancer progression affecting the behavior of both cancer and stromal cells. The effects of hypoxia on cancer cells can be essentially classified in: (1) shift to a glycolytic metabolism to circumvent lack of oxygen, (2) activation of pathways for survival to stressful conditions, (3) stimulation of *de novo* angiogenesis allowing nutrient/oxygen supply, (4) activation of Epithelial Mesenchymal Transition (EMT) program to escape from the hostile environment (Wilson and Hay 2011).

In addition, hypoxia strongly influences also stromal cells, essentially affecting the profibrogenic/proangiogenic behavior of CAFs (Giaccia and Schipani 2010).

Hypoxia-induced signaling is primarily mediated by the ubiquitous hypoxia-inducible factor-1 (HIF-1), a master regulator of O₂ homeostasis that consists of two subunits, HIF-1 α and HIF-1 β , sensitive or insensitive to O₂ modification, respectively. HIF-1-induced genes are involved in a wide range of cellular functions such as cell growth, survival, motility, angiogenesis, energy metabolism, and cellular differentiation (Ziello et al. 2007).

Several studies have demonstrated that angiogenesis, which is necessary for tumor progression, is influenced by the tumor microenvironment. Angiogenesis is the physiological process through which new blood vessels form from pre-existing vessels. However, angiogenesis performs a crucial role in development of cancer. To spread, solid tumors need to be supplied by blood vessels that bring oxygen and nutrients and remove metabolic wastes. In fact, oxygen and nutrients have difficulty diffusing to the cells in the center of the tumor, causing a state of cellular hypoxia that marks the onset of tumoral angiogenesis (Nishida et al. 2006). In this scenario, hypoxic tumor microenvironment has emerged as a primary physiological regulator of the angiogenic switch activating the transcription of various factors, including vascular endothelial growth factor (VEGF), angiopoietin 2, and fibroblast growth factor 2 (FGF2) (Semenza 2013). In addition, there is abundant evidence that stromal cells in the TME are instrumental in switching on and sustaining chronic angiogenesis in many tumor types. CAFs, for example, through chemokine secretion, promote angiogenesis by recruiting endothelial progenitor cells (EPCs) into carcinomas (Orimo et al. 2005). Importantly, also MSCs seems to be involved in the formation of new blood vessels. For instance, Suzuki et al. 2011 have demonstrated that combined administration of MSCs and tumor cells promoted tumor growth by enhancing angiogenesis in syngeneic tumor models. This enhanced neovascularization can likely be attributed to direct support of neovascularization by MSCs and to secretion of angiogenic factors, including VEGF and others, by MSCs.

1.2.4 TME: EMT and metastasis development

One of the main features of tumor milieu is the ability to elicit a clear escape adaptive strategy for cancer cells, called epithelial mesenchymal transition. EMT is an epigenetic program in which epithelial cells lose their cell polarity and cell-cell adhesion, undergo cytoskeleton reorganization, and gain morphological and functional characteristics of mesenchymal cells. EMT is essential for numerous developmental processes including mesoderm formation and neural tube formation. However, it has been shown that EMT occurs also in wound healing, in organ fibrosis and in metastasis initiation of cancer progression (Thiery et al. 2009). EMT is a regulated process in which the cell loses its epithelial markers and achieves expression of mesenchymal markers. A property of EMT is the loss of E-cadherin expression, correlated with tumor grade and stage (Giannoni et al. 2012). Cadherins mediate calcium-dependent cell-cell adhesion and play critical roles in normal tissue development. E-cadherin is considered an active suppressor of invasion and growth of many epithelial cancers. Recent studies indicate that

cancer cells have up-regulated N-cadherin in addition to loss of E-cadherin, causing the “cadherin switch” (Aigner et al. 2007).

Vimentin is an intermediate filament of mesenchymal origin and is present at early developmental stages. Vimentin is a clear marker of mesenchymal phenotype and its up-regulation concurs with the loss of E-cadherin expression (Kokkinos et al. 2007).

Others several transcription factors have been implicated in the control of EMT, including Snai1, Slug, Twist, zinc finger E-box binding homeobox-1 and -2 (ZEB1 and ZEB2) (Cannito et al. 2010).

Initiation of metastasis requires invasion, which is supported by EMT. Carcinoma cells in primary tumor lose cell-cell adhesion mediated by E-cadherin repression, break through the basement membrane with increased invasive properties, and enter the bloodstream through intravasation. Later, when these circulating tumor cells exit the bloodstream to form micrometastases, they undergo Mesenchymal Epithelial Transition (MET) for clonal outgrowth at these metastatic sites. Thus, EMT and MET form the initiation and completion of the invasion-metastasis cascade (Yao et al. 2011).

1.2.5 TME: Cancer stem cells (CSCs)

Stem cells, as classically defined, are cells with the ability to perform asymmetric cell divisions. Each cell, therefore, can self-renew in one that is identical to it, as well as generate a different one, in that it is more committed towards a certain differentiation pattern. (Cariati and Purushotham 2008).

In contrast to the ‘stochastic’ model of oncogenesis, where transformation results from random mutations and subsequent clonal selection, experimental and clinical data have accumulated to support the hypothesis that cancer may arise from mutations in stem cell populations (Cancer Stem Cell Hypothesis). Indeed, Cancer Stem Cells (CSCs) result involved in the pathologic manifestation of cancer affecting tumor initiation and metastatic progression, and increasing resistance of tumors to conventional cancer therapies (Reya et al. 2001).

Some functional environments, namely ‘cancer stem cell niches’, may support CSCs. CSC niches provide a unique microenvironment where CSCs interact closely with tumor stromal cells. Their maintenance, therefore, is subjected to regulation by microenvironmental signals, including cytokines, vascular effects, and modulation of immune responses. In this context, CSCs niche plays a crucial role in keeping CSCs in a quiescent stage leading them to preferentially survive tumor therapy, and persists long term to ultimately cause delayed cancer recurrence and metastatic progression (Kleffel and Schatton 2013).

1.2.6 TME: Mesenchymal stem cells (MSCs)

Mesenchymal stem cells are non-hematopoietic multipotent stromal cells widely distributed in a variety of adult tissues, including bone marrow, the umbilical cord, Wharton's Jelly, adipose tissue, peripheral blood, placenta and lung (Barcellos-de-Souza et al. 2013).

In such tissues, MSCs are either constantly present or their pool is replenished by the migration of bone marrow-derived MSCs (BM-MSCs) (Bergfeld and DeClerck 2010), thus representing the latter the most intriguing class of MSCs. Normally, MSCs are recruited into sites of injury and inflammation and differentiate into a variety of connective tissue cell types such as bone, cartilage, muscles, tendons and adipose tissue (Dominici et al. 2006).

Once at injury site, it has been widely reported that MSCs possess broad immunoregulatory capabilities by which they are capable to influence both adaptive and innate immune responses. In fact, MSCs can suppress immune responses by producing immunomodulatory molecules including tumor growth factor β (TGF- β) and nitric oxide, as well as, stimulating potent immunosuppressors as CD4⁺ or CD8⁺ regulatory T cells (Burr et al. 2013). Furthermore, MSCs have been showed to suppress the activity of a wide range of immune cells, including natural killer cells, dendritic cells, B cells, neutrophils, monocytes and macrophages (Zhao et al. 2010).

However, several studies have also reported that MSCs are rapidly recruited into tumor microenvironment in response to a variety of endo/paracrine signals that attracts them directly in a receptor-mediated manner (Korkaya et al. 2011). In particular, due to their remarkable ability to home to tumor sites and their immune privileged status, BM-MSCs have been used as carriers for delivering anti-tumor agents to the tumor microenvironment (Barcellos-de-Souza et al. 2012).

Nevertheless, BM-MSCs have a dual function. In fact, they have also been identified as pro-active tumor stroma associated cells that are implicated in promoting cell survival, angiogenesis, invasion, and metastasis, as reported in breast (Chaturvedi et al. 2013), lung (Suzuki et al. 2011), prostate (Jung et al. 2013), and colon (Shinagawa et al. 2010) carcinomas (Figure 2).

Within the tumor microenvironment, tumor-associated BM-MSCs increase the population of cancer stem cells (CSCs) with a high metastaticity, dormancy and chemoresistance (Liu et al. 2011 and Luo et al. 2014).

Importantly, BM-MSCs can differentiate into cancer-associated fibroblasts (CAFs), promoting EMT phenomenon required for establishing distant metastasis (Jung et al. 2013).

To date, the molecular mechanisms underlying these processes have remained elusive.

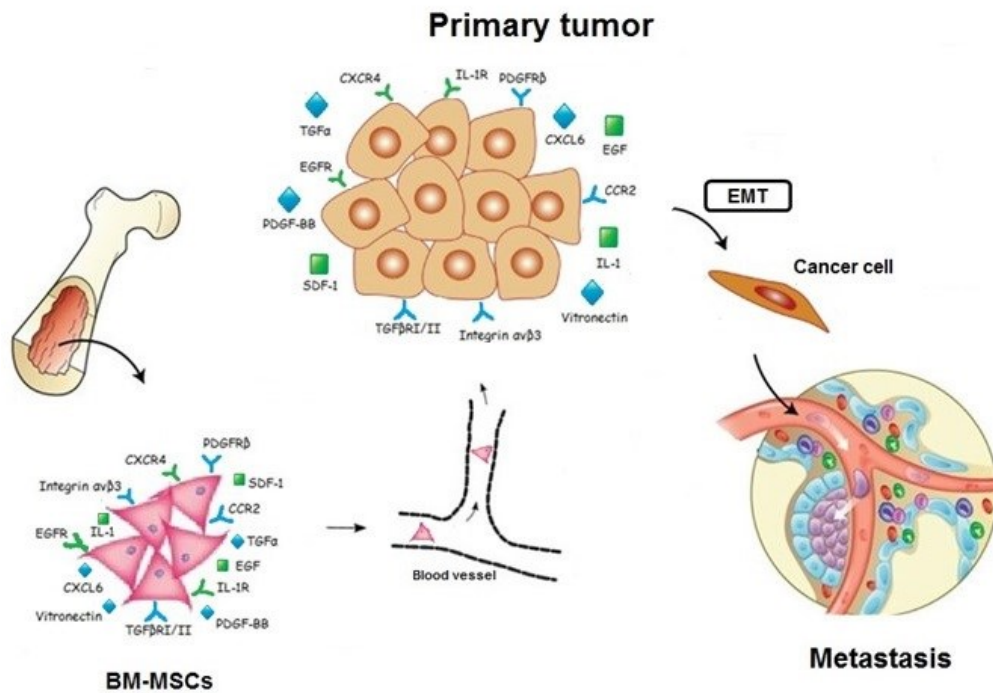


Figure 2. Bone marrow-derived mesenchymal stem cells (BM-MSCs) support tumor progression. The bidirectional signaling between BM-MSCs and cancer cells attracts BM-MSCs in a receptor-mediated manner into tumor sites. BM-MSC infiltration into pathogenic microenvironment promotes the malignant transformation of proliferating cancer cells to an EMT. EMT promotes the invasion-metastasis cascade.

1.3 Targeting tumor microenvironment for therapy

The key role played by stromal cells in determining or enhancing multiple hallmark capabilities in the tumor microenvironment of different types of cancer clearly prompts therapeutic targeting strategies aimed to inhibit their contributions. One benefit of therapies targeting the microenvironment is that these non-tumor cells are more genetically stable than tumor cells and thus are less likely to gain adaptive mutations and acquire drug resistance (Dimou et al. 2012).

However, a limitation of targeting stromal cells in the tumor microenvironment is that a fragile balance exists between their tumor-inhibitory and tumor-promoting functions (Li et al. 2007). As such, it become very important to identify and target key molecular differences between these cells under normal tissue homeostasis versus when they are co-opted or altered by the tumor microenvironment.

Recent studies have suggested various approaches to target different cell types in the tumor microenvironment (Figure 3).

As increasing data underline the important role by TAMs during tumorigenesis and cancer progression, a variety of pre-clinical studies were also performed to test the concept of TAM-based anti-cancer therapy. In 2006, Luo et al. presented a DNA vaccine based on legumain, which is over-expressed on TAM. The administration of the DNA vaccine in mouse induced a robust CD8+ T cell response against TAM. The distribution of TAM in tumor microenvironment was reduced and the production and release of pro-angiogenic factors such as, TGF- β , VEGF and matrix metalloproteinase 9 (MMP-9) from TAM was inhibited. As a sequence, the growth and metastases of a variety of tumors were significantly inhibited.

For their ability to enhance tumorigenicity, angiogenesis, and metastatic dissemination of cancer cells compared with normal fibroblasts, CAFs are considered a very attractive candidate for tumor-targeted therapies. For example, Loeffler et al. (2006) have shown that the use of DNA vaccines directed against fibroblast activation protein (FAP), resulted in the elimination of tumor growth, metastasis and recurrence in mouse tumor models.

Due to their capabilities to home to tumor sites and promote cancer progression, MSCs have become a promising target for attenuating the tumor malignancy in treating patients. In particular, recent studies have reported that the pro-tumorigenic effect of MSCs could be inhibited hampering the cross-talk between MSCs and tumor cells, and interfering with MSC-derived CAF differentiation within tumor microenvironment. Shinagawa et al. (2013), for example, have shown that interfering with platelet-derived growth factor (PDGF) signaling pathway impairs MSC migration and their tumor-promoting effect in an orthotopic colon tumor model. Furthermore, Shangguan et al. (2012) have reported that blocking TGF- β /Smad signaling in human BM-

MSCs prevented their differentiation to CAFs in tumor microenvironments and abolished their protumor effects.

Thus, in this scenario, investigate the involvement of specific signaling pathways underlying BM-MSc recruitment and role in tumor microenvironment, and develop innovative therapeutic tools to target and prevent their activity, may offer a novel way to treat cancer patients by targeting BM-MSCs.

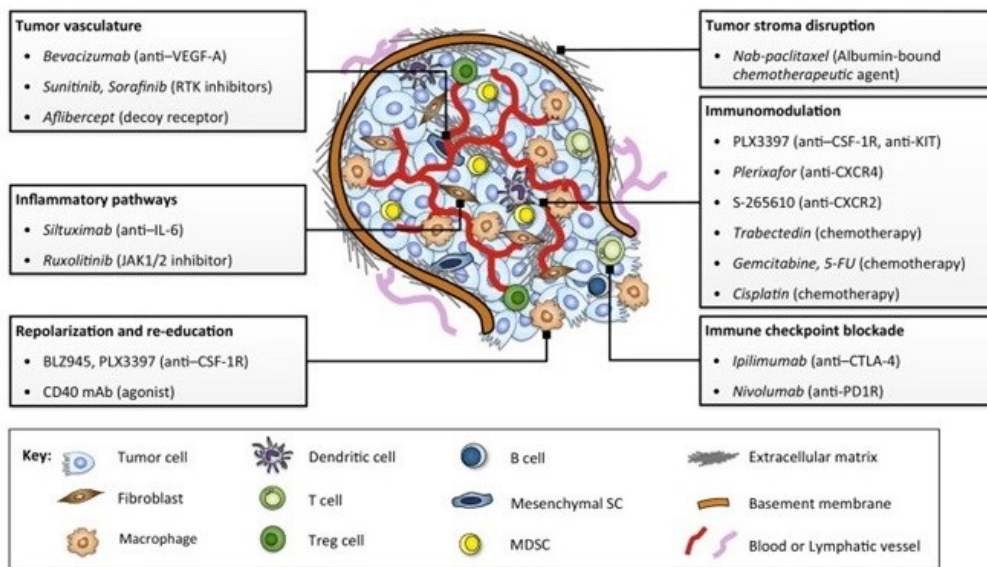


Figure 3. Tumor microenvironment targeted therapies. The tumor microenvironment comprises various cell types that modulate treatment response and are putative candidates for therapeutic intervention. Multiple strategies to target the tumor microenvironment are either currently in clinical use or are at different stages of clinical development.

1.4 CXCR4 and cancer

Chemokines are a family of small peptides that function as chemoattractant cytokines involved in cell activation, differentiation, and trafficking (Balkwill 2004).

Chemokines are expressed in discrete anatomical locations and act on chemokine receptors (CKRs), members of the seven-transmembrane domain G-protein-coupled receptor (GPCR) superfamily (Rajagopal et al. 2010). Most chemokines bind to multiple receptors, and the same receptor may bind to more than one chemokine. The C-X-C motif chemokine 12 (CXCL12), also known as stromal cell-derived factor-1 (SDF-1), for example, binds to CXC receptor 4 (CXCR4) (Murdoch 2000) and 7 (CXCR7) (Miao et al. 2007).

CXCR4 is an evolutionarily highly conserved GPCR expressed on monocytes, B cells, and naïve T cells in the peripheral blood. CXCL12 binding to CXCR4 triggers multiple signal transduction pathways that are able to regulate intracellular calcium flux, chemotaxis, transcription, and cell survival. As a G-protein-coupled receptor, the mechanism of CXCR4 receptor activation is mediated by coupling to an intracellular heterotrimeric G-protein associated with the inner surface of the plasma membrane. The heterotrimer is composed by $G\alpha$, $G\beta$ and $G\gamma$ subunits, and in its basal state binds the guanosine diphosphate (GDP). Upon activation by ligand binding, GDP is released and replaced by guanosine triphosphate (GTP), which leads to subunit dissociation into a $\beta\gamma$ dimer and the α monomer to which the GTP is bound. In turn, different subtypes of the α subunit impart different signals: $G\alpha_i$ subunits inhibit cyclic adenosine 3',5'-monophosphate (cAMP) formation via inhibition of adenylyl cyclase activity, and the $G\alpha_q$ subunits activate phospholipase C (PLC) generating diacylglycerol (DAG) and inositol 1,4,5 trisphosphate (IP3), which controls the release of intracellular Ca^{2+} . While inhibiting adenylyl cyclase, the $G\alpha_i$ subunits activate the nuclear factor kappa-light-chain-enhancer of activated B cells (NF- κ B), janus kinase-signal transducer and activator of transcription (JAK-STAT) and phosphatidylinositol-3-kinases-AKT (PI3K-AKT) pathways as well as, c-Jun N-terminal kinases (JNK)/p38 and mitogen-activated protein kinases (MAPKs) pathways, thus, regulating cell survival, proliferation, and chemotaxis (Teicher and Fricker 2010).

CXCL12 binding to CXCR4 also causes CXCR4 desensitization in which CXCR4 intracellular phosphorylation lead to β -arrestin recruitment and subsequent CXCR4 lysosomal degradation (Marchese 2014) (Figure 4).

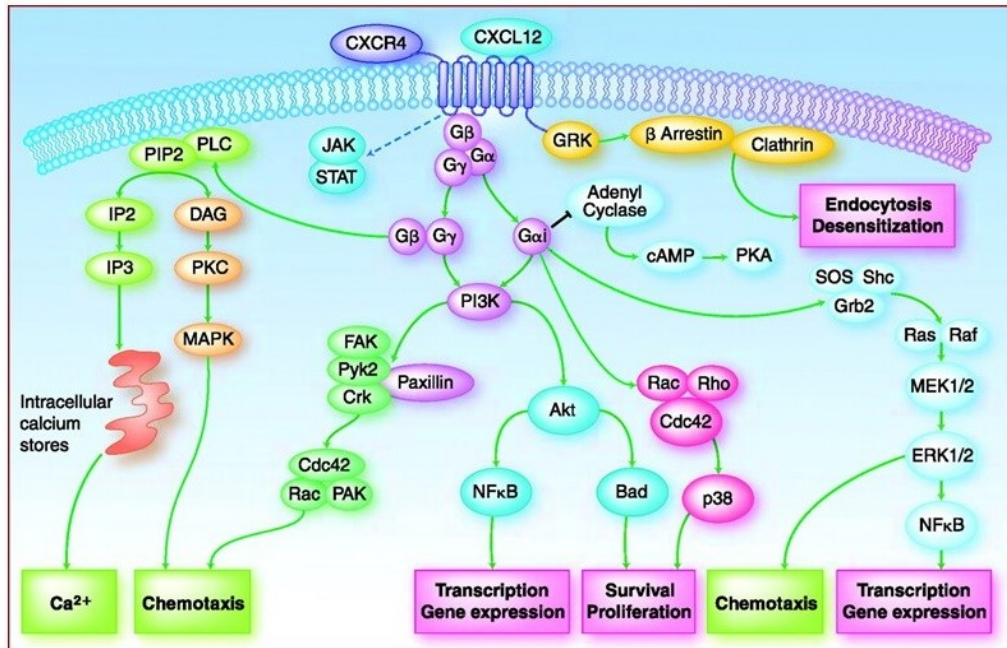


Figure 4. Pathway signaling of CXCL12-CXCR4 axis.

CXCR4 is over-expressed in more than 23 different types of human cancers as reported in kidney, lung, brain, prostate, breast, pancreas, ovarian and melanomas, and is involved in several aspects of tumor progression including angiogenesis, metastasis, and survival (Chatterjee et al. 2014). Several studies have shown that CXCR4 also contribute to the tumor-stromal interaction. In mouse models of human breast (Orimo et al. 2005) and prostate cancer (Olumi et al. 1999), high intratumoral CXCL12 levels attract CXCR4-positive inflammatory, vascular, and stromal cells into the tumors, where they eventually support tumor growth by secreting growth factors, cytokines, chemokines, and proangiogenic factors.

In particular, Orimo et al. (2005) have detected an increased expression of CXCR4 in CAFs, suggesting that the transdifferentiation of normal human mammary fibroblasts to tumor-promoting CAFs could be induced by CXCR4 expression.

Similarly, recent studies have demonstrated that the CXCR4/CXCL12 axis is critical for BM-MSC recruitment to tumor sites. As reported by Yu et al. (2015), for example, BM-MSCs can promote osteosarcoma cell proliferation and invasion *in vitro* involving the CXCR4/CXCL12 axis. In hepatocellular carcinoma, rat BM-MSCs enhance migration in a rat hepatoma cell line (CBRH-7919) by up-regulating CXCR4 (Li et al. 2015). Conversely, Li et al.

2015 (Eur. J. Med. Res.) showed that BM-MSCs promote proliferation of human hepatocellular carcinoma cells, but inhibit their migration.

As a result of its pleiotropic role in tumor development, the CXCL12/CXCR4 axis is considered an important potential target for cancer therapeutics.

Small molecular inhibitors of CXCR4 are being investigated in various disease settings. TG-0054 is an injectable small molecule CXCR4 antagonist that is currently in phase I/II clinical trials for multiple myeloma, non-Hodgkin lymphoma, and Hodgkin disease (Hsu et al. 2015). Another small molecule, AMD070, an orally active CXCR4 antagonist, is under clinical investigation for the prevention of T-tropic HIV infection (Murakami et al. 2009).

However, the bicyclam plerixafor (formerly known as AMD3100) represents the most effective CXCR4 therapeutic targeting. AMD3100 is a small molecule with two cyclam rings connected by a phenylene linker. At physiological pH, two nitrogens on each ring are protonated allowing specific charge-charge interactions with the carboxylate groups on CXCR4, thus inhibiting CXCL12 binding and downstream signaling events (De Clercq 2009). AMD3100 is approved by the Food and Drug Administration as an hematopoietic stem cell mobilizer in patients with non-Hodgkin lymphoma and multiple myeloma refractory to conventional protocols for mobilization (Vose et al. 2009). Nevertheless, Plerixafor has evoked some concerns regarding its cardiotoxicity and other adverse events and it is, therefore, not an ideal anticancer agent (Hendrix et al. 2004).

Thus, there is the urgent need to develop new specific CXCR4-targeting drugs to overcome AMD3100 toxicity, and for long-term use as anticancer agents.

1.4.1 Development of a novel CXCR4 antagonist

Recently, in order to develop new CXCR4 antagonists suitable for anticancer therapy, Portella et al. (2013), employing a ligand-based approach, conceived a new family of peptides to bind CXCR4 and antagonize its activity.

The analysis of short structural motifs in the ligand receptor-binding region (N-terminal region) of CXCL12 identified a three-residue segment R-Ar1-Ar2 (where Ar is an aromatic residue), making this motif a promising candidate scaffold to design short CXCR4-ligand peptides. This segment resulted similar to, but in reverse order (Ar1-Ar2-R), a peculiar inhibitory chemokine secreted by herpes virus 8 known as vMIP-II. Consequently, two motifs were used as templates to design cyclic peptides with the structure C-Ar1-Ar2-R-C and C-R-Ar1-Ar2-C, where the cysteines at each end in a disulfide-bridge are useful to stabilize the structure and provide protection from proteases. In addition, peptides were either elongated at their C-termini or, after sequence-reversal, at their N-termini, so as to mimic another possibly conserved basic residue motif (Italian Patent nu MI2010A000093; International Patent nu WO2011/ 092575

A1) (Amodeo et al. 2010). The *in vitro* evaluation of the CXCR4 inhibitory efficacy resulted in the selection of four peptides, named R, S, T and I, that showed concomitant antagonistic activity in four *in vitro* assays (competition with anti CXCR4 antibody binding, ligand dependent migration, calcium efflux and p-ERK induction). In order to identify the best CXCR4 inhibitor suitable for anticancer therapy, peptides R, I, S and T were selected for *in vivo* evaluation. Solubility limitations prevented the evaluation of peptide T *in vivo*, but peptides, R, I and S reduced lung metastases in mice injected with B16-CXCR4 mouse melanoma cells and K7M2 mouse osteosarcoma cells. In addition, peptides R, I and S inhibited primary tumor growth in a xenograft model of human renal cancer cells, SN12C. Peptide R especially revealed the best efficacy both in *in vitro* and *in vivo* analysis and its evaluation for a first in human Phase I trial is planned in patients with advanced tumors (Figure 5).

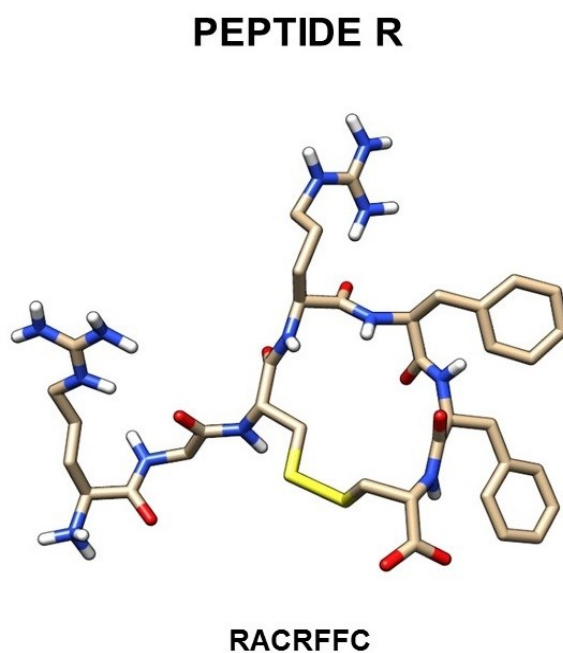


Figure 5. Representative structure of Peptide R.

1.4.2 CXCR4 as therapeutic target for osteosarcoma and hepatocellular carcinoma microenvironment

Osteosarcoma (OS) is the primary malignant bone tumor that most commonly affects children, adolescents and young adults. Specifically, it is an

aggressive malignant carcinoma that originates from primitive transformed cells of mesenchymal origin (and thus a sarcoma) and that shows osteoblastic differentiation and results in malignant osteoid. These tumors are typically locally aggressive and favor the development of early systemic metastases. More than 85% of metastatic disease occurs in the lung, whereas bone is the second most common site of distant disease. The current primary strategy for newly diagnosed osteosarcoma consists of neoadjuvant chemotherapy followed by surgical removal of the primary tumor as well as all clinically evident metastatic disease, plus the addition of adjuvant chemotherapy after surgery. As a result, the long-term cure rate for non-metastatic osteosarcoma following surgery has risen from 25 to 60%. However, despite these progresses, the survival rate for patients with osteosarcoma remains low, with novel effective therapeutic strategies required to target this disease (Luetke et al. 2014).

To date, molecular therapy for osteosarcoma patients has not been developed yet. Over past years, several studies have shown the involvement of the CXCR4/CXCL12 axis in the occurrence and metastatic potential of OS, suggesting that CXCR4 could be promising therapeutic target for the treatment of osteosarcoma patients (Lu et al. 2015; Perissinotto et al. 2005).

Importantly, recent evidence has demonstrated the involvement of tumor stroma cells in promoting osteosarcoma aggressiveness through the CXCR4/CXCL12 axis (Yu et al. 2015), indicating the possibility to target CXCR4 in order to interfere with the cross-talk between osteosarcoma microenvironment and tumor cells.

Hepatocellular carcinoma (HCC) is the fifth most common form of cancer worldwide and the third most common cause of cancer-related deaths. HCC is often secondary to either a viral hepatitis infection (hepatitis B or C) or cirrhosis. Surgical resection is currently considered the most curative strategy, but in the last decade highly satisfactory outcomes have been achieved with systemic targeted therapies focus on the critical steps of the carcinogenic pathways. To date, for patients with advanced HCC, sorafenib is the only approved therapy, but novel targeted agents and their combinations are developing (Raza and Sood 2014).

Recent evidence has shown that the role of the microenvironment in tumor initiation and progression in HCC is critical. The interaction between stromal and tumor cells is dynamic and dramatically modifies the behavior and aggressiveness of HCC. Recent studies, for example, have underlined the role of inflammatory pathways in the development of HCC in cirrhotic patients, suggesting the possibility to reprogram the immune microenvironment in tumors to improve the efficacy of standard anticancer treatments (Hernandez-Gea et al. 2013).

Importantly, in 2015 Li et al. have demonstrated that conditioned medium from rat BM-MSCs enhance migration of a rat hepatoma cell line (CBRH-7919) by up-regulating CXCR4. This evidence suggests the importance of investigating the role of BM-MSCs in HCC microenvironment, and how their interactions with cancer cells could be modulate targeting critical tumorigenic pathways.

1.5 PDGFR β and cancer

PDGFs are a family of potent mitogens for most mesenchyme-derived cells. The PDGF family consists of four polypeptides, A-D, forming five disulfide-linked dimeric proteins: PDGF-AA, -BB, -AB, -CC, and -DD, that signal through two structurally similar receptor tyrosine kinases (RTKs), PDGF receptors α and β (PDGFR α and PDGFR β) (Fredriksson et al. 2004). Ligands and receptors can form homodimers or heterodimers depending on cell type, receptor expression, and ligand availability. PDGF-BB and PDGF-DD are the primary activators of $\beta\beta$ homodimeric receptors. PDGF-AA activates only $\alpha\alpha$ receptor dimers, whereas PDGF-AB, PDGF-BB, and PDGF-CC activate $\alpha\alpha$ and $\alpha\beta$ receptor dimers (Yarden et al. 1986). The dimeric ligand molecules bind to two receptor proteins simultaneously and stimulate receptor dimerization, autophosphorylation of specific residues within the receptor's cytoplasmic domain, and intracellular signaling (Figure 6). PDGFR β signaling pathway activation induces several cellular processes, including cell proliferation, migration and angiogenesis (Cao et al. 2004; Ostman 2004).

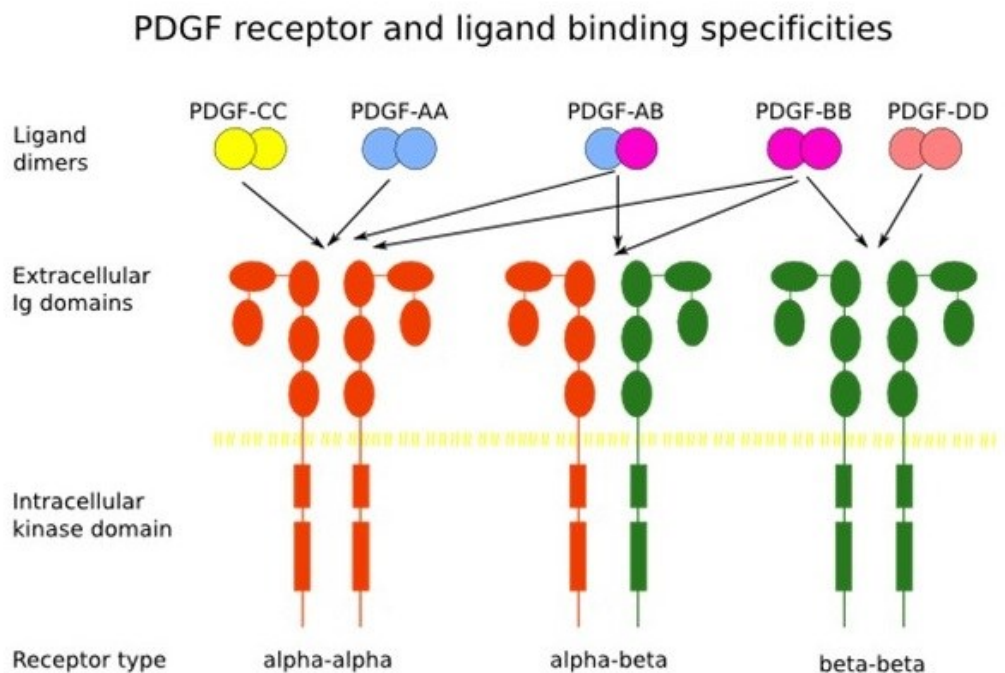


Figure 6. PDGF receptor family and their ligands.

Pathogenic roles of altered PDGFR β signaling have been determined for a number of human diseases including cancer. Preclinical studies have shown an important role for the overexpression, point mutations, deletions, and translocations of PDGFR β in tumorigenesis and maintenance of the malignant phenotype (Gilbertson and Clifford 2003), but have also proven that the targeted inhibition of PDGFR β signaling pathway has significant anticancer effects (Kilic et al. 2000).

Recently, MSCs have been reported to express abundant PDGFR β that plays a crucial role in specifying MSC commitment to mesenchymal lineages (Ng et al. 2008). Furthermore, PDGFR β signaling has also emerged as a predominant pathway in recruitment of BM-MSCs towards tumor sites (Veevers-Lowe et al. 2011), contributing to enhance the aggressive and invasive properties of a several types of cancer, including chronic lymphocytic leukemia (CLL) (Ding et al. 2010), pancreatic (Beckermann et al. 2008), and colon (Shinagawa et al. 2013) carcinomas.

Therefore, due to its crucial role in tumor progression, PDGFR β represents a valuable target for tumor therapeutic development.

To date, several tyrosine kinase inhibitors (TKIs) that act on a wide spectrum of tyrosine protein kinases including PDGFR β are under development as anticancer agents.

Among them, Imatinib mesylate (Gleevec®/STI571) was developed as TKI by inhibiting fusion proteins breakpoint cluster region-Abelson Tyrosine-Protein Kinase (Bcr-Abl) in chronic myeloid leukemia (Druker et al. 2001). However, it has been demonstrated that imatinib has clinical efficacy also in gastrointestinal stromal tumors by inhibiting c-Kit (Dagher et al. 2002), and in the treatment of a variety of dermatological diseases (Akhmetshina et al. 2009; Spiera et al. 2011). Many studies and clinical trials to assess its effectiveness in PDGFR β -expressing cancers are being performed (Cristofanilli et al. 2008; Maass et al. 2014; Wen et al. 2006).

Furthermore, Shinagawa et al. (2013) have reported that imatinib therapy impairs the tumor-promoting effect of BM-MSCs in an orthotopic transplantation model of colon cancer, suggesting that PDGFR β inhibition could prevent BM-MSC recruitment to tumor microenvironment.

Sunitinib malate (Sutent®/SU11248) is a broad-spectrum, orally available multitargeted TKI with activity against VEGFR, PDGFR, c-Kit, and FMS-like tyrosine kinase 3 (FLT-3). In several phase I/II/III studies, sunitinib was found to be effective as second and first line treatment in metastatic renal cell carcinoma (RCC). In fact, with a 37% response rate and an additional 48% stable disease, sunitinib became the drug of choice for first line treatment in RCC (Polyzos et al. 2008). In patients with gastrointestinal stromal tumors, sunitinib results also effective as second line treatment with 8% response rate, 70% stable disease and a 20-month median survival (Pilotte 2015). A phase II clinical trial in multi-treated women with breast cancer demonstrated that sunitinib has a moderate activity with 16% clinical benefit (Fratto et al. 2011).

Sorafenib (Nexavar®) is an inhibitor of Mitogen-activated protein kinases (MAPKs) pathway and of angiogenic receptor tyrosine kinases (RTKs) VEGFR2 and PDGFR β . Concerning PDGFR β targeting blockage, it has been shown that sorafenib inhibits oncogenic PDGFR β and overcome resistance to other TKi (Guida et al. 2007; Lierman et al. 2007). Several clinical trials have been performed to test sorafenib efficacy specially in treatment of advanced hepatocellular carcinoma (Keating and Santoro 2009; Ogasawara et al. 2016), and in metastatic thyroid cancer (Ferrari et al. 2015).

These TKIs might overcome molecular heterogeneity within or between cancer patients and, therefore, have a better chance of success; however, unnecessary targeting of multiple receptors could cause toxicity and limit drug effectiveness (Dancey and Chen 2006).

Neutralizing antibodies for PDGF ligands and receptors have been used in experiments evaluating the importance of PDGF signaling in pathogenic processes but, to date, none of such antibodies has entered the clinic (Shen et al. 2009).

Thus, there is the urgent need to design new PDGFR β -targeting drugs for a more specific and selective tumor therapy.

1.5.1 Targeting PDGFR β : Gint4.T aptamer

Aptamers are short single-stranded nucleic acid oligomers (ssDNA or RNA) with a specific and complex three-dimensional shape able to bind to a wide variety of targets from single molecules to complex target mixtures or whole organisms (Hermann and Patel 2000) (Figure 7A).

Unlike other small noncoding RNAs either natural or artificial, such as antisense, ribozymes, small interfering RNAs (siRNAs) and microRNAs (miRNAs) that inhibit gene expression, aptamers act by directly binding the protein target without interfering with its expression (Cerchia and de Franciscis 2006) (Figure 7B).

DNA or RNA aptamers are isolated from large pools of different oligonucleotides by an *in vitro* evolution-based approach named Systematic Evolution of Ligands by EXponential enrichment (SELEX). This process starts with a DNA library obtained from combinatorial chemical synthesis. The library usually consists of a random region of 20–80 nucleotides flanked by fixed 5' and 3' regions necessary for polymerase chain reaction (PCR) amplification and a promoter sequence for T7 RNA polymerase. Aptamers are selected, amplified by RT-PCR and then reselected at higher stringency with the process repeated as needed to achieve the desired affinity and specificity for the target. After cloning and sequencing, selected aptamer sequences can be synthesized and tested for their ability to bind specifically to the target molecule (Ellington et al. 1990).

Aptamers have a small size (8-15 kDa) which permits easy membrane penetration and short blood residence and can be chemically modified to improve their stability, bioavailability, and pharmacokinetic. In fact, aptamers generated by SELEX process, especially RNAs, are unstable in biological fluids. To protect RNA from digestion by nucleases, chemically modified nucleotides are incorporated into the oligonucleotide backbone. The most commonly employed functional group modifications are 2'-F, OMe, or NH₂ modifications of the nucleotides, all of which can be introduced at either the pre- or post-SELEX step (Keefe and Cloud 2008).

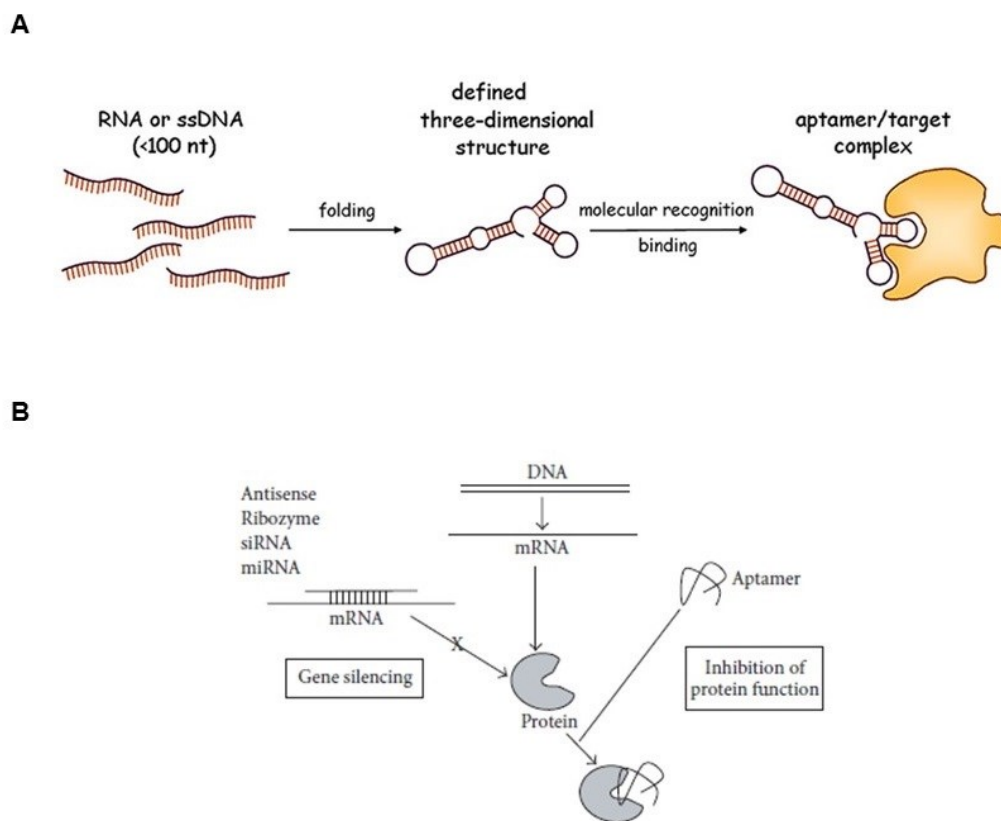


Figure 7. Aptamer functionality. **A)** Schematic representation of aptamer three-dimensional structure and functionality and **B)** its mechanism of action compared to that of other ncRNAs.

Among drugs used for molecular targeting, monoclonal antibodies have led great benefits in a wide range of applications. However, there are several limitations related to antibodies; monoclonal antibodies normally are unable of membrane penetration due to larger size and thus, are not ideal as carriers for

targeted delivery of molecules within cells. They are also immunogenic, temperature sensitive, and their production is laborious, expensive, time consuming and undergoes batch-to-batch variations.

Aptamers generally considered being oligonucleotides comparable to antibodies, rival antibodies in many ways. Aptamers fold to form unique tertiary structures, allowing them to bind to target proteins with high specificity and affinity, often leading to modulation of the target protein activity. In addition, aptamers small size enables them to access protein epitopes and be internalized better than antibodies. This feature allows aptamer to be used as bifunctional ligands that, along with recognition, can also be employed as delivery vehicles. These molecules are highly temperature-resistant and are stable over long-term storage. Their targeted binding properties can be controlled and modified as preferred, and molecules can be derivatized easily for downstream applications. Due to these advantages, aptamers gained immediate attention for clinical development, and shortly after the advent of the technology, a substantial number of aptamers entered clinical trials for a wide range of applications (Dua et al 2011).

Over last years, the development of aptamers as therapeutics has mainly involved aptamers that bind and hamper the activity of their protein targets. To date, the most successful therapeutic application of an aptamer is represented by the RNA-aptamer commercially known as Macugen (or Pegaptanib, marketed by Eyetech Pharmaceuticals/Pfizer), that binds and blocks VEGF activity. The aptamer has been approved by the Food and Drug Administration for the treatment of age-related macular degeneration (AMD) (Katz and Goldbaum 2006).

Recently, Camorani et al. (2014) have developed a new 33 mer nuclease-stabilized RNA aptamer, named Gint4.T that specifically binds PDGFR β by inhibiting the receptor activity and downstream signaling in glioblastoma multiforme (GBM) cells and *in vivo* (Figure 8). Gint4.T binds to PDGFR β at high affinity and specificity and dramatically inhibits *in vitro* GBM cell migration and cell proliferation. Importantly, the potent inhibitory effect of Gint4.T has been extended to a xenograft model of GBM in which Gint4.T induces a remarkable tumor growth inhibition.

Therefore, Gint4.T represents an innovative aptamer-based therapeutic tool that in combinations with conventional therapeutics may offer more effective alternative to treat cancer patients.

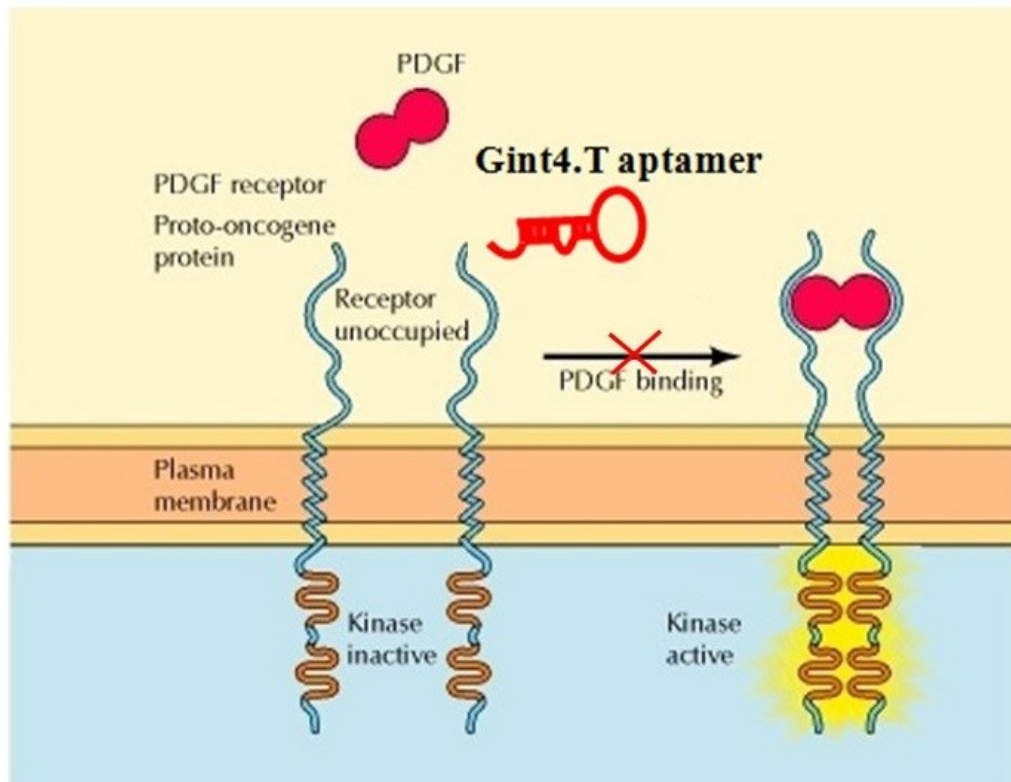


Figure 8. Gint4.T aptamer activity. Gint4.T specifically binds PDGFR β by inhibiting the receptor activation and downstream signaling.

1.5.2 Targeting Triple-Negative Breast Cancer microenvironment

Breast cancer is one of the most commonly diagnosed tumor and the second leading cause of cancer-related death in women after lung carcinoma (Siegel et al. 2012). Around 15% of invasive breast carcinoma is identified as triple negative breast cancer (TNBC), characterized for the lack expression of estrogen receptor (ER), progesterone receptor (PR) or Her2/neu. This renders it more difficult to treat since most chemotherapies target one of the three receptors, so triple-negative cancers often require combination therapies. TNBCs are generally of a higher grade, more prevalent in young and African-American people and are commonly associated with a poor outcome. The metastatic potential in TNBC is similar to that of other breast cancer subtypes, but these tumors are associated with a shorter median time to relapse and death (Hudis and Gianni 2011).

Over past years, a number of new strategies for TNBC were tested in clinical trials, including poly (ADP-ribose) polymerase (PARP), PI3K and MEK

inhibitors (Mayer et al. 2014). However, TNBC is clearly a complex disease and current treatments have shown unsatisfactory outcomes due to the dispersed nature of this tumor. Therefore, understanding new molecular mechanisms underlying breast cancer progression is required to provide new therapeutic targets.

Recent evidence has suggested that critical components of tumor stroma, including CAFs and TAMs, play a crucial role to promote breast cancer initiation, growth, migration, metastasis and therapeutic resistances (Mao et al. 2013). In addition, it has been widely shown that BM-MSCs can integrate into the tumor-associated stroma and promote the progression of TNBC through the activation of different mechanisms involving HIFs (Chaturvedi et al. 2013), TGF- β (McAndrews et al. 2015) and interleukin-1 beta (IL-1 β) (Escobar et al. 2015). Thus, exploring the interaction between cancer cells and stromal cells in the TNBC microenvironment may be useful to screen potential candidate markers and offer a great impact in TNBC therapy in the future.

2. AIM OF THE STUDY

Tumor is a complex system in which cancer cells perform an intricate cross-talk with microenvironment. A tumor can influence its microenvironment by releasing extracellular signals, promoting tumor angiogenesis and inducing the inflammatory response, whereas the stroma cells in the microenvironment can prompt tumor growth and promote metastatic phenotype.

Thus, in this scenario, multi-targeted approaches, for both tumor cells and tumor microenvironment and/or the signaling pathways involved in their communication, may provide a more efficient anti-cancer therapy.

Among several cell types that compose the tumor milieu, bone marrow-derived mesenchymal stem cells (BM-MSCs) selectively migrate toward tumor microenvironment and promote cancer progression and metastasis by supporting tumor stroma activity.

The aim of this study is to investigate the role of BM-MSCs in tumor processes, deepening the involvement of specific signaling pathways underlying their recruitment and activity into tumor microenvironment.

In particular, innovative therapeutic tools targeting specific receptor involved in the cross-talk between BM-MSCs and tumor cells have been developed and characterized to:

- inhibit BM-MSC-mediated growth and aggressiveness of osteosarcoma (OS) and hepatocellular carcinoma (HCC) cell lines through modulation of CXCR4 signaling using a novel antagonist, named Peptide R.
- interfere with BM-MSC recruitment by triple negative breast cancer (TNBC) cells through modulation of PDGFR β signaling using Gint4.T aptamer.

3. MATERIALS AND METHODS

3.1 Cell lines and culture conditions

Human tumor cell lines were cultured in three different media:

- osteosarcoma (OS) cells U2OS and Saos-2 were cultured in McCoy's 5A medium;
- hepatocellular carcinoma (HCC) cells SNU-398 and Hep3B, U87MG glioblastoma and MCF7 breast cancer cells were grown in Dulbecco's modified Eagle's medium (DMEM);
- triple-negative breast cancer cell lines (TNBC) MDA-MB-231 and BT-549 were grown in RPMI 1640.

All cell lines came from American Type Culture Collection, whereas OS cell lines were purchased from Sigma Aldrich.

All types of media were supplemented with 10% fetal bovine serum (FBS), 100 U/ml penicillin and 100 µg/ml streptomycin. The cells were maintained in a humidified incubator in 5% CO₂ at 37 °C.

3.2 Isolation, culture and immunophenotypic characterization of human bone-marrow mesenchymal stem cells (BM-MSCs)

Bone marrow (BM) samples were obtained from 3 male patients (29, 35 and 49 years old) who underwent surgery at the Rizzoli Orthopaedic Institute after informed consent was obtained according to a protocol approved by the Ethics Committee. The isolation of cells and the expansion of cultures of human BM-MSCs were performed, using gradient separation and plastic adherence methods (Pierini et al. 2012). BM-MSCs were recognized by their ability to proliferate in culture and their adherent, spindle-shape morphology. Furthermore, BM-MSCs were characterized using a FC500 flow cytometer (Beckman Coulter, Brea, CA, USA) with staminal markers; cells positive for CD44, CD73, CD90, CD105, and CD146 and negative for CD34 and CD45 were isolated.

BM-MSCs, after isolation and characterization, were grown in Alpha MEM medium supplemented with 20% FBS, 2mM GlutaMax (Gibco) and 100 U/ml penicillin and 100 µg/ml streptomycin.

To obtain conditioned medium (BM-MSC-CM), BM-MSCs were grown in medium with 1% FBS for 48 h. The medium was then collected, centrifuged at 1000 × g for 10 min, and filtered through 0.22-µm filters (Millipore, Billerica,

MA), before being added to tumor cells. BM-MSCs were used at passage 2–3 in this study.

3.3 Aptamers and treatments

2'F-Py RNA aptamers (Gint4.T and CL4Scrambled) were synthesized by TriLink Biotechnologies and purchased from Tebu-bio srl (Magenta, Milan, Italy).

Before each treatment, aptamer proper folding was accomplished by a short denaturation/ renaturation step (85 °C for 5 minutes, snap-cooled on ice for 2 minutes, and allowed to warm up to 37 °C). For cell incubation longer than 24 hours, the aptamer treatment was renewed each day and the RNA concentration was determined to ensure the continuous presence of at least 400 nmol/l concentration, taking into account the 6 hours-half-life of the aptamer in 10% serum (Camorani et al. 2014).

Gint4.T aptamer, PDGFR β inhibitor:

5'-UGUCGUGGGGCAUCGAGUAAAUGCAAUUCGACA-3'.

The scrambled sequence of CL4 aptamer (Esposito et al. 2011) has been used as a negative control; herein indicated as unrelated:

5'-UUCGUACCGGGUAGGUUGGCUUGCACAUAGAACGUGUCA-3'.

3.4 Cell viability assay

Cell viability was assessed with CellTiter 96 AQueous One Solution Cell Proliferation Assay (Promega, Madison, WI) according to the supplier's instructions. The number of viable cells was detected by determining the bioreduction of 3-(4,5-dimethylthiazol- 2yl)-5-(3-carboxymethoxy-phenyl)-2-(4-sulfophenyl)-2H tetrazolium (MTS) to formazan salt crystals.

U2OS and SNU-398 cells were seeded in their media at a density of 5000 cells per well in 96-well flat-bottomed plates and allowed to recover for 24 h. Then, tumor cells were grown in the presence of medium with 10% FBS or BM-MSC-CM, or they were co-cultured with BM-MSCs (ratio 1:1) for 24 h and 48 h in a humidified incubator with 5% CO₂ at 37 °C. In co-cultures, BM-MSCs and tumor cells were grown in a Boyden chamber with a 0.4 μ m membrane. The upper chambers were seeded with BM-MSCs, and the lower chambers were seeded with OS or HCC cells.

BM-MSCs were seeded at a density of 4000 cells per well in 96-well flat-bottomed plates and allowed to recover for 24 h. Then, BM-MSCs were treated

for 72 hours with 400nmol/l Gint4.T and the unrelated aptamer, or 1 μ mol/l Imatinib mesylate (Santa Cruz Biotechnology).

After 1 h of incubation with MTS, the absorbance was read using a plate reader (Multiskan RC, Thermo Scientific) at a wavelength of 490 nm. Each sample was analyzed in triplicate. The data are expressed as the percentage of viable cells, considering 100% to represent the number of cells grown in the medium supplemented with 10% FBS, which was used as control.

3.5 Cell lysate preparation and western blot analysis

Cells were washed twice in ice-cold PBS and lysed in lysis buffer (40mM HEPES pH 7.5, 120mM NaCl, 5mM MgCl₂, 1mM EGTA, 0.5 mM EDTA, and 1% Triton X-100) containing protease (Complete Tablets, EDTA-free, Roche) and phosphatase inhibitors (20mM α -glycerol-3-phosphate and 2.5 mM Na-pyrophosphate). The suspension was homogenized and centrifuged for 15 min at 13,000 \times g at 4 °C. Western blot analysis of proteins from whole cell lysates was performed using a standard protocol. Equal amounts of proteins from cells (50 μ g) were separated using SDS-PAGE under reducing conditions and transferred to PVDF membranes. After blocking to prevent non-specific protein binding, the membranes were incubated with primary antibodies overnight at 4 °C. The following primary antibodies were used: rabbit polyclonal anti-CXCR4 (C8227, Sigma-Aldrich), rabbit polyclonal anti phospho-AKT (CST-9271, Cell Signaling, indicated as pAKT), rabbit polyclonal anti-AKT (CST-9272, Cell Signaling), rabbit polyclonal anti phospho-ERK (CST-9101, Cell Signaling, indicated as p-ERK), rabbit polyclonal anti-ERK (CST-9102, Cell Signaling), goat anti E-cadherin (sc-1500, Santa Cruz Biotechnology), rabbit polyclonal anti-vimentin (CST-5741, Cell Signaling), anti phospho-PDGFR β (CST-3173, Cell Signaling indicated as pPDGFR β), anti-PDGFR β (CST-3169, Cell Signaling) and mouse monoclonal anti- β -actin (A4700, Sigma-Aldrich). The filters were then incubated with 1:2000 peroxidase-labeled anti-mouse, anti-rabbit or anti-goat Ig antibodies (Amersham Biosciences Europe, Freiburg, Germany) for 1 h at 22 °C. After extensive washing, the immunoreactions were revealed using an enhanced chemiluminescence detection system (ECL) according to the manufacturer's recommendations. Densitometric analyses were performed on at least two different expositions to assure the linearity of each acquisition using ImageJ software (v1.46r).

3.6 RNA isolation and realtime-polymerase chain reaction (Real time-PCR)

Total RNA was extracted from tumor cells and BM-MSCs using TRIzol reagent (Invitrogen, Grand Island, NY). Total extracted RNA (200 ng) was reverse transcribed using Superscript II RNase H-reverse transcriptase according to the manufacturer's instructions (Invitrogen/Life Technologies, Carlsbad, CA, USA). Real-time PCR was performed using approximately 10 ng of cDNA in a 25- μ l SYBR Green reaction mixture, and an ABI Prism 7000 (Applied Biosystems, Carlsbad, CA, USA) robocycler was used for amplification. The cycling conditions for the PCRs were as follows: initial denaturation (one cycle of 10 min at 95 °C) followed by 40 cycles of denaturation (15 s at 95 °C) and annealing (1 min at 60 °C). Subsequently, CXCR4 mRNA levels in tumor cells were quantified, and these expression levels were compared to GUSB mRNA levels. Instead, for quantitative analysis of PDGFR β mRNA levels in BM-MSCs, they were compared to β -actin mRNA levels.

The gene-specific primers used for the amplifications were as follows:

CXCR4: 5'-TGAGAAGCATGACGGACAAG-3' (forward)
5'-AGGGAAGCGTGATGACAAAG-3' (reverse)

GUSB: 5'-AGCCAGTTCCTCATCAATGG-3' (forward)
5'-GGTAGTGGCTGGTACGGAAA-3' (reverse)

PDGFR β : 5'-AGGACACGCAGGAGGTCAT-3' (forward)
5'-TTCTGCCAAAGCATGATGAC-3' (reverse)

β -actin: 5'-CAAGAGATGGCCACGGCTGCT-3' (forward)
5'-TCCTTCTGCATCCTGTCTGGCA-3' (reverse)

3.7 RNA interference

CXCR4-targeting siRNA (L-005139-00-05) and a corresponding control non-targeting siRNA (D-001810-10-05) were purchased from Dharmacon. Saos-2 and Hep3B cells were transfected using DharmaFECT siRNA transfection reagent and 100 nmol/l siRNAs according to the manufacturer's protocol. Saos-2 and Hep3B cells were grown in culture medium after transfection for 72 h, and the down-regulation of targeted protein expression was assessed using Western blot analysis.

3.8 Analysis of OS and HCC cell migration by wound healing assay

OS and HCC cell lines were seeded in 6-well plates and grown to confluent cell monolayers. Cells were then scratched with pipette tips to make wounds. The cells were then rinsed with PBS to remove the loosened cell debris. Culture medium containing 1% FBS, 10% FBS, BM-MSC-CM, BM-MSC-CM with the CXCR4 antagonist AMD3100 (10 μ M) (Sigma-Aldrich) or Peptide R (10 μ M) were then added to the cells and the plates were incubated at 37 °C in 5% CO₂ for 24 h and 48 h. In addition, wound healing assays were performed using Saos-2 and Hep3B cells that were grown in the presence of CXCR4 siRNA or Scr siRNA for 72 h. The wounds were observed using phase contrast microscopy. As the cells migrated to fill the scratched area, images were captured using a digital camera (Canon) that was attached to a microscope (Leica) at time 0 and after 24 and 48 hours. The distance between the edges of the scratch was measured using ImageJ, the average distance was quantified and the extent of wound closure was determined as follows: wound closure (%) = $1 - (\text{wound width tx} / \text{wound width t0}) \times 100$.

3.9 Analysis of BM-MSC migration using Boyden chamber

To test BM-MSC migration a 24-well Boyden chambers (Corning, NY) containing inserts of polycarbonate membranes with 8 μ m pores were used. BM-MSCs were harvested, suspended in serum free medium, and counted. Cells (0.2×10^5 in 100 μ l serum-free medium per well) were then plated into each top chamber in the presence of 400 nmol/l Gint4.T and the unrelated aptamer or 5 μ mol/l Imatinib mesylate, and exposed to PDGF-BB (100 ng/ml), MDA-MB-231, BT-549 cells, or 10% FBS as inducers of migration (0.6 ml, lower chamber).

After incubation for 24 h at 37 °C in a humidified incubator in 5% CO₂, the non-migrating cells were removed from the top chamber using a cotton swab, and the cells that had migrated to the lower surface of the membrane insert were visualized by staining with 0.1% crystal violet in 25% methanol. The percentage of migrated cells was evaluated by eluting the crystal violet with 1% sodium dodecyl sulfate and reading the absorbance at a 570 nm wavelength.

3.10 Tumor cell invasion assay

To perform invasion assays, the top compartment of Boyden chambers was coated with 50 μL of diluted (1:3 in PBS) Matrigel (BD Biosciences, San Jose, CA). After coating, chambers were incubated at 37°C for 1h to allow Matrigel to solidify. OS (U2OS and Saos-2) and HCC (SNU-398 and Hep3B) cells were harvested, suspended in serum free medium, and counted. Cells (2.5×10^5 in 100 μL serum-free medium per well) were then added to each top chamber. Medium containing 1% FBS (negative control), 10% FBS (positive control), BM-MS-CM or BM-MSCs was added to the lower chamber as a chemoattractant. After incubation for 48 h at 37 °C in a humidified incubator in 5% CO₂, migrated cells were visualized and analyzed as described above. To block CXCR4, the cells were incubated with the CXCR4 inhibitors AMD3100 or Peptide R at a concentration of 10 μM during the invasion assays.

3.11 NIR fluorescent BM-MS-C-labeling

VivoTrack 680 Fluorescent Cell Labeling Agent (MW: 1173 g mol^{-1} ; A: 676 nm; Em: 696 nm) was commercially obtained from PerkinElmer (Waltham, MA), dissolved in 1.3 mL of warm sterile PBS (final volume of 2.0 mL). BM-MSCs (3×10^6) were resuspended in 200 μL of sterile PBS and incubated with VivoTrack 680 (ratio 1:1, v/v) for 30 min at 37°C under agitation in the dark. Afterwards, the suspension was washed three times with PBS containing 1% FBS to remove excess cell labeling agent. At that time, VivoTrack 680-labeled cell viability was assessed microscopically by Tripan-blue exclusion (Gibco™). To verify that the labelling process had been successfully succeeded, labelled cells were examined by flow cytometry (BD Accuri™ C6), using appropriate lasers and filters for detection of 680 nm wavelength.

3.12 *In vivo* BM-MS-C tracking by Fluorescence Molecular Tomography

Human breast cancer cell line MDA-MB-231 were used for development of animal tumor models using nude CD-1 (Crl:CD1-Foxn1tm) mice (Charles River Laboratories, Wilmington, MA). Briefly, MDA-MB-231 xenografts were established by subcutaneous inoculation of 10×10^6 cells into the right posterior flank of female nude CD-1 mice, 5 week old and weighing 15–20 g, and allowed to grow for 3 weeks.

To perform *in vivo* imaging studies, 1×10^6 VivoTrack 680-labeled BM-MSCs were administered by caudal vein injection in MDA-MB-231 xenografts. Mice under isoflurane anesthesia were analyzed at different time points by FMT 4000 (Fluorescence Molecular Tomography) imaging system (PerkinElmer, Waltham, MA).

Epifluorescence (2D) and tomography (3D) datasets were both acquired and analyzed by FMT system software (TrueQuant™ v4.0) from PerkinElmer (Waltham, MA). Volumes of interest (VOI's) were drawn encompassing each tumor and quantitative measurement of fluorescence was performed and fluorochrome concentration to the pmol was obtained.

All animal experimental procedures were conducted in accordance with Italian law for animal protection and were approved by the Italian Ministry of Health, Animal Welfare Direction.

3.13 Statistical analysis

Results were obtained from at least three independent experiments and are expressed as the mean \pm standard deviation. The data were analyzed using GraphPad Prism statistical software 6.0 (GraphPad Software, La Jolla, CA, USA), and significance was determined using Student's t-tests. A P-value <0.05 was considered statistically significant.

4. RESULTS

4.1 BM-MSCs promote tumor cell growth and increase p-AKT and p-ERK levels in human osteosarcoma (OS) and human hepatocellular carcinoma (HCC) cell lines

To determine the effects of BM-MSCs on human osteosarcoma (U2OS) and human hepatocellular carcinoma cells (SNU-398) proliferation, cells were grown in medium supplemented with 10% FBS (control), in BM-MSC-conditioned medium or co-cultured with BM-MSCs for 24 and 48 hours, and cell viability was then tested using an MTS assay. As shown in Figure 9A, when U2OS cells were grown in the presence of BM-MSC-CM for 24 and 48 hours, a 2-fold significant increase in proliferation was observed compared to proliferation in the control cells ($P < 0.01$). Consistent with these results, I found that when U2OS cells were co-cultured with BM-MSCs (1:1 ratio), their growth was also significantly enhanced by 3- and 3.5-fold at 24 and 48 hours, respectively ($P < 0.01$) (Figure 9A). Similarly, I observed an increase in SNU-398 cell proliferation when cells were grown in the presence of BM-MSC-CM (1.8-fold at 24h and 2.1-fold at 48h; $P < 0.01$) or co-cultured with BM-MSCs (1:1 ratio) (1.5-fold at 24h and 1.8-fold at 48h; $P < 0.01$) compared to proliferation in the control cells (Figure 9B). Thus, BM-MSCs and factors released by BM-MSCs promoted cell growth in U2OS and SNU-398 cells.

To investigate the mechanisms underlying the promotion of tumor growth by BM-MSCs, I next analyzed the activation of cell survival-related intracellular signals in the PI3K/AKT and extracellular signal-regulated kinase 1/2 (ERK1/2) pathways. As shown in Figure 9C, conditioned medium from BM-MSCs increased p-AKT and p-ERK levels in both tumor cell lines compared to the levels observed in cells grown in medium supplemented with 10% FBS (control), whereas no increase was observed in AKT and ERK levels. I found that BM-MSC-CM caused a 2.54-fold and a 2.44-fold increase in p-AKT levels in U2OS and SNU-398 cells, respectively, whereas p-ERK was increased by 1.3-fold in U2OS and 1.9-fold in SNU-398 cells compared to the levels observed in the controls (Figure 9C).

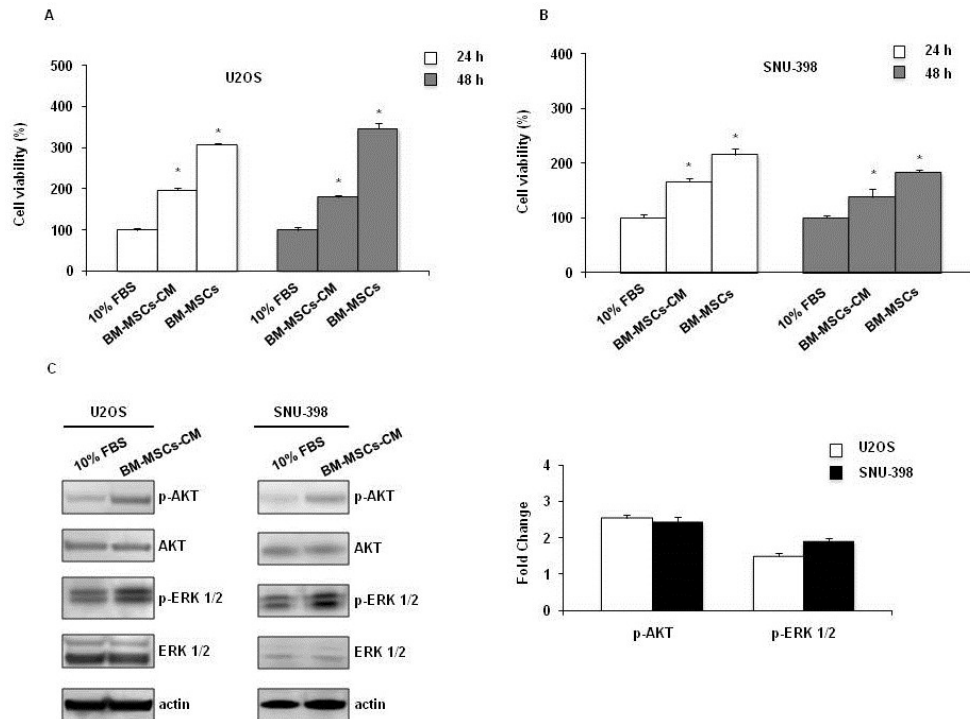


Figure 9. BM-MSCs enhance cell viability and activate AKT and ERK pathways in U2OS and SNU-398 tumor cell lines. (A, B) U2OS and SNU-398 cells were co-cultured with BM-MSCs or grown in the presence of BM-MSC-CM for 24 and 48 hours, and then their viability was tested using MTS assays. The data are expressed as the percentage of viable cells by considering 100% to represent the number of cells grown in medium supplemented with 10% FBS (controls). All experiments were performed at least three times independently (* $P < 0.01$). **(C)** Western blots show the effect of BM-MSC-CM after 24h on downstream signaling in tumor cells. Actin was used as an equal loading control. Representative data are shown from one of three experiments. The fold changes in p-AKT and p-ERK levels are shown in tumor cells grown in presence of BM-MSC-CM compared to their levels in control cells grown in medium containing 10% FBS, which were arbitrarily determined to be 1.

4.2 BM-MSCs increase CXCR4 mRNA and protein expression in OS and HCC cell lines

To test whether the expression of CXCR4 could be affected by treatment with BM-MSC-CM, OS (U2OS and Saos-2) and HCC cells (SNU-398 and Hep3B) were treated for 24h with BM-MSC-CM and a significant increase was observed in CXCR4 mRNA and protein levels (Figure 10).

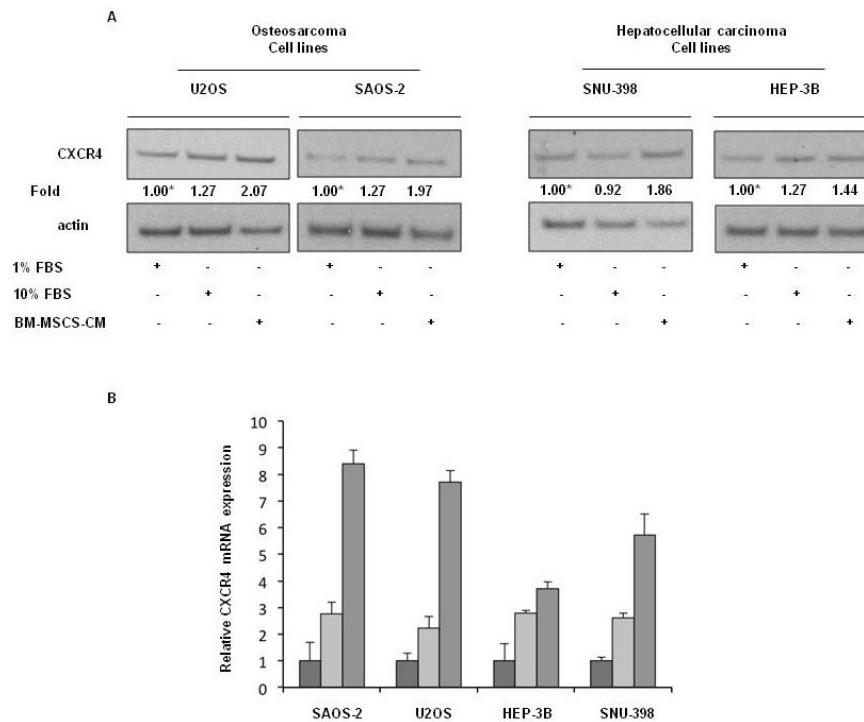


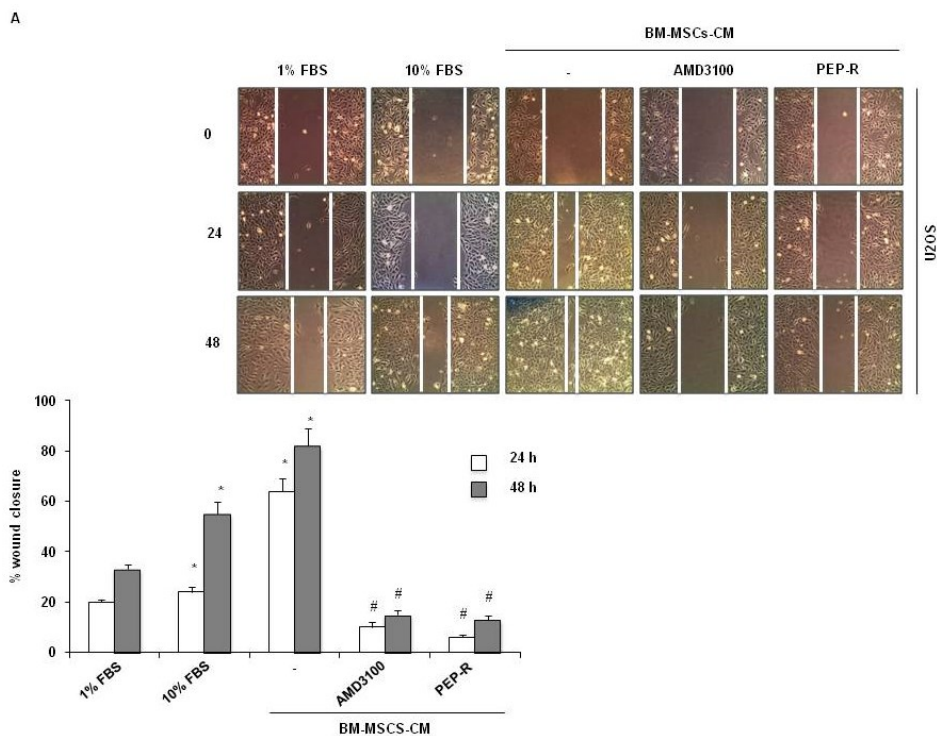
Figure 10. BM-MSCs increase CXCR4 mRNA and protein levels in OS and HCC cell lines. (A) Western blot analysis of CXCR4 expression in tumor cell lines after treatment with BM-MSC-CM for 24h. Actin was used as an equal loading control. The values below the blot indicate signal levels relative to controls, which were arbitrarily set to 1 (labeled with asterisk). Representative data from one of three experiments are shown. (B) CXCR4 mRNA levels as detected using real-time PCR in OS and HCC cell lines grown for 24h in the presence of BM-MSC-CM, medium with 1% FBS or medium with 10% FBS, as indicated.

4.3 A novel CXCR4 antagonist, Peptide R, prevents BM-MSC-dependent wound healing in OS and HCC cells

Because CXCR4 expression is correlated with tumor cell migration and metastatic potential (Thiery et al. 2009), I investigated whether BM-MSC-CM would be able to affect wound healing. Monolayers of U2OS and SNU-398 cells were scratched, and images were taken at 0, 24 and 48 hours after wounding (Figure 11A and B). BM-MSC-CM caused a significant increase in wound closure in U2OS cells (64% and 82% at 24h and 48h, respectively) compared to closure in the control cells (1% FBS) ($P < 0.01$). When U2OS cells were grown in the presence of BM-MSC-CM and treated with 10 μ M of CXCR4 antagonist Peptide R (indicated as PEP-R) or, alternatively, with 10

μM of AMD3100, wound healing was significantly delayed compared to cells treated with BM-MSC-CM alone ($P < 0.001$) (Figure 11A). In SNU-398 cells, BM-MSC-CM caused a significant increase in wound closure (40% and 50% at 24h and 48h, respectively) compared to closure in control cells, although this increase was lower than that observed for U2OS cells. These results suggest that Peptide R, as well as AMD3100, significantly reduced the wound closure induced by BM-MSC-CM ($P < 0.001$) (Figure 11B).

To confirm that inhibition of CXCR4 expression reduced the BM-MSC-induced wound closure, Saos-2 and Hep3B cells were transiently transfected with a pool of non-targeting Scr siRNAs or CXCR4-specific siRNAs. A significant reduction was observed in CXCR4 levels in both cell lines when they were transfected with CXCR4 siRNAs compared to cells transfected with Scr siRNAs for 72h (Figure 12A and B). Similar to what was observed in U2OS and SNU-398 cells, I observed that Saos-2 and Hep3B cells that were treated with BM-MSC-CM showed a significant increase in wound closure compared to closure in the control (1% FBS). Whereas when these cells were treated with BM-MSC-CM in presence of Peptide R (10 μM) or, alternatively, AMD3100 (10 μM), wound healing was significantly delayed ($P < 0.001$). Furthermore, when Saos-2 and Hep3B cells were transfected with CXCR4-specific siRNAs, a significant reduction was observed in wound closure compared to closure in cells transfected with Scr siRNAs ($P < 0.001$) (Figure 12A and B).



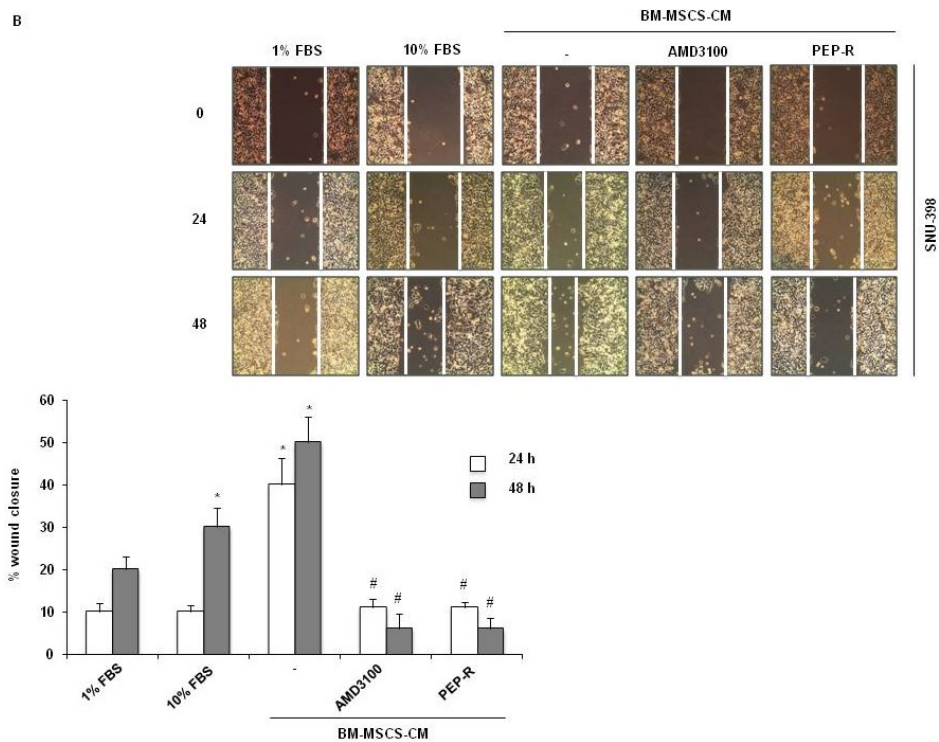
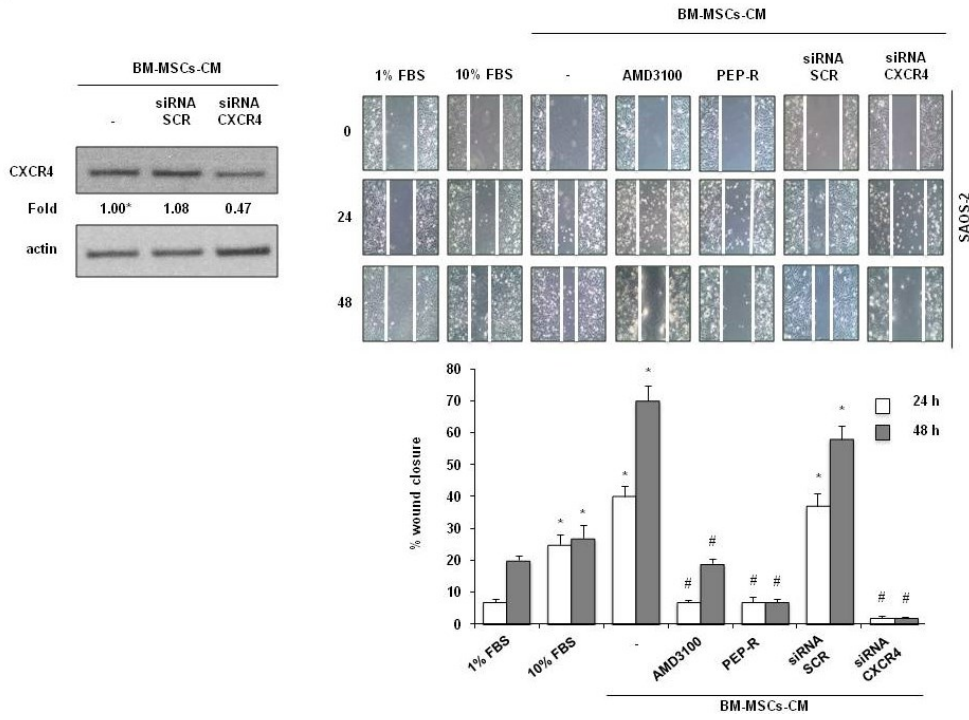


Figure 11. BM-MSCs induced an increase in wound healing in U2OS and SNU-398 tumor cells that was inhibited by Peptide R. (A) U2OS cells, after wounds were made by scratching with pipette tips, were grown for 24 and 48 hours in medium containing 1% FBS or 10% FBS or with conditioned medium obtained from cultured BM-MSCs (BM-MSC-CM) in the presence of Peptide R (10 μ M) or AMD3100 (10 μ M) used as positive control. **(B)** SNU-398 cells were tested in wound healing assays using the same experimental conditions described above for U2OS cells. The distance between edges of the scratch was measured using ImageJ, the average distance was quantified, and the extent of wound closure was determined as follows: wound closure (%) = $1 - (\text{wound width tx}/\text{wound width t0}) \times 100$. All experiments were performed at least three times. * $P < 0.01$ compared to the control (medium with 1% FBS); # $P < 0.001$ compared to treatment with BM-MSC-CM.

A



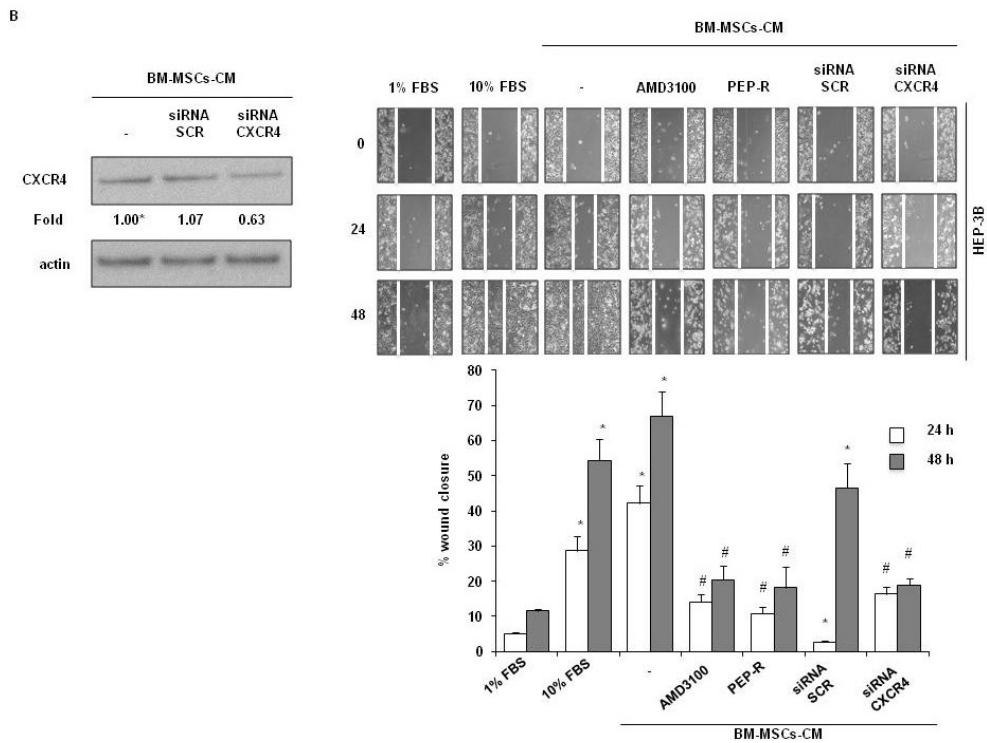


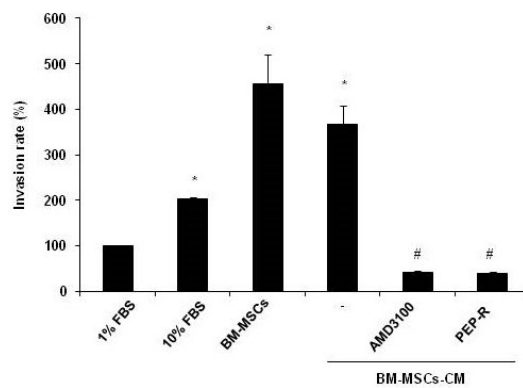
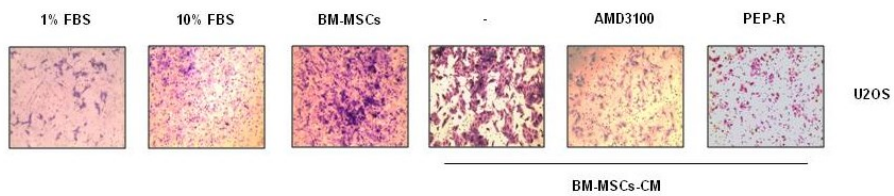
Figure 12. The increase in wound healing in Saos-2 and Hep3B tumor cells induced by BM-MSCs was inhibited by Peptide R. (A) Saos-2 cells transfected for 72 h with CXCR4-specific siRNAs or non-targeting siRNAs (used as the negative control) were analyzed to determine CXCR4 protein levels using western blot analysis. Saos-2 cells, after wounds were induced by scratching with pipette tips, were grown for 24 and 48 hours in medium containing 1% FBS or 10% FBS or with conditioned medium obtained from BM-MSCs (BM-MSC-CM) in the presence of CXCR4 inhibitor Peptide R (10 μ M) or, alternatively, AMD3100 (10 μ M), CXCR4 siRNAs or Scr siRNAs, as indicated. (B) Hep3B cells were transfected and tested in wound healing assays using the same experimental conditions described above for Saos-2 cells. The distance between edges of the scratch was measured using ImageJ, the average distance was quantified, and the extent of wound closure was determined as follows: wound closure (%) = $1 - (\text{wound width tx} / \text{wound width t0}) \times 100$. All experiments were performed at least three times. *P < 0.01 compared to the control (medium containing 1% FBS); #P < 0.001 compared to BM-MSC-CM.

4.4 A novel CXCR4 antagonist, Peptide R, prevents BM-MSC-dependent U2OS and SNU-398 cell invasion

To test whether BM-MSCs could affect the invasiveness of U2OS and SNU-398 cells, Boyden chambers coated with Matrigel were used. Figure 13A and B

demonstrate that a significant increase was observed in tumor cell invasiveness when the tumor cell line was exposed for 48 hours to BM-MSC-CM or BM-MSCs (ratio 1:1), which was added to the lower chamber as chemoattractant, compared to the invasiveness observed in the control cells (1% FBS used as the medium) ($P < 0.001$). The inhibition of CXCR4 using Peptide R or AMD3100 as positive control, dramatically suppressed the invasiveness of U2OS and SNU-398 cells that was promoted by BM-MSCs ($P < 0.001$). A similar inhibitory effect on BM-MSC-induced invasiveness was observed on Saos-2 and Hep3B cells when they were also cultured in the presence of Peptide R, as well as AMD3100. (Figure 14A and B).

A



B

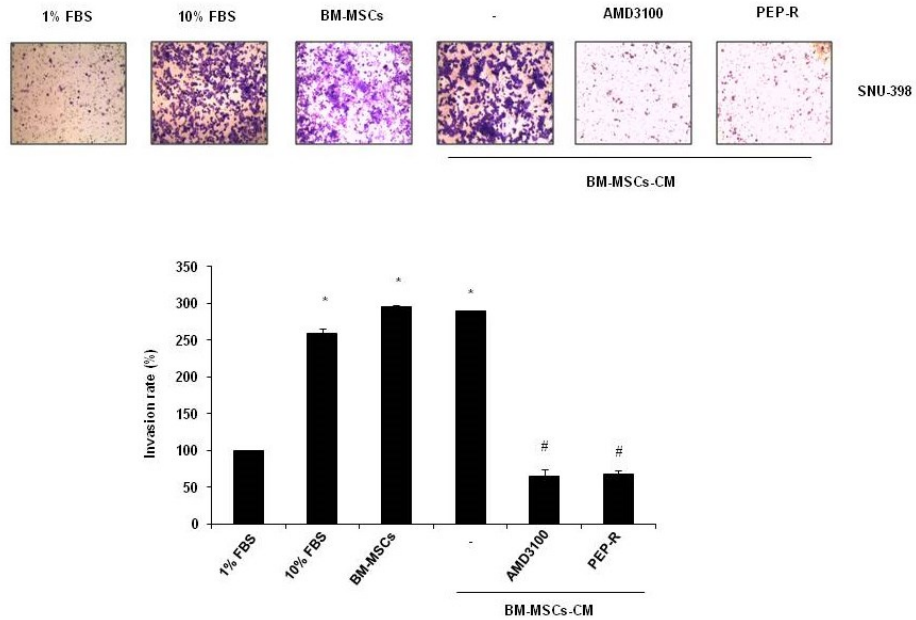
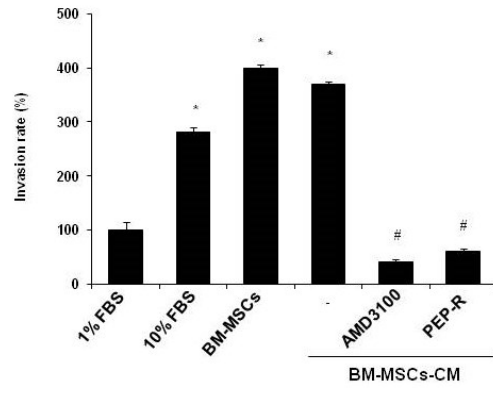
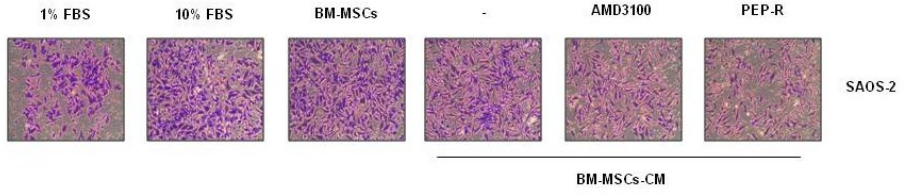


Figure 13. Peptide R prevents BM-MSC-mediated U2OS and SNU-398 tumor cell invasion. Tumor cells were seeded into upper chambers containing 8 μm pore-size filters that were coated with Matrigel basement membrane matrix in the presence or absence of Peptide R (10 μM) or, alternatively, AMD3100 (10 μM). Medium containing 1% FBS or 10% FBS, BM-MSCs or conditioned medium obtained from cultured BM-MSCs (BM-MSC-CM) were added to the lower chamber as a chemoattractant. The invasiveness of U2OS and SNU-398 cells is described in panels **A** and **B**, respectively. All experiments were performed at least three times. * $P < 0.001$ compared to the control (medium with 1% FBS); # $P < 0.001$ compared to BM-MSCs.

A



B

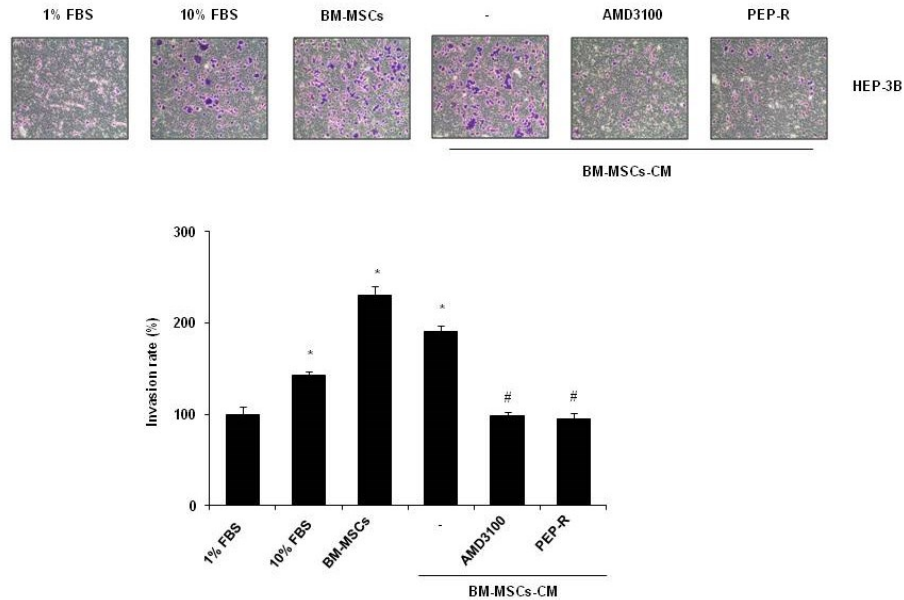


Figure 14. Peptide R prevents BM-MSC-mediated Saos-2 and Hep3B tumor cells invasion. Tumor cells were seeded into upper chambers containing 8 μm pore-size filters that were coated with Matrigel basement membrane matrix in the presence or absence of Peptide R (10 μM) or, alternatively, AMD3100 (10 μM). Medium containing 1% FBS, medium containing 10% FBS, BM-MSCs or BM-MSC-CM were added to the lower chambers as chemoattractants. The invasion of Saos-2 cells and Hep3B cells is shown in panels **A** and **B**, respectively. All experiments were performed at least three times. * $P < 0.001$ compared to the control (medium containing 1% FBS); # $P < 0.001$ compared to BM-MSCs.

4.5 Peptide R prevents BM-MSC-dependent ERK and AKT activation and Epithelial-Mesenchymal Transition in OS and HCC cell lines

To further characterize the involvement of ERK and AKT pathways in OS and HCC migration and invasion induced by BM-MSCs and triggered by CXCR4, I analyzed p-ERK and p-AKT expression after that cells were treated with the CXCR4-specific antagonist Peptide R and AMD3100 used as positive control. As shown in Figure 15, I observed a significant reduction in p-ERK and p-AKT levels when all cell lines, grown in presence of BM-MSC-CM, were treated with Peptide R, as well as, AMD3100. The epithelial–mesenchymal transition (EMT) of tumor cells is widely accepted to be closely correlated with cancer metastasis (Yao et al. 2011). To explore whether

CXCR4 promotes EMT process in OS and HCC cell lines grown in the presence of BM-MSC-CM, I analyzed E-cadherin and vimentin levels after cell treatment with Peptide R and AMD3100. As shown in Figure 16, Peptide R as AMD3100 caused an increase in E-cadherin and a reduction in vimentin levels in cells that were grown in the presence of BM-MSC-CM.

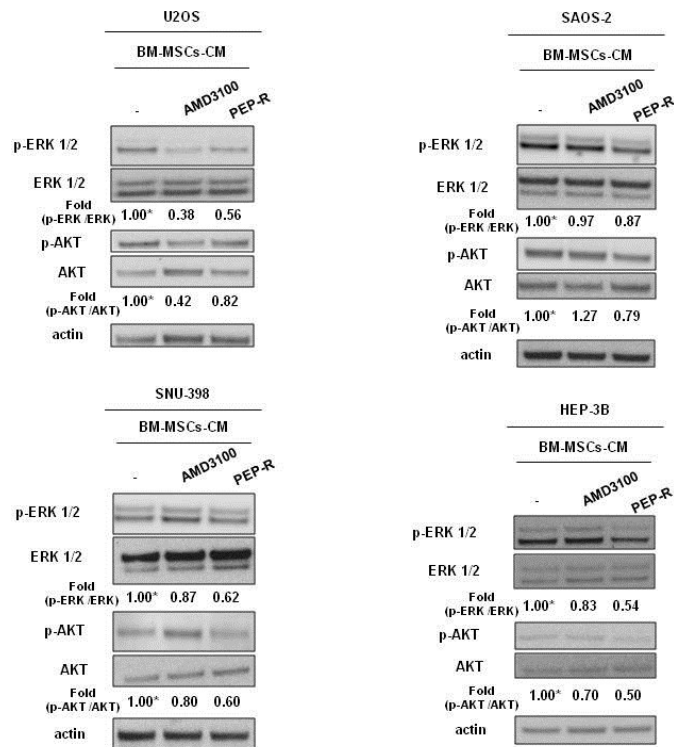


Figure 15. Peptide R prevents BM-MSC-dependent activation of ERK and AKT signaling pathways in OS and HCC cell lines. Tumor cell lines grown in the presence of BM-MSC-CM were treated with Peptide R, using AMD3100 as positive control, for 24h and then analyzed for p-ERK, ERK, p-AKT, and AKT levels. Actin was used as an equal loading control. Values below the blot indicate signal levels relative to controls (BM-MSC-CM), which were arbitrarily set to 1 (labeled with an asterisk). Representative data from one of three experiments are shown.

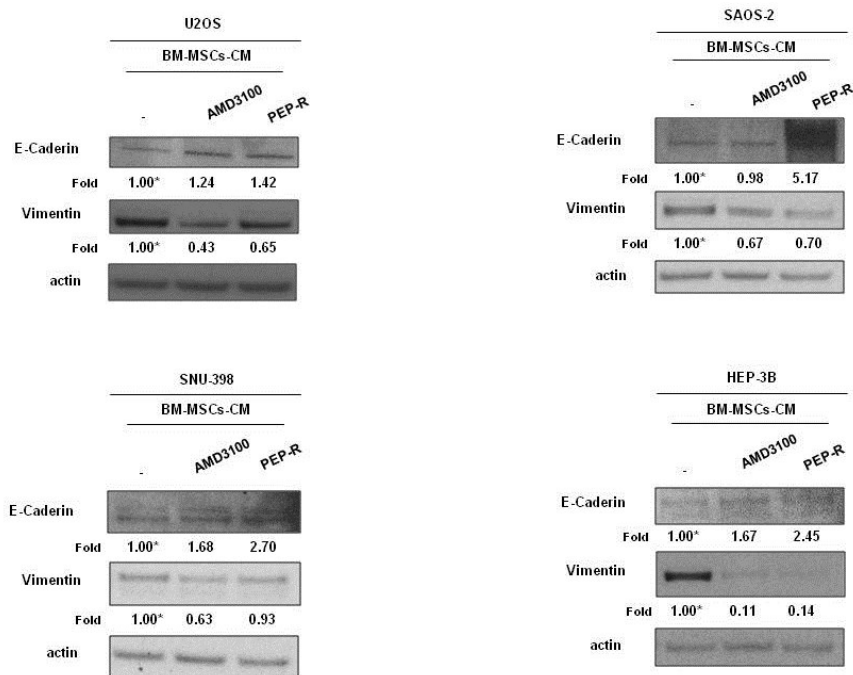


Figure 16. Peptide R prevents BM-MSC-dependent EMT in OS and HCC cell lines. Tumor cell lines grown in the presence BM-MSC-CM were treated with Peptide R, using AMD3100 as positive control, and analyzed for E-cadherin and Vimentin levels. Actin was used as an equal loading control. Values below the blot indicate signal levels relative to controls (BM-MSC-CM), which were arbitrarily set to 1 (labeled with an asterisk). Representative data from one of three experiments are shown.

4.6 BM-MSCs show high levels of PDGFR β mRNA and protein

Firstly, to determine BM-MSC expression of PDGFR β , western blotting and Real Time-PCR analysis were performed using human glioblastoma cells U87MG and human breast cancer cells MCF7 as positive and negative control, respectively. BM-MSCs showed higher levels of PDGFR β protein (**A**) and mRNA (**B**) than U87MG cells used as positive control (Figure 17).

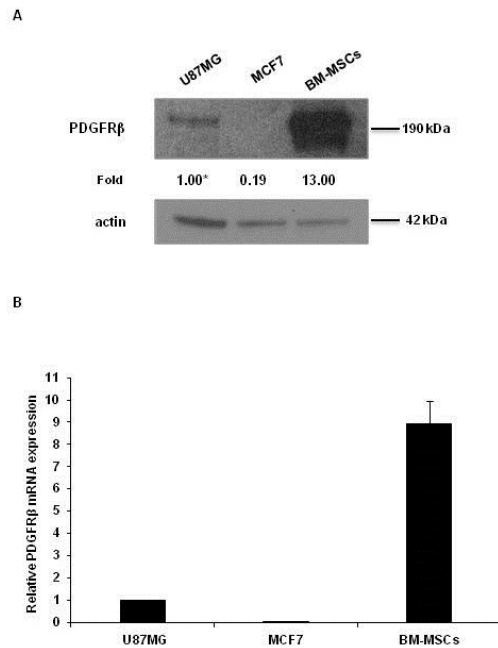


Figure 17. BM-MSCs present high PDGFR β mRNA and protein levels. (A) Western blot analysis of PDGFR β expression in BM-MSCs compared to U87MG and MCF7 cells as positive and negative control, respectively. Equal loading was confirmed by immunoblot with anti-actin antibody. Values below the blots indicate signal levels relative to U87MG cells arbitrarily set to 1 (labeled with asterisk). Representative data from one of three experiments are shown. (B) PDGFR β mRNA levels as detected using Real Time-PCR in BM-MSCs compared to U87MG and MCF7 cells used as positive and negative control, respectively.

4.7 Gint4.T aptamer inhibits PDGFR β -mediated signaling pathway in BM-MSCs

As a next step, I asked whether, because of its binding to PDGFR β , Gint4.T aptamer could interfere with BM-MSC ligand-dependent activation of the receptor and downstream signaling. As shown in Figure 18A, Gint4.T (400 nmol/l) treatment reduced the tyrosine-phosphorylation of PDGFR β induced by PDGF-BB in BM-MSCs. No effect was observed when BM-MSCs were treated with the unrelated sequence used as a negative control. Furthermore, a substantial reduction of PDGF-BB-dependent phosphorylation of ERK1/2 and PKB/AKT kinase was observed in the presence of Gint4.T treatment (Figure 18B).

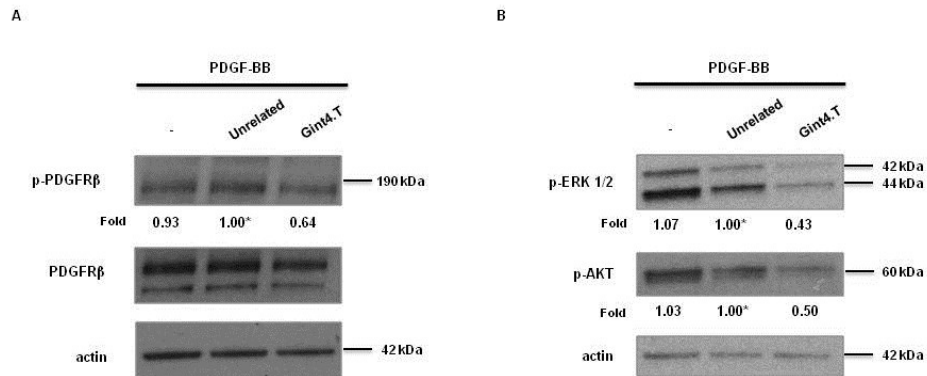


Figure 18. Gint4.T aptamer inhibits PDGF-BB-dependent PDGFR β activation in BM-MSCs. Serum-starved BM-MSCs were stimulated with PDGF-BB in the presence of Gint4.T or the unrelated aptamer (used as a negative control), as indicated. Cell lysates were immunoblotted with (A) anti-p-PDGFR β and anti-PDGFR β , and with (B) anti-p-ERK and anti-p-AKT. Values below the blots indicate signal levels relative to PDGF-BB stimulated cells in the presence of unrelated aptamer, arbitrarily set to 1 (labeled with asterisk). Equal loading was confirmed by immunoblot with anti-actin antibody. Representative data are shown from one of three experiments.

4.8 Gint4.T aptamer inhibits BM-MSC proliferation and migration

Based on the Gint4.T inhibitory potential on the activation of ERK1/2 and the PKB/AKT pathways in BM-MSCs, I investigated whether PDGFR β inhibition by Gint4.T aptamer could affect BM-MSC viability. Cells were treated with Gint4.T or an unrelated aptamer for 72 h and their growth was evaluated by MTS assay. As shown in Figure 19A, Gint4.T aptamer significantly inhibited cell viability of BM-MSCs and its effect was stronger than imatinib, a well known inhibitor of PDGFR β activity (Maass et al. 2014). Remarkably, no cytotoxicity was observed when BM-MSCs were treated with the unrelated aptamer.

Because PDGFR β intracellular pathway has been reported to be involved in BM-MSC tropism for tumor sites (Hata et al. 2010), I determined whether Gint4.T aptamer could affect *in vitro* migration of BM-MSCs. BM-MSCs were seeded into the upper compartment of Boyden chamber, and grown in presence or not of Gint4.T aptamer for 24 h. Medium supplemented with 10% FBS was added into the lower compartment and used as chemoattractant. As shown in Figure 19B, the treatment with Gint4.T aptamer or imatinib strongly reduced BM-MSC migration whereas no effect was observed when cells were treated with an unrelated aptamer.

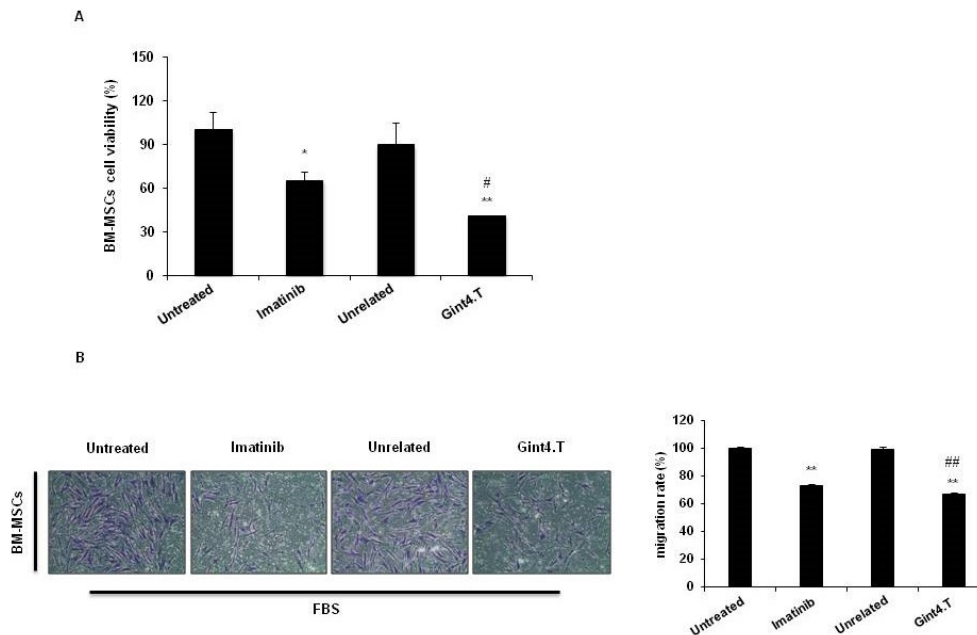


Figure 19. Gint4.T aptamer inhibits BM-MSc proliferation and migration. (A) BM-MSCs were treated for 72 hours with Gint4.T (400 nmol/l), the unrelated aptamer (400 nmol/l) used as a negative control or imatinib (1 μ mol/l) used as positive control. Cell viability is expressed as percent of viable cells and untreated cells are reported as 100%. All experiments were performed at least three times. * $P < 0.01$ imatinib vs untreated; ** $P < 0.001$ Gint4.T vs untreated; ## $P < 0.01$ Gint4.T compared vs unrelated aptamer. (B) Migration of BM-MSCs was analyzed by Boyden chamber in the presence of 400 nmol/l Gint4.T and the unrelated aptamer or 5 μ mol/l imatinib for 24 hours toward 10% FBS as chemoattractant. The migrated cells were stained with crystal violet. Representative photographs of at least three different experiments are shown. The results are expressed as percent of migrated cells respect untreated cells reported as 100%. All experiments were performed at least three times. ** $P < 0.001$ for imatinib and Gint4.T vs untreated; ## $P < 0.001$ for Gint4.T vs unrelated aptamer.

4.9 Gint4.T aptamer prevents BM-MSc migration towards triple negative breast cancer (TNBC) cells

To evaluate the role of PDGFR β in BM-MSc migration towards TNBC cells, BM-MSCs were seeded in presence or not of Gint4.T aptamer into the upper compartment of Boyden chamber whereas two TNBC cell lines (MDA-MB-231 or BT-549), and PDGF-BB were added into lower chamber as chemoattractants. As shown in Figure 20, the treatment of BM-MSCs with Gint4.T aptamer strongly reduced their migration towards MDA-MB-231 cells

(A), BT-549 cells (B) and PDGF-BB (C), whereas no effect was observed after the unrelated aptamer treatment.

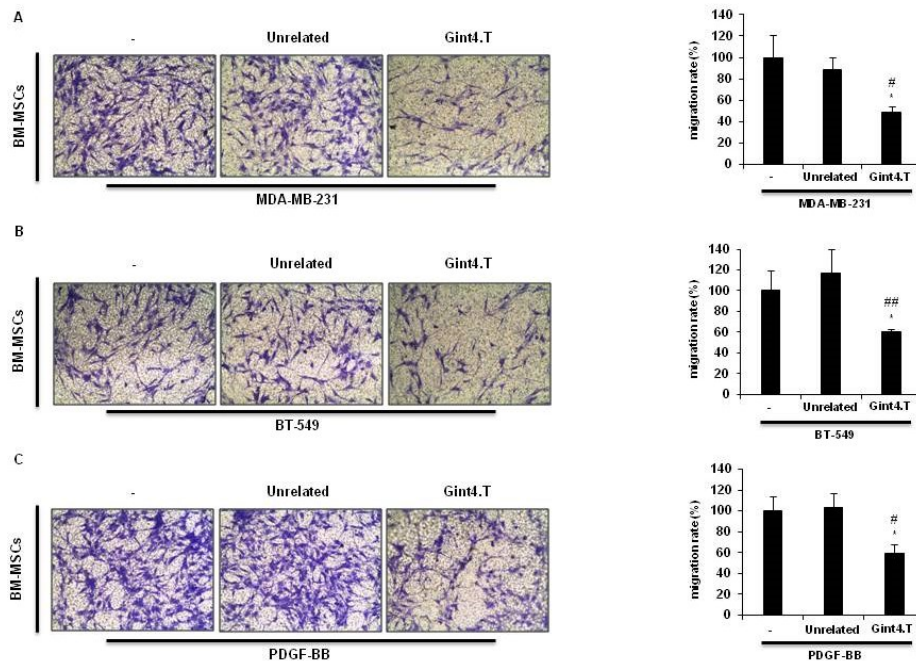


Figure 20. Gint4.T aptamer inhibits BM-MSC migration towards TNBC cells. Migration of BM-MSCs was analyzed by Boyden chamber in the presence of Gint4.T or the unrelated aptamer, used as a negative control, for 24 hours. MDA-MB-231 cells (A), BT-549 cells (B) and PDGFBB (C) were added to the lower chambers. The migrated cells were stained with crystal violet. Representative photographs of at least three different experiments were shown. The results are expressed as percent of migrated cells and untreated cells are reported as 100%. All experiments were performed at least three times. * $P < 0.01$ compared to untreated cells; # $P < 0.01$ compared to the unrelated aptamer; ## $P < 0.001$ compared to the unrelated aptamer.

4.10 *In vivo* tracking of BM-MSC recruitment into TNBC xenograft by Fluorescence Molecular Tomography

To test the ability of BM-MSCs to migrate towards tumors, cells were labeled with VivoTrack 680 Fluorescent Cell Labeling Agent and, then, examined for viability. There was essentially no significant loss of cell viability after incubation with VivoTrack 680. Therefore, these results demonstrated that an incubation time of 30 min with a dye concentration of 0.2 mg/ml was appropriate for stem cell labeling. The labeling efficiency of VivoTrack 680

was more than 99% at this labeling condition as established by flow cytometry (Figure 21).

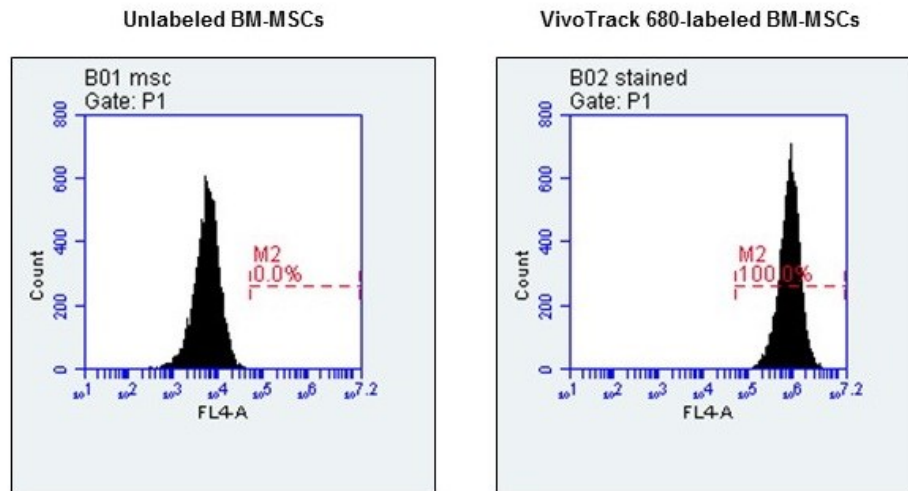


Figure 21. VivoTrack 680 efficiently labels BM-MSCs. BM-MSCs were incubated with VivoTrack 680 for 30 min and the dye uptake was analyzed by flow cytometry. Unlabeled and labeled BM-MSC mean fluorescence intensity is shown.

Because VivoTrack 680 showed superior properties for stem cell labeling, the next aim was to investigate its feasibility for *in vivo* cell imaging and tracking. Nude mice bearing MDA-MB-231 xenografts, that received intravenous injections of 1×10^6 VivoTrack 680-labeled BM-MSCs, were analyzed with Fluorescence Molecular Tomography (FMT) at different time-points. Mice were analyzed in dorsal and lateral views and 3D images were reconstructed. Then, volumes of interest (VOIs) were generated around the tumor. The fluorescence signal of BM-MSCs was visualized in tumor at 3 h post-injection and remained visualized up to 24 and 48 h post-injection (Figure 22A and B). Because VivoTrack 680 emits at NIR wavelength where autofluorescence and tissue absorbance are minimal, a low fluorescence was observed in the tissues around the tumor.

A



B

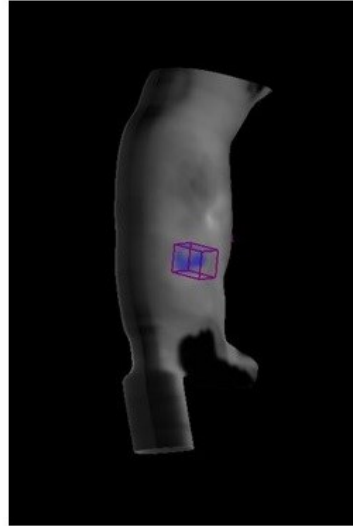


Figure 22. *In vivo* imaging of VivoTrack 680-labeled BM-MSCs in Triple Negative breast cancer by Fluorescence Molecular Tomography. (A) Whole body lateral view of nude mouse bearing MDA-MB-231 xenograft (arrow) **(B)** Representative 3D image of tumor 3 h after intravenous injection of VivoTrack 680-labeled BM-MSCs. The fluorescence signal was specifically detected in the tumor.

5. DISCUSSION

Since the tumor microenvironment contributes to many aspects of carcinogenesis and cancer progression, the different stromal cell types which play key roles in determining or enhancing several hallmark capabilities in different TMEs, should be taken into account to stimulate future anticancer drug development. In particular, the recent discovery that mesenchymal stem cells (MSCs) can be recruited into tumor microenvironment and promote cancer progression has led to consider MSCs as a suitable target for an anti-cancer therapy. In fact, great interest has been shown in developing therapeutic targeting strategies aimed to inhibit MSC support thus improving therapeutic efficacy in treating cancer (Shangguan et al. 2012, Shinagawa et al. 2013).

In this study, I test two innovative therapeutic tools that, by targeting specific signaling pathways, prevent bone marrow-derived mesenchymal stem cells (BM-MSC) recruitment and activity into tumor microenvironment.

Over last years, several studies have demonstrated that the effects of MSCs on tumor cells are numerous and controversial, which make the analysis of their role in cancer progression more complex. An increasing number of evidence has shown that MSCs can be recruited into primary tumors and become active components of the tumor microenvironment, including cancer-associated fibroblasts (CAFs) (Bergfeld and DeClerck 2010, Jung et al. 2013). Importantly, tumor associated-MSCs contribute to tumor cell growth and metastatic behavior in a variety of cancers, including breast (Chaturvedi et al. 2013, Karnoub et al. 2007, Zhang et al. 2013), prostate (Jung et al. 2013, Luo et al. 2014, Zhang et al. 2013), osteosarcoma (Tu et al. 2012, Yu et al. 2015), and colon (Hogan et al. 2013, Liu et al. 2011, Shinagawa et al. 2013) cancers. In contrast, recent evidence showed that MSCs inhibit tumor progression. In glioblastoma multiforme (GBM), for example, MSCs seem to reduce tumor growth by inhibiting angiogenesis (Ho et al. 2013). Thus, in this scenario, the starting point for MSC targeted therapy is the identification of specific molecular pathways involved in pro-tumorigenic cross-talk between MSCs and cancer cells.

In osteosarcoma (OS) several molecular pathways involved in MSC-mediated tumor progression were identified, including Interleukin-6/ Signal transducer and activator of transcription 3 (IL6/STAT3) (Tu et al. 2012), Chemokine (C-C motif) ligand 5 (CCL5) (Xu et al. 2009) and CXCR4/VEGF (Yu et al. 2015). For hepatocellular carcinoma (HCC), few studies have reported on the molecular mechanisms underlying the crosstalk between MSCs and HCC cells. Recently, Li et al. (2015) have showed that conditioned medium from rat BM-MSCs enhance migration of a rat hepatoma cell line (CBRH-7919) by up-regulating CXCR4. All these reports have demonstrated that in both, OS and HCC, the interaction between MSCs and cancer cells through specific signal pathways, promotes cell proliferation and migration/invasion *in vitro*, as well as tumor growth and metastasis development *in vivo*.

The delineation of key molecular pathways, that underlie the interactions between cancer and stroma cells, has improved the knowledge of the biology of tumor microenvironment, tumor spreading, and carcinogenesis. The complexities of cell-cell communication and the opportunities for modulation provide new possibility for cancer treatments. However, the understanding of the dynamic regulation of relationships between cells in the tumor microenvironment is still unclear. During tumor progression, cancer cells and the surrounding microenvironment constantly communicate each other through a biochemical and/or a biophysical signal. In this regard, paracrine molecules secreted by MSCs can act as ligands for receptors that are expressed on tumor cells, thereby inducing the activation of the PI3K/AKT and Ras/ERK pathways, which are involved in tumor cell progression (Huang et al. 2013). Consistent with these studies, I found that conditioned medium obtained from BM-MSCs causes parallel increases in OS and HCC cell growth and p-AKT/p-ERK levels, suggesting the activation of the PI3K/AKT as well as the Ras/ERK intracellular cascades.

Emerging evidence has shown that BM-MSCs may accelerate human breast tumor growth and metastasis by regulating the cancer stem cell population through a microenvironmental network of cytokines and growth factors (Liu et al. 2011). In addition, it was reported that MSCs are recruited into prostate tumors through CXCL16 and that they are then converted in to CAFs. In turn, CAFs secrete CXCL12, which binds to CXCR4 on tumor cells to induce EMT, which ultimately promotes metastasis to secondary tumor sites (Jung et al. 2013). Thus, the CXCR4/CXCL12 axis results important for MSCs to promote cancer cells capacity to migration and invasion, making this pathway an important potential target for cancer therapeutics. In this study, when OS and HCC cells were treated with conditioned medium obtained from BM-MSCs an increase of mRNA and protein levels of CXCR4 was observed, suggesting that the cross-talk between BM-MSCs and tumor cells involved the CXCR4/CXCL12 axis.

Recently, in order to overcome the toxicity of the well-known CXCR4 antagonist AMD3100, Portella et al. (2013) developed a novel CXCR4 antagonist suitable for anticancer therapy, Peptide R. In fact, although AMD3100 (known as Plerixafor) represents the most effective CXCR4 therapeutic targeting, it has evoked some concerns regarding its cardiotoxicity and it is, therefore, not an ideal anticancer agent (Hendrix et al. 2004). Thus, in order to develop new CXCR4 antagonists suitable for anticancer therapy, the short structural motifs in the ligand receptor-binding region of CXCL12 was analyzed and, based on this scaffold, were designed short CXCR4-ligand peptides. Importantly, the entire peptide library was first evaluated for cytotoxicity on several human cancer cell lines and showed no toxicity. Subsequently, CXCR4 developed peptides were tested for their capability to bind CXCR4 and antagonize its activity, and Peptide R especially revealed the best efficacy both in *in vitro* and *in vivo* analysis on animal tumor models.

Here, for the first time it has been shown that Peptide R inhibits OS and HCC cells migration and invasion in response to BM-MSCs. In addition, to elucidate the mechanism underlying Peptide R activity, I have analyzed the role of PI3K/AKT and Ras/ERK pathways. I have demonstrated that Peptide R prevents BM-MSC-dependent phosphorylation of ERK and AKT, thus inhibiting these signaling pathways in OS and HCC cell lines.

Furthermore, I have investigated the role of BM-MSCs in another important mechanism involved in tumor progression, Epithelial-Mesenchymal Transition (EMT) process. EMT consists in the transition of tumor cells from epithelial to mesenchymal phenotype due to paracrine molecules produced by stromal cells of tumor microenvironment (Giannoni et al. 2012). This mesenchymal phenotype is associated with an increase of cellular motility and invasion that in turn enhances tumor malignancy. Here, I have demonstrated that Peptide R, targeting and inhibiting CXCR4, prevents EMT of OS and HCC cells promoted by BM-MSCs. Indeed, I have observed an increase of E-cadherin, epithelial marker, and a decrease of vimentin (mesenchymal marker) levels in tumor cells exposed to conditioned medium from BM-MSCs and treated with Peptide R.

Thus, in this study for the first time, it has been assessed the possibility to use a novel CXCR4 inhibitor, Peptide R, as therapeutic agent to prevent the cancer progression and spreading that is regulated by cross-talk between BM-MSCs and tumor cells.

Given the importance to identify mechanisms that underlie the recruitment of MSCs into tumor microenvironment, in this study, I have also analyzed one of the most important signaling pathway involved in the bidirectional communication between cancer cells and MSCs, the PDGFR β pathway.

Over past years, several studies have shown that MSCs express high levels of PDGFR β (Ng et al. 2008, Spitzer et al. 2012), suggesting that it could play a crucial role in processes in which MSCs are involved. In fact, it is widely reported that PDGFR β is implicated in specifying MSC commitment to mesenchymal lineages (Ng et al. 2008) as well as in MSC proliferation and self-renewal (Gharibi et al. 2012).

Furthermore, PDGFR β signaling has emerged as a predominant pathway in recruitment of MSCs towards tumor sites (Veevers-Lowe et al. 2011). Hata et al. (2010), for example, have demonstrated that PDGFR β was involved in MSC tropism for malignant gliomas, providing direct evidence that tumor was capable of attracting MSCs in an *in vivo* intracranial glioma model through PDGFR β pathway. In addition, due to MSC capability to suppress tumor growth in glioma (Ho et al. 2013, Nakamizo et al. 2005), Hata et al. suggested the possibility to exploit their findings for advancing MSC glioma treatment. In contrast with positive effects provided by MSCs in glioma, several studies have reported that PDGFR β -mediated MSC recruitment into tumor microenvironment, contributed to enhance the aggressive and invasive properties of many types of tumor, including chronic lymphocytic leukemia (CLL) (Ding et al. 2010), pancreatic (Beckermann et al. 2008) and colon (Shinagawa et al. 2013) carcinomas.

However, although PDGFR β inhibitors have already been tested for their capability to target and interfere with receptor activity in MSCs (Ball et al. 2012, Gharibi et al. 2012, Hata et al. 2010), no studies have still demonstrated the possibility to target PDGFR β to prevent pro-tumorigenic effect of MSCs into tumor microenvironment. Moreover, the current class of PDGFR β drugs consist of small molecule TKIs that show limited specificity and modest efficacy whereas no antibodies have entered the clinic. To give more effective alternative to currently used PDGFR β inhibitors, recently, Camorani et al. (2014) have developed a new 33 mer nuclease-stabilized RNA aptamer suitable for anticancer therapy, named Gint4.T. Aptamers respond to many requirements because they can discriminate among thousand proteins and do so in a short time. They can distinguish between small proteins that are otherwise relatively similar in structure, a necessary property if proteins are differentiated on the cell surface.

Here, for the first time, I have tested an innovative aptamer-based therapeutic tool to interfere with PDGFR β -dependent BM-MSc recruitment into breast cancer microenvironment.

Accordingly with the involvement of PDGFR β in MSC proliferation and migration (Gharibi et al. 2012, Veevers-Lowe et al. 2011), I have showed that Gint4.T significantly inhibits *in vitro* BM-MSc cell migration and blocks cell proliferation. To elucidate the mechanism underlying Gint4.T aptamer activity, I have investigated the role of PDGFR β downstream pathways. I have found that the binding of the Gint4.T to PDGFR β prevents ligand-dependent phosphorylation of the receptor and the consequent activation of ERK1/2 and AKT signaling.

Recent evidence has widely shown that BM-MScs can integrate into the tumor-associated stroma and promote the progression of triple negative breast cancer (TNBC) through the activation of different mechanisms involving HIFs (Chaturvedi et al. 2013), TGF- β (McAndrews et al. 2015) and interleukin-1 beta (IL-1 β) (Escobar et al. 2015).

Up to now, no work has demonstrated the involvement of PDGFR β pathway in MSC recruitment toward TNBC microenvironment, as well as MSC-mediated TNBC progression. In this study I have showed that Gint4.T aptamer, inhibiting PDGFR β , strongly reduces BM-MSc migration stimulated by two different TNBC cell lines, MDA-MB-231 and BT-549, as well as by PDGFBB ligand. This result underlines the importance of PDGFR β in mediating MSC migration towards TNBC cells and highlights Gint4.T aptamer to specifically prevent PDGFR β -mediated MSC tropism for tumor microenvironment.

These data demonstrated that Gint4.T aptamer not only hampers PDGFR β phosphorylation and downstream signaling in BM-MScs, but it also interferes with recruitment of BM-MScs in breast cancer microenvironment.

Thus, for the first time, it has been assessed the possibility to use a novel aptamer-based PDGFR β inhibitor as therapeutic agent to prevent BM-MSc recruitment and eventually interfere with their pro-tumorigenic activity within tumor microenvironment.

6. CONCLUSIONS

Knowing that BM-MSCs have a key role in promoting cancer progression, in my thesis I have investigated the possible pathways underlying their recruitment and their pro-tumorigenic activity within tumor microenvironment. I demonstrated that CXCR4 is involved in tumor BM-MSC-mediated osteosarcoma and hepatocellular carcinoma invasion, whereas PDGFR β plays a key role in BM-MSC migration towards triple negative breast cancer cells, a well-known aggressive phenotype of breast cancer.

After establishing the involvement of CXCR4 and PDGFR β signaling pathways in the cross-talk between BM-MSCs and tumor cells, I validated the possibility to interfere with them by using two novel therapeutic tools, Peptide R and Gint4.T aptamer, respectively.

In conclusion, this study provides insight into BM-MSC interactions with aggressive cancer cells and identifies potential therapeutic targets. Furthermore, for the first time innovative therapeutic tools targeting BM-MSCs and preventing their recruitment and activity are developed and validated.

ACKNOWLEDGEMENTS

If any value is to be recognized to this work, much of it is due to the endless support that I received from many people.

I would greatly to thank my supervisor Dr. Antonella Zannetti for the opportunity of this Ph.D, for her help during these years solving many problems and making me more confident in science. I am very grateful to her because she has helped me to coordinate my project especially in writing this dissertation.

Dr. Laura Cerchia and Simona Camorani for the helpfulness, scientific advices and for continuous collaboration.

Dr. Vittorio de Franciscis because he has suggested me to start this experience and then he has supported and motivated me during my first year of this Ph.D.

All my lab friends and in particular Simona, Martina e Tiziano for helping me with experiments and especially for sharing several funny moments.

Dr. de Franciscis and Prof. Condorelli's labs, starting from Dr. Carla L. Esposito for her help in scientific experiments and thanks everybody for their friendship having spent so much time together.

My sincere thanks also goes to IBB researchers who provided me an opportunity to feel a part of their team, and who gave access to the laboratory and research facilities.

Thanks to the Department of Molecular Medicine and Medical Biotechnology. It has provided the support and equipment I have needed to produce and complete my dissertation.

Many friends have helped me stay sane through these difficult years.

My greatest gratitude goes to Gennaro D'Oriano, Anna Rienzo, Maria Rosaria Mollo, Imma Fichera, Sonia Autorino e Anna Sirico.

Anna Musto, you are simply my best friend.

Special thanks goes to Margherita Iaboni for sharing my difficulties during these years supporting me. She has been patient with me and has trusted me all along this experience. Thanks for her guidance, advices and encouragement in

each single minute of my Ph.D. Without her precious support none of this would have been possible.

Most importantly, I would especially thank my parents and my beautiful family for their love, patience and unconditional support throughout my life and my studies. I don't have enough words to show my gratitude all days of my life.

REFERENCES

- Aigner K, Dampier B, Descovich L, Mikula M, Sultan A, Schreiber M, Mikulits W, Brabletz T, Strand D, Obrist P, Sommergruber W, Schweifer N, Wernitznig A, Beug H, Foisner R, Eger A. The transcription factor ZEB1 (deltaEF1) promotes tumour cell dedifferentiation by repressing master regulators of epithelial polarity. *Oncogene* 2007;26(49):6979-88.
- Akhmetshina A, Venalis P, Dees C, Busch N, Zwerina J, Schett G, Distler O, Distler JH. Treatment with imatinib prevents fibrosis in different preclinical models of systemic sclerosis and induces regression of established fibrosis. *Arthritis Rheum.* 2009;60(1):219-24.
- Amodeo P, Vitale RM, De Luca S, Scala S, Castello G, Siani A. (2010). Cyclic peptides binding CXCR4 receptor and relative medical and diagnostic uses. Italian patent: no. MI2010A 000093; international patent nu WO2011/092575 A.
- Balkwill F. Cancer and the chemokine network. *Nat Rev Cancer.* 2004 Jul;4(7):540-50.
- Ball SG, Shuttleworth A, Kielty CM. Inhibition of platelet-derived growth factor receptor signaling regulates Oct4 and Nanog expression, cell shape, and mesenchymal stem cell potency. *Stem Cells* 2012;30(3):548-60.
- Banchereau J, Steinman RM. Dendritic cells and the control of immunity. *Nature* 1998;392(6673):245–252.
- Barcellos-de-Souza P, Gori V, Bambi F, Chiarugi P. Tumor microenvironment: bone marrow-mesenchymal stem cells as key players. *Biochim. Biophys. Acta* 2013;1836(2):321–335.
- Beckermann BM, Kallifatidis G, Groth A, Frommhold D, Apel A, Mattern J, Salnikov AV, Moldenhauer G, Wagner W, Diehlmann A, Saffrich R, Schubert M, Ho AD, Giese N, Büchler MW, Friess H, Büchler P, I Herr. VEGF expression by mesenchymal stem cells contributes to angiogenesis in pancreatic carcinoma. *Br J Cancer* 2008;99(4):622-31.

Bergfeld SA, and DeClerck YA. Bone marrow-derived mesenchymal stem cells and the tumor microenvironment. *Cancer Metastasis Rev.* 2010;29, 249–261.

Biswas SK, Mantovani A. Macrophage plasticity and interaction with lymphocyte subsets: cancer as a paradigm. *Nature Immunology* 2010;11(10):889–896.

Brennen WN, Rosen DM, Wang H, Isaacs JT, Denmeade SR. Targeting carcinoma-associated fibroblasts within the tumor stroma with a fibroblast activation protein-activated prodrug. *J Natl Cancer Inst.* 2012;104:1320–34.

Burr SP, Dazzi F, Garden OA. Mesenchymal stromal cells and regulatory T cells: the Yin and Yang of peripheral tolerance? *Immunol Cell Biol.* 2013;91(1):12-8.

Camorani S, Esposito CL, Rienzo A, Catuogno S, Iaboni M, Condorelli G, de Franciscis V, Cerchia L. Inhibition of receptor signaling and of glioblastoma-derived tumor growth by a novel PDGFR β aptamer. *Mol Ther.* 2014;22(4):828-41.

Cannito S, Novo E, di Bonzo LV, Busletta C, Colombatto S, Parola M. Epithelial-mesenchymal transition: from molecular mechanisms, redox regulation to implications in human health and disease. *Antioxid. Redox. Signal.* 2010;12(12):1383-430.

Cao R, Björndahl MA, Religa P, Clasper S, Garvin S, Galter D, Meister B, Ikomi F, Tritsarlis K, Dissing S, Ohhashi T, Jackson DG, Cao Y. PDGF-BB induces intratumoral lymphangiogenesis and promotes lymphatic metastasis. *Cancer Cell* 2004;6(4):333-45.

Cariati M, Purushotham AD. Stem cells and breast cancer. *Histopathology* 2008 ;52(1):99-107.

Cerchia L, De Franciscis V. Noncoding RNAs in cancer medicine. *J Biomed Biotechnol.* 2006;2006(4):73104.

Chatterjee S, Behnam Azad B, Nimmagadda S. The intricate role of CXCR4 in cancer. *Adv Cancer Res.* 2014;124:31-82.

Chaturvedi P, Gilkes DM, Wong CC, Kshitiz W, Luo W, Zhang H, Wei H, Takano N, Schito L, Levchenko A, Semenza GL. Hypoxia-inducible factor-dependent breast cancer-mesenchymal stem cell bidirectional signaling promotes metastasis. *J. Clin. Invest.* 2013; 123(1):189–205.

Coussens LM, Zitvogel L, Palucka AK. Neutralizing tumor-promoting chronic inflammation: a magic bullet? *Science*. 2013;339(6117):286–291.

Cristofanilli M, Morandi P, Krishnamurthy S, Reuben JM, Lee BN, Francis D, Booser DJ, Green MC, Arun BK, Puzstai L, Lopez A, Islam R, Valero V, Hortobagyi GN. Imatinib mesylate (Gleevec) in advanced breast cancer-expressing C-Kit or PDGFR-beta: clinical activity and biological correlations. *Ann Oncol*. 2008;19(10):1713-9.

Dagher R, Cohen M, Williams G, Rothmann M, Gobburu J, Robbie G, Rahman A, Chen G, Staten A, Griebel D, Pazdur R. Approval summary: imatinib mesylate in the treatment of metastatic and/or unresectable malignant gastrointestinal stromal tumors. *Clin Cancer Res*. 2002;8(10):3034-8.

Dancey JE, Chen HX. Strategies for optimizing combinations of molecularly targeted anticancer agents. *Nat Rev Drug Discov*. 2006;5(8):649-59.

Ding W, Knox TR, Tschumper RC, Wu W, Schwager SM, Boysen JC, Jelinek DF, Kay NE. Platelet-derived growth factor (PDGF)-PDGF receptor interaction activates bone marrow-derived mesenchymal stromal cells derived from chronic lymphocytic leukemia: implications for an angiogenic switch. *Blood* 2010;116(16):2984-93.

Druker BJ, Talpaz M, Resta DJ, Peng B, Buchdunger E, Ford JM, Lydon NB, Kantarjian H, Capdeville R, Ohno-Jones S, Sawyers CL. Efficacy and safety of a specific inhibitor of the BCR-ABL tyrosine kinase in chronic myeloid leukemia. *N Engl J Med*. 2001;344(14):1031-7.

De Clercq E. The AMD3100 story: the path to the discovery of a stem cell mobilizer (Mozobil). *Biochem. Pharmacol*. 2009;77(11):1655–64.

de Visser KE, Korets LV, Coussens LM. De novo carcinogenesis promoted by chronic inflammation is B lymphocyte dependent. *Cancer Cell* 2005;7(5):411–423.

Dimou A, Syrigos KN, Saif MW. Overcoming the stromal barrier: Technologies to optimize drug delivery in pancreatic cancer. *Ther. Adv. Med. Oncol*. 2012;4(5):271-9.

Dominici M, Le Blanc K, Mueller I, Slaper-Cortenbach I, Marini F, Krause D, Deans R, Keating A, Prockop D, Horwitz E. Minimal criteria

for defining multipotent mesenchymal stromal cells. The International Society for Cellular Therapy position statement. *Cytotherapy* 2006;315–317.

Dua P, Kim S, Lee DK. Nucleic acid aptamers targeting cell-surface proteins. *Methods* 2011;54(2):215-25.

Ellington AD, Szostak JW. In vitro selection of RNA molecules that bind specific ligands. *Nature*. 1990;346(6287):818-22.

Escobar P, Bouclier C, Serret J, Bièche I, Brigitte M, Caicedo A, Sanchez E, Vacher S, Vignais ML, Bourin P, Geneviève D, Molina F, Jorgensen C, Lazennec G. IL-1 β produced by aggressive breast cancer cells is one of the factors that dictate their interactions with mesenchymal stem cells through chemokine production. *Oncotarget* 2015;6(30):29034-47.

Esposito CL, Passaro D, Longobardo I, Condorelli G, Marotta P, Affuso A, de Franciscis V, Cerchia L. A neutralizing RNA aptamer against EGFR causes selective apoptotic cell death. *PLoS One* 2011; 6(9):e24071.

Ferrari SM, Politti U, Spisni R, Materazzi G, Baldini E, Ulisse S, Miccoli P, Antonelli A, Fallahi P. Sorafenib in the treatment of thyroid cancer. *Expert Rev Anticancer Ther*. 2015;15(8):863-74.

Fratto ME, Imperatori M, Vincenzi B, Tomao F, Santini D, Tonini G. New perspectives: role of Sunitinib in breast cancer. *Clin Ter*. 2011;162(3):251-7.

Fredriksson, L, Li H and Eriksson U. The PDGF family: four gene products form five dimeric isoforms. *Cytokine Growth Factor Rev*. 2004;15:197–204.

Fridman WH, Pages F, Sautes-Fridman C, Galon J. The immune contexture in human tumours: impact on clinical outcome. *Nature Reviews: Cancer*. 2012;12(4):298–306.

Gharibi B, Ghuman MS, Hughes FJ. Akt- and Erk-mediated regulation of proliferation and differentiation during PDGFR β -induced MSC self-renewal. *J Cell Mol Med*. 2012;16(11):2789-801.

Giaccia AJ, Schipani E. Role of carcinoma-associated fibroblasts and hypoxia in tumor progression. *Curr Top Microbiol Immunol*. 2010;345:31-45.

Giannoni E, Parri M, Chiarugi P. EMT and oxidative stress: a bidirectional interplay affecting tumor malignancy. *Antioxid. Redox. Signal.* 2012;16(11):1248-63.

Gilbertson RJ, Clifford SC. PDGFRB is overexpressed in metastatic medulloblastoma. *Nat Genet.* 2003;35(3):197-8.

Guida T, Anaganti S, Provitera L, Gedrich R, Sullivan E, Wilhelm SM, Santoro M, Carlomagno F. Sorafenib inhibits imatinib-resistant KIT and platelet-derived growth factor receptor beta gatekeeper mutants. *Clin Cancer Res.* 2007;13(11):3363-9.

Hanahan D, Coussens LM. Accessories to the crime: functions of cells recruited to the tumor microenvironment. *Cancer Cell* 2012;21(3):309-22.

Hata N, Shinojima N, Gumin J, Yong R, Marini F, Andreeff M, Lang FF. Platelet-derived growth factor BB mediates the tropism of human mesenchymal stem cells for malignant gliomas. *Neurosurgery* 2010;66(1):144-56.

Hendrix CW, Collier AC, Lederman MM, Schols D, Pollard RB, Brown S, Jackson JB, Coombs RW, Glesby MJ, Flexner CW, Bridger GJ, Badel K, MacFarland RT, Henson GW, Calandra G; AMD3100 HIV Study Group. Safety, pharmacokinetics, and antiviral activity of AMD3100, a selective CXCR4 receptor inhibitor, in HIV-1 infection. *J Acquir Immune Defic Syndr.* 2004;37(2):1253-62.

Hermann T, Patel DJ. Adaptive recognition by nucleic acid aptamers. *Science* 2000;287(5454):820-5.

Hernandez-Gea V, Toffanin S, Friedman SL, Llovet JM. Role of the microenvironment in the pathogenesis and treatment of hepatocellular carcinoma. *Gastroenterology* 2013;144(3):512-27.

Ho IA, Toh HC, Ng WH, Teo YL, Guo CM, Hui KM, Lam PY. Human bone marrow-derived mesenchymal stem cells suppress human glioma growth through inhibition of angiogenesis. *Stem Cells* 2013;31(1):146-55.

Hogan NM, Joyce MR, Murphy JM, Barry FP, O'Brien T, Kerin MJ, Dwyer RM. Impact of mesenchymal stem cell secreted PAI-1 on colon cancer cell migration and proliferation. *Biochem Biophys Res Commun.* 2013;435(4):574-9.

Hsu WT, Jui HY, Huang YH, Su MY, Wu YW, Tseng WY, Hsu MC, Chiang BL, Wu KK, Lee CM. CXCR4 Antagonist TG-0054 Mobilizes Mesenchymal Stem Cells, Attenuates Inflammation, and Preserves Cardiac Systolic Function in a Porcine Model of Myocardial Infarction. *Cell Transplant*. 2015;24(7):1313-28.

Huang WH, Chang MC, Tsai KS, Hung MC, Chen HL, Hung SC. Mesenchymal stem cells promote growth and angiogenesis of tumors in mice. *Oncogene* 2013;32(37):4343-54.

Hudis CA, Gianni L. Triple-negative breast cancer: an unmet medical need. *Oncologist* 2011;16 Suppl 1:1-11.

Jung Y, Kim JK, Shiozawa Y, Wang J, Mishra A, Joseph J, Berry JE, McGee S, Lee E, Sun H, Wang J, Jin T, Zhang H, Dai J, Krebsbach PH, Keller ET, Pienta KJ, Taichman RS. Recruitment of mesenchymal stem cells into prostate tumours promotes metastasis. *Nat Commun*. 2013;4:1795.

Karnoub AE, Dash AB, Vo AP, Sullivan A, Brooks MW, Bell GW, Richardson AL, Polyak K, Tubo R, Weinberg RA. Mesenchymal stem cells within tumour stroma promote breast cancer metastasis. *Nature*. 2007;449(7162):557-63.

Katz B, Goldbaum M. Macugen (pegaptanib sodium), a novel ocular therapeutic that targets vascular endothelial growth factor (VEGF). *Int Ophthalmol Clin*. 2006;46(4):141-54.

Keating GM, Santoro A. Sorafenib: a review of its use in advanced hepatocellular carcinoma. *Drugs* 2009;69(2):223-40.

Keefe AD, Cload ST. SELEX with modified nucleotides. *Curr Opin Chem Biol*. 2008;12(4):448-56.

Kilic T, Alberta JA, Zdunek PR, Acar M, Iannarelli P, O'Reilly T, Buchdunger E, Black PM, Stiles CD. Intracranial inhibition of platelet-derived growth factor-mediated glioblastoma cell growth by an orally active kinase inhibitor of the 2-phenylaminopyrimidine class. *Cancer Res* 2000;60(18):5143-50.

Kim Y, Lin Q, Glazer PM, Yun Z. Hypoxic tumor microenvironment and cancer cell differentiation. *Curr Mol Med*. 2009;9(4):425-34.

Kleffel S, Schatton T. Tumor dormancy and cancer stem cells: two sides of the same coin? *Adv Exp Med Biol*. 2013;734:145-79.

Kokkinos MI, Wafai R, Wong MK, Newgreen DF, Thompson EW, Waltham M. Vimentin and epithelial-mesenchymal transition in human breast cancer--observations in vitro and in vivo. *Cells Tissues Organs* 2007;185(1-3):191-203.

Korkaya H, Liu S, Wicha MS. Breast cancer stem cells, cytokine networks, and the tumor microenvironment. *J Clin Invest*. 2011;121(10):3804-9.

Li H, Fan X, Houghton J. Tumor microenvironment: the role of the tumor stroma in cancer. *J Cell Biochem*. 2007;101(4):805-15.

Li X, Luo Q, Sun J, Song G. Conditioned medium from mesenchymal stem cells enhances the migration of hepatoma cells through CXCR4 up-regulation and F-actin remodeling. *Biotechnol. Lett*. 2015;37(3):511-21.

Li T, Zhao S, Song B, Wei Z, Lu G, Zhou J, Huo T. Effects of transforming growth factor β -1 infected human bone marrow mesenchymal stem cells on high- and low-metastatic potential hepatocellular carcinoma. *Eur. J. Med. Res*. 2015;20:56.

Lierman E, Lahortiga I, Van Miegroet H, Mentens N, Marynen P, Cools J. The ability of sorafenib to inhibit oncogenic PDGFRbeta and FLT3 mutants and overcome resistance to other small molecule inhibitors. *Haematologica* 2007;92(1):27-34.

Liu S, Ginestier C, Ou SJ, Clouthier SG, Patel SH, Monville F, Korkaya H, Heath A, Dutcher J, Kleer CG, Jung Y, Dontu G, Taichman R, Wicha MS. Breast cancer stem cells are regulated by mesenchymal stem cells through cytokine networks. *Cancer Res*. 2011; 71(2):614-24.

Liu Y, Han ZP, Zhang SS, Jing YY, Bu XX, Wang CY, Sun K, Jiang GC, Zhao X, Li R, Gao L, Zhao QD, Wu MC, Wei LX. Effects of inflammatory factors on mesenchymal stem cells and their role in the promotion of tumor angiogenesis in colon cancer. *J Biol Chem*. 2011;286(28):25007-15.

Loeffler M, Krüger JA, Niethammer AG, Reisfeld RA. Targeting tumor-associated fibroblasts improves cancer chemotherapy by increasing intratumoral drug uptake. *J Clin Invest*. 2006;116(7):1955-62.

Lu Y, Guan GF, Chen J, Hu B, Sun C, Ma Q, Wen YH, Qiu XC, Zhou Y. Aberrant CXCR4 and β -catenin expression in osteosarcoma correlates with patient survival. *Oncol Lett.* 2015;10(4):2123-2129.

Luetke A, Meyers PA, Lewis I, Juergens H. Osteosarcoma treatment - where do we stand? A state of the art review. *Cancer Treat Rev.* 2014;40(4):523-32.

Luo J, Ok Lee S, Liang L, Huang CK, Li L, Wen S, Chang C. Infiltrating bone marrow mesenchymal stem cells increase prostate cancer stem cell population and metastatic ability via secreting cytokines to suppress androgen receptor signaling. *Oncogene* 2014; 33(21) 2768–78.

Luo Y, Zhou H, Krueger J, Kaplan C, Lee SH, Dolman C, Markowitz D, Wu W, Liu C, Reisfeld RA, Xiang R. Targeting tumor-associated macrophages as a novel strategy against breast cancer. *J Clin Invest.* 2006;116(8):2132-2141.

Maass N, Schem C, Bauerschlag DO, Tiemann K, Schaefer FW, Hanson S, Muth M, Baier M, Weigel MT, Wenners AS, Alkatout I, Bauer M, Jonat W, Mundhenke C. Final safety and efficacy analysis of a phase I/II trial with imatinib and vinorelbine for patients with metastatic breast cancer. *Oncology* 2014;87(5):300-10.

Mao Y, Keller ET, Garfield DH, Shen K, Wang J. Stromal cells in tumor microenvironment and breast cancer. *Cancer Metastasis Rev.* 2013;32(1-2):303-15.

Marchese A. Endocytic trafficking of chemokine receptors. *Curr Opin Cell Biol.* 2014;27:72-7.

Mayer IA, Abramson VG, Lehmann BD, Pietenpol JA. New strategies for triple-negative breast cancer--deciphering the heterogeneity. *Clin Cancer Res.* 2014;20(4):782-90.

McAndrews KM, McGrail DJ, Ravikumar N, Dawson MR. Mesenchymal Stem Cells Induce Directional Migration of Invasive Breast Cancer Cells through TGF- β . *Sci Rep.* 2015;5:16941.

Miao Z, Luker KE, Summers BC, Berahovich R, Bhojani MS, Rehemtulla A, Kleer CG, Essner JJ, Nasevicius A, Luker GD, Howard MC, Schall TJ. CXCR7 (RDC1) promotes breast and lung tumor growth in vivo and is expressed on tumor-associated vasculature. *Proc Natl Acad Sci U S A.* 2007;104(40):15735-40.

Mishra PJ, Mishra PJ, Humeniuk R, Medina DJ, Alexe G, Mesirov JP, Ganesan S, Glod JW, Banerjee D. Carcinoma-associated fibroblast-like differentiation of human mesenchymal stem cells. *Cancer Res.* 2008;68:4331–4339.

Murakami T, Kumakura S, Yamazaki T, Tanaka R, Hamatake M, Okuma K, Huang W, Toma J, Komano J, Yanaka M, Tanaka Y, Yamamoto N. The novel CXCR4 antagonist KRH-3955 is an orally bioavailable and extremely potent inhibitor of human immunodeficiency virus type 1 infection: comparative studies with AMD3100. *Antimicrob Agents Chemother.* 2009;53(7):2940-8.

Murdoch C. CXCR4: chemokine receptor extraordinaire. *Immunol Rev.* 2000;177:175-84.

Nakamizo A, Marini F, Amano T, Khan A, Studeny M, Gumin J, Chen J, Hentschel S, Vecil G, Dembinski J, Andreeff M, Lang FF. Human bone marrow-derived mesenchymal stem cells in the treatment of gliomas. *Cancer Res.* 2005;65(8):3307-18.

Ng F, Boucher S, Koh S, Sastry KS, Chase L, Lakshmiathy U, Choong C, Yang Z, Vemuri MC, Rao MS, Tanavde V. PDGF, TGF-beta, and FGF signaling is important for differentiation and growth of mesenchymal stem cells (MSCs): transcriptional profiling can identify markers and signaling pathways important in differentiation of MSCs into adipogenic, chondrogenic, and osteogenic lineages. *Blood* 2008; 112(2):295-307.

Nishida N, Yano H, Nishida T, Kamura T, Kojiro M. Angiogenesis in cancer. *Vasc Health Risk Manag.* 2006;2(3):213-9.

Ogasawara S, Chiba T, Ooka Y, Suzuki E, Kanogawa N, Saito T, Motoyama T, Tawada A, Kanai F, Yokosuka O. Post-progression survival in patients with advanced hepatocellular carcinoma resistant to sorafenib. *Invest New Drugs* 2016; [Epub ahead of print].

Olumi AF, Grossfeld GD, Hayward SW, Carroll PR, Tlsty TD, Cunha GR. Carcinoma-associated fibroblasts direct tumor progression of initiated human prostatic epithelium. *Cancer Res.* 1999;59(19):5002-11.

Orimo A, Gupta PB, Sgroi DC, Arenzana-Seisdedos F, Delaunay T, Naeem R, Carey VJ, Richardson AL, Weinberg RA. Stromal fibroblasts present in invasive human breast carcinomas promote tumor growth and angiogenesis through elevated SDF-1/CXCL12 secretion. *Cell* 2005;121(3):335-48.

Ostman A. A PDGF receptors-mediators of autocrine tumor growth and regulators of tumor vasculature and stroma. *Cytokine Growth Factor Rev.* 2004;15:275–286.

Perissinotto E, Cavalloni G, Leone F, Fonsato V, Mitola S, Grignani G, Surrenti N, Sangiolo D, Bussolino F, Piacibello W, Aglietta M. Involvement of chemokine receptor 4/stromal cell-derived factor 1 system during osteosarcoma tumor progression. *Clin Cancer Res.* 2005;11(2 Pt 1):490-7.

Pierini M, Dozza B, Lucarelli E, Tazzari PL, Ricci F, Remondini D, di Bella C, Giannini S, Donati D. Efficient isolation and enrichment of mesenchymal stem cells from bone marrow. *Cytotherapy* 2012;14(6):686-93.

Pilotte AP. Current management of patients with gastrointestinal stromal tumor receiving the multitargeted tyrosine kinase inhibitor sunitinib. *Curr Med Res Opin.* 2015;31(7):1363-76.

Polyzos A. Activity of SU11248, a multitargeted inhibitor of vascular endothelial growth factor receptor and platelet-derived growth factor receptor, in patients with metastatic renal cell carcinoma and various other solid tumors. *J Steroid Biochem Mol Biol.* 2008;108(3-5):261-6.

Portella L, Vitale R, De Luca S, D'Alterio C, Ieranò C, Napolitano M, Riccio A, Polimeno MN, Monfregola L, Barbieri A, Luciano A, Ciarmiello A, Arra C, Castello G, Amodeo P, Scala S. Preclinical development of a novel class of CXCR4 antagonist impairing solid tumors growth and metastases. *PLoS One.* 2013;8(9):e74548.

Quail DF, Joyce JA. Microenvironmental regulation of tumor progression and metastasis. *Nat. Med.* 2013;19(11):1423–1437.

Rajagopal S, Rajagopal K, Lefkowitz RJ. Teaching old receptors new tricks: biasing seven-transmembrane receptors. *Nat Rev Drug Discov.* 2010;9(5):373-86.

Raza A, Sood GK. Hepatocellular carcinoma review: current treatment, and evidence-based medicine. *World J Gastroenterol.* 2014;20(15):4115-27.

Reya T, Morrison SJ, Clarke MF, Weissman IL. Stem cells, cancer, and cancer stem cells. *Nature* 2001;414(6859):105-11.

Rønnov-Jessen L, Petersen OW. A function for filamentous alpha-smooth muscle actin: retardation of motility in fibroblasts. *J Cell Biol.* 1996;134(1):67-80.

Semenza GL. Cancer-stromal cell interactions mediated by hypoxia-inducible factors promote angiogenesis, lymphangiogenesis, and metastasis. *Oncogene* 2013;32(35):4057-63.

Shangguan L, Ti X, Krause U, Hai B, Zhao Y, Yang Z, Liu F. Inhibition of TGF- β /Smad signaling by BAMBI blocks differentiation of human mesenchymal stem cells to carcinoma-associated fibroblasts and abolishes their protumor effects. *Stem Cells* 2012;30(12):2810-9.

Shen J, Vil MD, Prewett M, Damoci C, Zhang H, Li H, Jimenez X, Deevi DS, Iacolina M, Kayas A, Bassi R, Persaud K, Rohoza-Asandi A, Balderes P, Loizos N, Ludwig DL, Tonra J, Witte L, Zhu Z. Development of a fully human anti-PDGFRbeta antibody that suppresses growth of human tumor xenografts and enhances antitumor activity of an anti-VEGFR2 antibody. *Neoplasia* 2009; 11(6):594-604.

Shinagawa K, Kitadai Y, Tanaka M, Sumida T, Kodama M, Higashi Y, Tanaka S, Yasui W, Chayama K. Mesenchymal stem cells enhance growth and metastasis of colon cancer. *Int. J. Cancer* 2010; 127(10):2323-33.

Shinagawa K, Kitadai Y, Tanaka M, Sumida T, Onoyama M, Ohnishi M, Ohara E, Higashi Y, Tanaka S, Yasui W, Chayama K. Stroma-directed imatinib therapy impairs the tumor-promoting effect of bone marrow-derived mesenchymal stem cells in an orthotopic transplantation model of colon cancer. *Int J Cancer.* 2013;132(4):813-23.

Siegel R, Naishadham D, Jemal A. Cancer statistics, 2012. *CA Cancer J Clin.* 2012;62(1):10-29.

Spiera RF, Gordon JK, Mersten JN, Magro CM, Mehta M, Wildman HF, Kloiber S, Kirou KA, Lyman S, Crow MK. Imatinib mesylate (Gleevec) in the treatment of diffuse cutaneous systemic sclerosis: results of a 1-year, phase IIa, single-arm, open-label clinical trial. *Ann Rheum Dis.* 2011;70(6):1003-9.

Spitzer TL, Rojas A, Zelenko Z, Aghajanova L, Erikson DW, Barragan F, Meyer M, Tamareisis JS, Hamilton AE, Irwin JC, Giudice LC. Perivascular human endometrial mesenchymal stem cells express

pathways relevant to self-renewal, lineage specification, and functional phenotype. *Biol Reprod.* 2012;86(2):58.

Suzuki K, Sun R, Origuchi M, Kanehira M, Takahata T, Itoh J, Umezawa A, Kijima H, Fukuda S, Saijo Y. Mesenchymal stromal cells promote tumor growth through the enhancement of neovascularization, *Mol. Med.* 2011; 17(7-8):579–87.

Talmadge JE, Gabrilovich DI. History of myeloid-derived suppressor cells. *Nature Reviews: Cancer* 2013;13(10):739–752.

Teicher BA, Fricker SP. CXCL12 (SDF-1)/CXCR4 pathway in cancer. *Clin Cancer Res.* 2010;16(11):2927-31.

Thiery JP, Acloque H, Huang RY, Nieto MA. Epithelial-mesenchymal transitions in development and disease. *Cell* 2009;139(5):871-90.

Tu B, Du L, Fan QM, Tang Z, Tang TT. STAT3 activation by IL-6 from mesenchymal stem cells promotes the proliferation and metastasis of osteosarcoma. *Cancer Lett.* 2012 1;325(1):80-8.

Veevers-Lowe J, Ball SG, Shuttleworth A, Kielty CM. Mesenchymal stem cell migration is regulated by fibronectin through $\alpha 5\beta 1$ -integrin-mediated activation of PDGFR- β and potentiation of growth factor signals. *J Cell Sci.* 2011;124(Pt 8):1288-300.

Vivier E, Tomasello E, Baratin M, Walzer T, Ugolini S. Functions of natural killer cells. *Nature Immunology* 2008;9(5):503–510.

Vose JM, Ho AD, Coiffier B, Corradini P, Khouri I, Sureda A, Van Besien K, Dipersio J. Advance in mobilization for the optimization of autologous stem cell transplantation. *Leuk. Lymphoma* 2009;50(9):1412–21.

Wen PY, Yung WK, Lamborn KR, Dahia PL, Wang Y, Peng B, Abrey LE, Raizer J, Cloughesy TF, Fink K, Gilbert M, Chang S, Junck L, Schiff D, Lieberman F, Fine HA, Mehta M, Robins HI, DeAngelis LM, Groves MD, Puduvalli VK, Levin V, Conrad C, Maher EA, Aldape K, Hayes M, Letvak L, Egorin MJ, Capdeville R, Kaplan R, Murgo AJ, Stiles C, Prados MD. Phase I/II study of imatinib mesylate for recurrent malignant gliomas: North American Brain Tumor Consortium Study 99-08. *Clin Cancer Res.* 2006;12(16):4899-907.

Wilson WR, Hay MP. Targeting hypoxia in cancer therapy, *Nat. Rev. Cancer* 2011;11(6):393-410.

Xing F, Saidou J, Watabe K. Cancer associated fibroblasts (CAFs) in tumor microenvironment. *Front Biosci (Landmark Ed)* 2010;15:166-79.

Xu WT, Bian ZY, Fan QM, Li G, Tang TT. Human mesenchymal stem cells (hMSCs) target osteosarcoma and promote its growth and pulmonary metastasis. *Cancer Lett.* 2009 18;281(1):32-41.

Yao D, Dai C, Peng S. Mechanism of the mesenchymal-epithelial transition and its relationship with metastatic tumor formation. *Mol Cancer Res.* 2011;9(12):1608-20.

Yarden Y, Escobedo JA, Kuang WJ, Yang-Feng TL, Daniel TO, Tremble PM, Chen EY, Ando ME, Harkins RN, Francke U, Fried VA, Ullrich A and Williams LT. Structure of the receptor for platelet-derived growth factor helps define a family of closely related growth factor receptors. *Nature* 1986; 323: 226–232.

Yu FX, Hu WJ, He B, Zheng YH, Zhang QY, Chen L. Bone marrow mesenchymal stem cells promote osteosarcoma cell proliferation and invasion. *World J. Surg. Oncol.* 2015;13:52.

Zeng H, Chi H. The interplay between regulatory T cells and metabolism in immune regulation. *Oncoimmunology* 2013;2(11):e26586.

Zhang T, Lee YW, Rui YF, Cheng TY, Jiang XH, Li G. Bone marrow-derived mesenchymal stem cells promote growth and angiogenesis of breast and prostate tumors. *Stem Cell Res Ther.* 2013;4(3):70.

Zhao S, Wehner R, Bornhäuser M, Wassmuth R, Bachmann M, Schmitz M. Immunomodulatory properties of mesenchymal stromal cells and their therapeutic consequences for immune-mediated disorders. *Stem Cells Dev.* 2010;19(5):607-14.

Ziello JE, Jovin IS, Huang Y. Hypoxia-Inducible Factor (HIF)-1 regulatory pathway and its potential for therapeutic intervention in malignancy and ischemia. *Yale J Biol Med.* 2007;80(2):51-60.



Original Articles

A novel antagonist of CXCR4 prevents bone marrow-derived mesenchymal stem cell-mediated osteosarcoma and hepatocellular carcinoma cell migration and invasion



Raffaella Fontanella ^{a,1}, Alessandra Pelagalli ^{a,b,1}, Anna Nardelli ^a, Crescenzo D'Alterio ^c, Caterina Ieranò ^c, Laura Cerchia ^d, Enrico Lucarelli ^e, Stefania Scala ^c, Antonella Zannetti ^{a,*}

^a Istituto di Biostrutture e Bioimmagini, CNR, Naples, Italy

^b Dipartimento di Scienze Biomediche Avanzate, Università degli Studi di Napoli "Federico II", Naples, Italy

^c Istituto Nazionale per lo Studio e la Cura dei Tumori "Fondazione Giovanni Pascale", IRCCS, Naples, Italy

^d Istituto per l'Endocrinologia e l'Oncologia Sperimentale "G. Salvatore", CNR, Naples, Italy

^e Istituto Ortopedico Rizzoli, Bologna, Italy

ARTICLE INFO

Article history:

Received 20 July 2015

Received in revised form 16 October 2015

Accepted 19 October 2015

Keywords:

Bone marrow-derived mesenchymal stem cells (BM-MSCs)

Tumor invasion

Chemokine receptor type 4 (CXCR4)

Novel CXCR4 inhibitor

ABSTRACT

Recent findings suggest that bone marrow-derived mesenchymal stem cells (BM-MSCs) are recruited into the microenvironment of developing tumors, where they contribute to metastatic processes. The aim of this study was to investigate the role of BM-MSCs in promoting osteosarcoma and hepatocellular carcinoma cell progression *in vitro* and the possible mechanisms involved in these processes.

U2OS and SNU-398 are osteosarcoma and hepatocellular carcinoma cell lines, respectively, that can be induced to proliferate when cultured in the presence of BM-MSCs. To determine the effect of BM-MSCs on U2OS and SNU-398 cells, the AKT and ERK signaling pathways were investigated, and increases were observed in active P-Akt and P-Erk forms. Moreover, BM-MSCs caused an increase in tumor cell migration and invasion that was derived from the enhancement of CXCR4 levels.

Thus, when tumor cells were treated with the CXCR4 antagonist AMD3100, a reduction in their migration and invasion was observed. Furthermore, a new CXCR4 inhibitor, Peptide R, which was recently developed as an anticancer agent, was used to inhibit BM-MSC-mediated tumor invasion and to overcome AMD3100 toxicity. Taken together, these results suggest that inhibiting CXCR4 impairs the cross-talk between tumor cells and BM-MSCs, resulting in reduced metastatic potential in osteosarcoma and hepatocellular carcinoma cells.

© 2015 Elsevier Ireland Ltd. All rights reserved.

Introduction

Tumor progression is a multistep process during which tumor-associated stromal cells perform an intricate cross-talk with tumor cells to supply appropriate signals that may promote tumor survival, proliferation and aggressiveness. A tumor can influence its microenvironment by releasing extracellular signals, promoting tumor angiogenesis and inducing the inflammatory response, while the immune cells in the microenvironment can affect the growth and evolution of cancer cells. The relationship between cancer cells and their microenvironment contributes to tumor heterogeneity [1].

Mesenchymal stem cells (MSCs) are non-hematopoietic multipotent stromal cells that are involved in tissue homeostasis and regeneration. Normally, MSCs are rapidly recruited into sites

of injury and inflammation, where they differentiate into a variety of connective tissue cell types [2]. Early studies demonstrated that bone marrow-derived mesenchymal stem cells (BM-MSCs) possess a remarkable ability to home in to tumor sites and putative immune-privileged status that renders them suitable carriers for delivering anti-tumor agents to the tumor microenvironment [3]. However, BM-MSCs have also been identified as pro-active tumor stroma-associated cells that are implicated in promoting cell survival, angiogenesis, invasion, and metastasis in addition to the evasion of the immune system [4]. Recently, tumor-associated BM-MSCs have been reported to differentiate within the tumor microenvironment and to act as local sources for other tumor stromal cells, such as cancer-associated fibroblasts (CAF) [5]. Furthermore, BM-MSCs increased the population of cancer stem cells (CSCs) in breast [6] and prostate carcinomas [7]. The cross-talk between tumor cells and stromal cells induced the production of growth factors, cytokines and chemokines that can specifically attract BM-MSCs to invade the tumor microenvironment, as has been shown in *breast* [8], *lung* [9], *prostate* [10] and *colon* [11] carcinomas. Even though BM-MSCs have

* Corresponding author. Tel.: +39 0812203431; fax: +39 0812203498.

E-mail address: antonella.zannetti@cnr.it (A. Zannetti).

¹ These authors contributed equally to this work.

been shown to integrate into the tumor stroma and promote tumor progression, the molecular mechanisms underlying these processes have remained elusive.

BM-MSC-derived chemokines, such as CXCL1, CXCL2 or CXCL12, have been shown to promote cancer cell proliferation through the related receptors CXCR2 and CXCR4 in a number of cancer models [12,13].

The chemokine CXCL12, by binding to the CXCR4 and CXCR7 receptors, activates signaling pathways that result in cell proliferation, cell migration and the transcriptional regulation of genes that are critical for cell inflammation and cancer metastases [13,14]. CXCR4 expression was first correlated with breast and melanoma cancer cell metastatic progression [14,15]. As a result of its pleiotropic role in tumor development, the CXCL12/CXCR4 axis is considered an important potential target for cancer therapeutics. A CXCR4 inhibitor, the bicyclam plerixafor (formerly known as AMD3100), is approved by the FDA as a hematopoietic stem cell mobilizer in patients with non-Hodgkin lymphoma and multiple myeloma refractory to conventional protocols for mobilization [16]. Nevertheless, Plerixafor has evoked some concerns regarding its toxicity and is therefore not an ideal anticancer agent [17,18].

It has been shown that the CXCL12/CXCR4 pathway regulates mobilization, trafficking and homing in normal stem cells and metastasis in cancer stem cells [19]. Portella et al. [20] described a new family of peptides that were rationally designed and that were not derived from the naturally occurring CXCR4 inhibitor polyphemusin-II, which has been used as a template to design several classes of CXCR4 inhibitors. These CXCR4 antagonists reduced lung metastasis in mice injected with B16-CXCR4 mouse melanoma cells and K7M2 mouse osteosarcoma cells [20].

Several studies have reported that BM-MSCs promoted the progression of osteosarcoma through different mechanisms involving IL-6/STAT3 [21], the chemokine CCL5 [22], VEGF [23] and CXCR4 [24]. In hepatocellular carcinoma, rat BM-MSCs enhanced migration in a rat hepatoma cell line (CBRH-7919) by up-regulating CXCR4 [25]. Conversely, Li T. et al. showed that BM-MSCs promoted proliferation in human hepatocellular carcinoma cells but inhibited their migration [26].

In our study, we focused on two of the most common cancers with a poor prognosis and metastatic recurrence in children and adults: osteosarcoma (OS) and hepatocellular carcinoma (HCC) [27,28]. Thus, we investigated the role of BM-MSCs in controlling growth and aggressiveness in OS and HCC cell lines, and we analyzed the involvement of CXCR4 in these processes. Furthermore, to interfere with cross-talk between BM-MSCs and tumor cells, we tested a new CXCR4 inhibitor, Peptide R, which was developed to overcome the toxicity of the well-known CXCR4 inhibitor AMD3100.

Materials and methods

Cell lines and culture conditions

The human osteosarcoma cell lines (OS) U2OS and Saos-2 were cultured in McCoy's 5A medium according to the instructions provided by Sigma-Aldrich. The hepatocellular carcinoma (HCC) cell lines SNU-398 and Hep3B were purchased from the American Type Culture Collection and grown in Dulbecco's modified Eagle's medium (DMEM). Both types of media were supplemented with 10% FBS, 100 U/ml penicillin and 100 µg/ml streptomycin. The cells were maintained in a humidified incubator in 5% CO₂ at 37 °C.

Isolation, culture and immunophenotypic characterization of human bone-marrow mesenchymal stem cells (BM-MSC)

Bone marrow (BM) samples were obtained from 3 male patients (29, 35 and 49 years old) who underwent surgery at the Rizzoli Orthopaedic Institute after informed consent was obtained according to a protocol approved by the Ethics Committee. The isolation of cells and the expansion of cultures of human BM-MSCs were performed as previously described [29], using gradient separation and plastic adherence methods. BM-MSCs were recognized by their ability to proliferate in culture and their adherent, spindle-shape morphology. Furthermore, BM-

MSCs were characterized using a FC500 flow cytometer (Beckman Coulter, Brea, CA, USA) with staminal markers, and cells that were positive for CD44, CD73, CD90, CD105, and CD146 and negative for CD34 and CD45 were isolated. BM-MSCs, after isolation and characterization, were grown in medium with 1% fetal bovine serum for 48 h to obtain conditioned medium (BM-MSC-CM). The medium was then collected, centrifuged at 1000 × g for 10 min, and filtered through 0.22-µm filters (Millipore, Billerica, MA) before being added to tumor cells. The BM-MSCs were used at passage 2–3 in this study.

Cell viability assay

To investigate the effects of BM-MSCs on cell viability, a 3-(4,5-dimethylthiazol-2-yl)-5-(3-carboxymethoxy-phenyl)-2-(4-sulfophenyl)-2H tetrazolium (MTS) assay was performed according to the manufacturer's instructions (Promega). As previously described [30], this colorimetric method allows the determination of the number of viable cells based on the bioreduction of MTS to formazan salt crystals. In co-cultures, BM-MSCs and tumor cells were grown in a Boyden chamber with a 0.4 µm membrane. The upper chambers were seeded with BM-MSCs, and the lower chambers were seeded with tumor cells. Briefly, tumor cells were seeded at a density of 5000 cells per well in 96-well flat-bottomed plates and allowed to recover for 24 h. Then, tumor cells were grown in the presence of medium with 10% FBS or BM-MSC-derived conditioned medium, or they were co-cultured with BM-MSCs (ratio 1:1) for 24 h and 48 h in a humidified incubator with 5% CO₂ at 37 °C. After 1 h of incubation with MTS, the absorbance was read using a plate reader (Multiskan RC, Thermo Scientific) at a wavelength of 490 nm. Each sample was analyzed in triplicate. The data are expressed as the percentage of viable cells, considering 100% to represent the number of cells grown in the medium supplemented with 10% FBS, which was used as the control. All experiments were independently performed at least three times.

Cell lysate preparation and western blot analysis

Whole-cell lysates were prepared as previously described [31]. Briefly, cells were homogenized in lysis buffer (40 mM HEPES pH 7.5, 120 mM NaCl, 5 mM MgCl₂, 1 mM EGTA, 0.5 mM EDTA, and 1% Triton X-100) containing protease (Complete Tablets, EDTA-free, Roche) and phosphatase inhibitors (20 mM α-glycerol-3-phosphate and 2.5 mM Na-pyrophosphate). The suspension was homogenized and centrifuged for 15 min at 13,000 × g at 4 °C. Western blot analysis of proteins from whole cell lysates was performed using a standard protocol. Equal amounts of proteins from cells (50 µg) were separated using SDS-PAGE under reducing conditions and transferred to PVDF membranes. After blocking to prevent non-specific protein binding, the membranes were incubated with primary antibodies overnight at 4 °C. The following primary antibodies were used: rabbit polyclonal anti-CXCR4 (C8227, Sigma-Aldrich), rabbit polyclonal anti-AKT (CST-9272, Cell Signaling), rabbit polyclonal anti-P-AKT (CST-9271, Cell Signaling), rabbit polyclonal anti-ERK (CST-9102, Cell Signaling), rabbit polyclonal anti-P-ERK (CST-9101, Cell Signaling), goat anti E-cadherin (sc-1500, Santa Cruz Biotechnology), rabbit polyclonal anti-vimentin (CST-5741, Cell Signaling) and mouse monoclonal anti-β-actin (A4700, Sigma-Aldrich). The filters were then incubated with 1:2000 peroxidase-labeled anti-mouse, anti-rabbit or anti-goat Ig antibodies (Amersham Biosciences Europe, Freiburg, Germany) for 1 h at 22 °C. After extensive washing, the immunoreactions were revealed using an enhanced chemiluminescence detection system (ECL) according to the manufacturer's recommendations. Densitometric analyses were performed on at least two different exposures to assure the linearity of each acquisition using ImageJ software (v1.46r). The blots shown representative of at least three independent experiments.

RNA isolation and real-time reverse transcription polymerase chain reaction (PCR)

Total RNA was extracted from tumor cells using TRIzol reagent (Invitrogen, Grand Island, NY). Total extracted RNA (200 ng) was reverse transcribed using Superscript II RNase H-reverse transcriptase according to the manufacturer's instructions (Invitrogen/Life Technologies, Carlsbad, CA, USA). Real-time PCR was performed using approximately 10 ng of cDNA in a 25-ml SYBR Green reaction mixture, and an ABI Prism 7000 (Applied Biosystems, Carlsbad, CA, USA) robcycler was used for amplification. The cycling conditions for the PCRs were as follows: initial denaturation (one cycle of 10 min at 95 °C) followed by 40 cycles of denaturation (15 s at 95 °C) and annealing (1 min at 60 °C). Subsequently, CXCR4 mRNA levels were quantified, and these expression levels were compared to GUSB mRNA levels. All of the samples were analyzed in triplicate using real-time PCR.

The gene-specific primers used for the amplifications were as follows:

CXCR4: 5'-TGAGAAGCATGACGGACAAG-3' (forward)
5'-AGGGAAGCGTGATGACAAAG-3' (reverse)
GUSB: 5'-AGCCAGTTCCTCATCAATGG-3' (forward)
5'-GGTAGTGGCTGGTACGGAAA-3' (reverse)

RNA interference

CXCR4-targeting siRNA (L-005139-00-05) and a corresponding control non-targeting siRNA (D-001810-10-05) were purchased from Dharmacon. Saos-2 and

Hep3B cells were transfected using DharmaFECT siRNA transfection reagent and 100 nmol/l siRNAs according to the manufacturer's protocol. Saos-2 and Hep3B cells were grown in culture medium after transfection for 72 h, and the down-regulation of targeted protein expression was assessed using Western blot analysis.

Wound healing assays

OS and HCC cell lines were seeded in 6-well plates and grown to confluent cell monolayers. Cells were then scratched with pipette tips to make wounds. The cells were then rinsed with PBS to remove the loosened cell debris. Culture medium containing 1% FBS, 10% FBS, BM-MSC-CM, BM-MSC-CM with the CXCR4 antagonist AMD3100 (10 μ M) (Sigma-Aldrich) or Peptide R (10 μ M) were then added to the cells and the plates were incubated at 37 °C in 5% CO₂ for 24 h and 48 h. In addition, wound healing assays were performed using Saos-2 and Hep3B cells that were grown in the presence of CXCR4 siRNA or Scr siRNA for 72 h. The wounds were observed using phase contrast microscopy. As the cells migrated to fill the scratched area, images were captured using a digital camera (Canon) that was attached to a microscope (Leica) at time 0 and after 24 and 48 hours. The distance between the edges of the scratch was measured using ImageJ, the average distance was quantified and the extent of wound closure was determined as follows: wound closure (%) = 1 – (wound width t_x /wound width t_0) \times 100. All experiments were performed at least three times.

Cell invasion assays

To perform invasion assays, 24-well trans-well chambers (Corning, NY) containing inserts with polycarbonate membranes with 8 μ m pores were used. The top chamber, which contained the filter, was coated with 50 μ l of diluted (1:3 in PBS) Matrigel (BD Biosciences, San Jose, CA) following standard protocols. OS (U2OS and Saos-2) and HCC (SNU-398 and Hep3B) cells were harvested, suspended in serum-free medium, and counted. Cells (2.5×10^5 in 100 μ l serum-free medium per well) were then added to each top chamber. Medium containing 1% FBS (negative control), 10% FBS (positive control), BM-MSC-CM or BM-MSCs was added to the lower chamber as a chemoattractant. After incubation for 48 h at 37 °C in a humidified incubator in 5% CO₂, the non-invading cells were removed from the top chamber using a cotton swab, and the cells that had migrated to the lower surface of the membrane insert were visualized by staining with 0.1% crystal violet in 25% methanol. The percentage of migrated cells was evaluated by eluting the crystal violet with 1% sodium dodecyl sulfate and reading the absorbance at a 570 nm wavelength. The data were obtained from three independent experiments. To block CXCR4, the cells were in-

cubated with the CXCR4 inhibitors AMD3100 or Peptide R at a concentration of 10 μ M during the invasion assays.

Statistical analysis

Results were obtained from at least three independent experiments and are expressed as the mean \pm standard deviation. The data were analyzed using GraphPad Prism statistical software 6.0 (GraphPad Software, La Jolla, CA, USA), and significance was determined using Student's *t*-tests. A *P*-value <0.05 was considered statistically significant.

Results

BM-MSCs promote tumor cell growth and increase P-Akt and P-Erk levels

To determine the effects of BM-MSCs on human osteosarcoma cell (U2OS) and human hepatocellular carcinoma cell (SNU-398) growth, cells were grown in medium supplemented with 10% FBS (control), in conditioned medium obtained from BM-MSC cultures or co-cultured with BM-MSCs for 24 and 48 hours, and cell viability was then tested using an MTS assay. As shown in Fig. 1A, when U2OS cells were grown in the presence of BM-MSC-CM for 24 and 48 hours, a 2-fold significant increase in proliferation was observed compared to proliferation in the control cells ($P < 0.01$). Consistent with these results, we found that when U2OS cells were co-cultured with BM-MSCs (1:1 ratio), their growth was also significantly enhanced by 3- and 3.5-fold at 24 and 48 hours, respectively ($P < 0.01$) (Fig. 1A). Similarly, we observed an increase in SNU-398 cell proliferation when cells were grown in the presence of BM-MSC-CM (1.8-fold at 24 h and 2.1-fold at 48 h; $P < 0.01$) or co-cultured with BM-MSCs (1:1 ratio) (1.5-fold at 24 h and 1.8-fold at 48 h; $P < 0.01$) compared to proliferation in the control cells

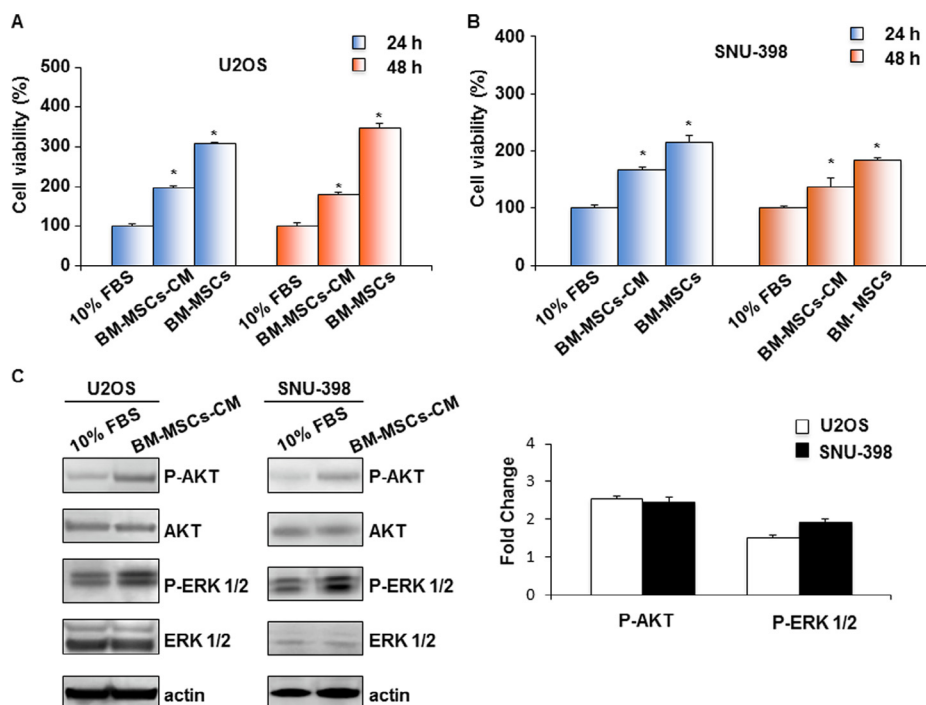


Fig. 1. BM-MSCs enhance cell viability and activate the P-AKT/AKT and P-ERK/ERK pathways in U2OS and SNU-398 tumor cell lines. (A) U2OS and SNU-398 cells were co-cultured with BM-MSCs or grown in the presence of BM-MSC-CM for 24 and 48 hours, and then their viability was tested using MTS assays. The data are expressed as the percentage of viable cells by considering 100% to represent the number of cells grown in medium supplemented with 10% FBS (controls). All experiments were performed at least three times independently ($*P < 0.01$). (B) Western blots show the effect of BM-MSC-CM after 24 h on downstream signaling in tumor cells. Actin was used as an equal loading control. Representative data are shown from one of three experiments. The fold changes in P-AKT and P-ERK levels are shown in tumor cells grown in presence of BM-MSC-CM compared to their levels in control cells grown in medium containing 10% FBS, which were arbitrarily determined to be 1.

(Fig. 1B). Thus, BM-MSCs and factors released by BM-MSCs promoted cell growth in U2OS and SNU-398 cells.

To investigate the mechanisms underlying the promotion of tumor growth by BM-MSCs, we next analyzed the activation of cell survival-related intracellular signals in the phosphatidylinositol-3-kinase (PI3K)/Akt and extracellular signal-regulated kinase 1/2 (Erk1/2) pathways. As shown in Fig. 1C, conditioned medium from BM-MSCs increased P-Akt and P-Erk levels in both tumor cell lines compared to the levels observed in cells grown in medium supplemented with 10% FBS (control), whereas no increase was observed in Akt and Erk levels. We found that BM-MSC-CM caused a 2.54-fold and a 2.44-fold increase in P-Akt levels in U2OS and SNU-398 cells, respectively, whereas P-Erk was increased by 1.3-fold in U2OS and 1.9-fold in SNU-398 cells compared to the levels observed in the controls (Fig. 1C).

BM-MSCs increase CXCR4 mRNA and protein expression in OS and HCC cell lines

We analyzed whether the expression of chemokine receptor type 4 (CXCR4), which is known to play a key role in cancer metastasis, was affected by treatment with BM-MSC-CM. When OS cells (U2OS and Saos-2) and HCC cells (SNU-398 and Hep3B) were treated for 24 h with conditioned medium from BM-MSCs, a significant increase was observed in CXCR4 mRNA and protein levels (Fig. 2).

Inhibiting CXCR4 prevents BM-MSCs-dependent wound healing in OS and HCC cells

Because CXCR4 expression is correlated with tumor cell migration and metastatic potential [14], we investigated whether

conditioned medium from BM-MSCs would be able to affect wound healing. Monolayers of U2OS and SNU-398 cells were scratched, and images were taken at 0, 24 and 48 hours after wounding (Fig. 3A and B). BM-MSC-CM caused a significant increase in wound closure in U2OS cells (64% and 82% at 24 h and 48 h, respectively) compared to closure in the control cells (1% FBS) ($P < 0.01$). When U2OS cells were grown in the presence of BM-MSC-CM and treated with the CXCR4 antagonists AMD3100 (10 μ M) or peptide R (10 μ M), wound healing was significantly delayed compared to cells treated with BM-MSC-CM alone ($P < 0.001$) (Fig. 3A). In SNU-398 cells, BM-MSC-CM caused a significant increase in wound closure (40% and 50% at 24 h and 48 h, respectively) compared to closure in control cells, although this increase was lower than that observed for U2OS cells. Both of the CXCR4 inhibitors, AMD3100 and peptide R, significantly reduced the wound closure induced by BM-MSC-CM ($P < 0.001$) (Fig. 3B). To confirm that inhibition of CXCR4 expression reduced the wound closure that was induced by BM-MSCs, Saos-2 and Hep3B cells were transiently transfected with non-targeting Scr siRNAs or CXCR4-specific siRNAs. A significant reduction was observed in CXCR4 levels in both cell lines when they were transfected with CXCR4 siRNAs compared to cells transfected with Scr siRNAs for 72 h (Supplementary Fig. S1A and B). Similar to what was observed in U2OS and SNU-398 cells, we observed that Saos-2 and Hep3B cells that were treated with BM-MSC-CM showed a significant increase in wound closure compared to closure in the control (1% FBS), whereas when these cells were treated with BM-MSC-CM in the presence of the CXCR4 antagonists AMD3100 (10 μ M) or peptide R (10 μ M), wound healing was significantly delayed ($P < 0.001$). Furthermore, when Saos-2 and Hep3B cells were transfected with CXCR4-specific siRNAs, a significant reduction was observed in wound closure compared to closure in the cells transfected with Scr siRNAs ($P < 0.001$) (Supplementary Fig. S1A and B).

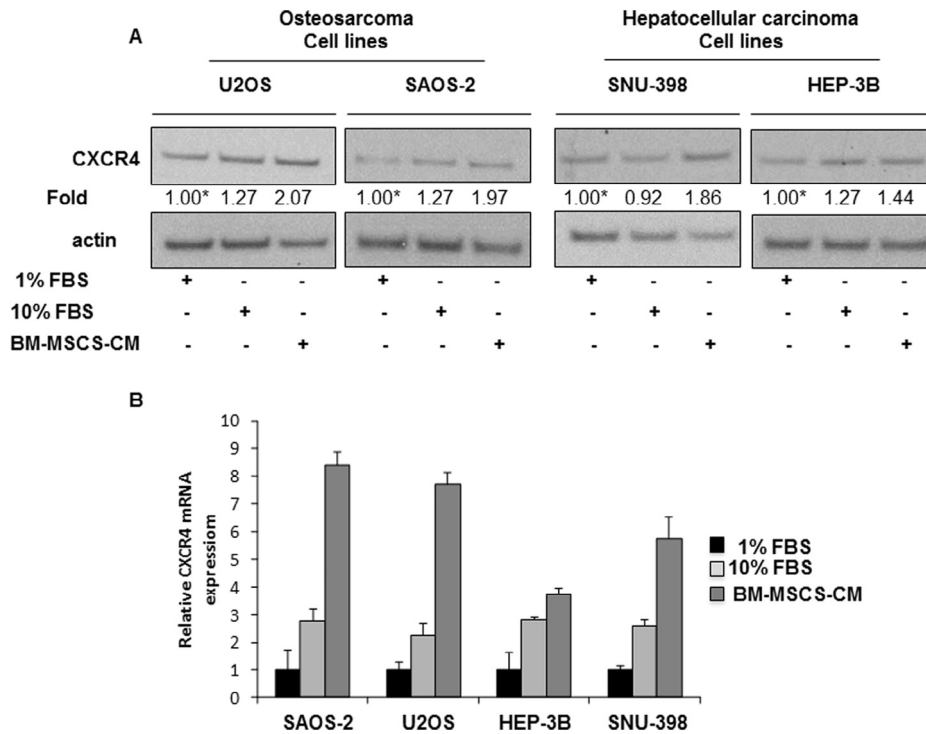
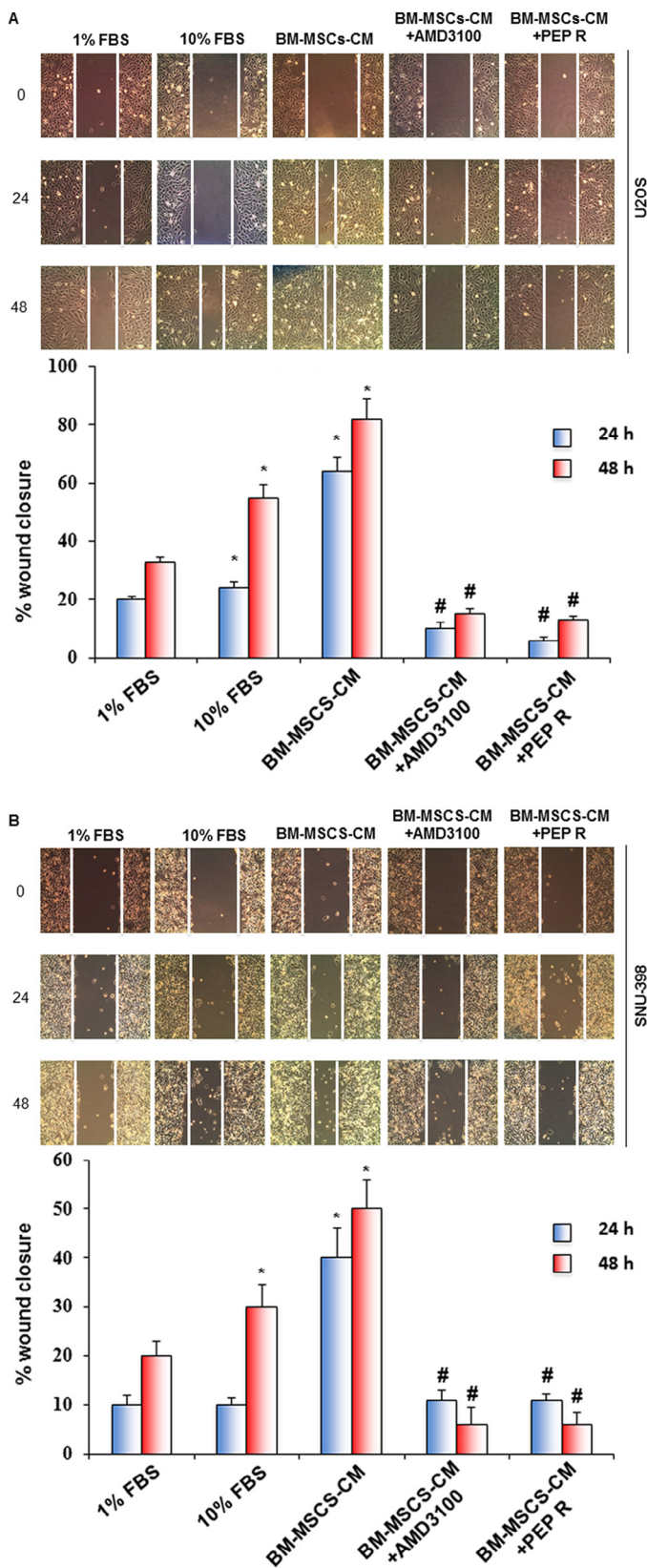


Fig. 2. BM-MSCs increase CXCR4 mRNA and protein levels in OS and HCC cell lines. (A) Western blot analysis of CXCR4 expression in tumor cell lines after treatment with BM-MSC-CM for 24 h. Actin was used as an equal loading control. The values below the blot indicate signal levels relative to controls, which were arbitrarily set to 1 (labeled with asterisk). Representative data from one of three experiments are shown. (B) CXCR4 mRNA levels as detected using real-time PCR in OS and HCC cell lines grown for 24 h in the presence of BM-MSC-CM, medium with 1% FBS or medium with 10% FBS, as indicated.



CXCR4 inhibitors prevent BM-MSC-dependent U2OS and SNU-398 cell invasion

We then examined the effect of BM-MSCs on the invasiveness of U2OS and SNU-398 cells using trans-well chambers coated with

Fig. 3. BM-MSCs induced an increase in wound healing in U2OS and SNU-398 tumor cells that was inhibited by CXCR4 antagonists. (A) U2OS cells, after scratch wounds were made using pipette tips, were grown for 24 and 48 hours in medium containing 1% FBS or 10% FBS or with conditioned medium obtained from cultured BM-MSCs (BM-MSC-CM) in the presence of the CXCR4 inhibitors AMD3100 (10 μ M) or Peptide R (10 μ M). (B) SNU-398 cells were tested in wound healing assays using the same experimental conditions described above for U2OS cells. The distance between the edges of the scratch was measured using ImageJ, the average distance was quantified, and the extent of wound closure was determined as follows: wound closure (%) = $1 - (\text{wound width } t_x / \text{wound width } t_0) \times 100$. All experiments were performed at least three times. * $P < 0.01$ compared to the control (medium with 1% FBS); # $P < 0.001$ compared to treatment with BM-MSC-CM.

Matrigel. Fig. 4A and B demonstrate that a significant increase was observed in tumor cell invasiveness when either tumor cell line was exposed to BM-MSC-CM or BM-MSCs (ratio 1:1), which was added to the lower chamber as chemoattractant, compared to the invasiveness observed in the control cells (1% FBS used as the medium) for 48 hours ($P < 0.01$). Inhibiting CXCR4 using AMD3100 or peptide R dramatically suppressed the invasiveness of U2OS and SNU-398 cells that was promoted by BM-MSCs ($P < 0.001$). A similar inhibitory effect on BM-MSCs-induced invasiveness was observed on Saos-2 and Hep3B cells when they were also cultured in the presence of AMD3100 or peptide R (Supplementary Fig. S2A and B).

CXCR4 inhibitors prevent BM-MSC-dependent ERK and AKT activation and EMT in OS and HCC cell lines

To further characterize the involvement of the ERK and AKT pathways in BM-MSC-induced, CXCR4-mediated OS and HCC migration and invasion, we analyzed P-Erk and P-Akt expression after cells were treated with the CXCR4-specific antagonists AMD3100 and peptide R and a specific CXCR7 antibody. Recent studies reported that CXCR7 expression is correlated with the CXCL12-CXCR4 axis during tumor progression and furthermore that CXCR7 activates the same intracellular signaling pathways activated by CXCR4 [32]. As shown in Fig. 5, we observed a significant reduction in P-Erk and P-Akt levels when all cell lines that were grown in the presence of BM-MSC-CM were treated with CXCR4 inhibitors, whereas a validated anti-CXCR7 monoclonal antibody [33] was particularly effective in HCC cell lines. The epithelial–mesenchymal transition (EMT) of tumor cells is widely accepted to be closely correlated with cancer metastasis. To explore whether CXCR4 promotes the EMT process in OS and HCC cell lines grown in the presence of BM-MSC-CM, we analyzed E-cadherin and vimentin levels after cells were treated with AMD3100 and peptide R. We found that CXCR4 antagonists caused an increase in E-cadherin and a reduction in vimentin levels in cells that were grown in the presence of BM-MSC-CM (Fig. 6).

Discussion

Several studies have reported that BM-MSCs, which are known to be involved in tissue homeostasis and regeneration, can be recruited into primary tumors and become active components of the tumor microenvironment, such as cancer-associated fibroblasts (CAFs) [34,35]. BM-MSCs contribute to tumor cell growth and metastatic behavior in a variety of cancers, including breast [8,36,37], prostate [7,10,36], osteosarcoma [21–24] and colon [11,38,39] cancers. In contrast, there is evidence showing that MSCs inhibit tumor progression [39]. In glioblastoma multiforme (GBM), BM-MSCs seem to reduce tumor growth by inhibiting angiogenesis [40].

In the present study, we investigated the role of BM-MSCs in promoting growth and invasion in osteosarcoma and hepatocellular carcinoma cell lines. Several previous studies have reported that MSCs promoted the progression of different osteosarcoma cell lines through different molecular pathways, including

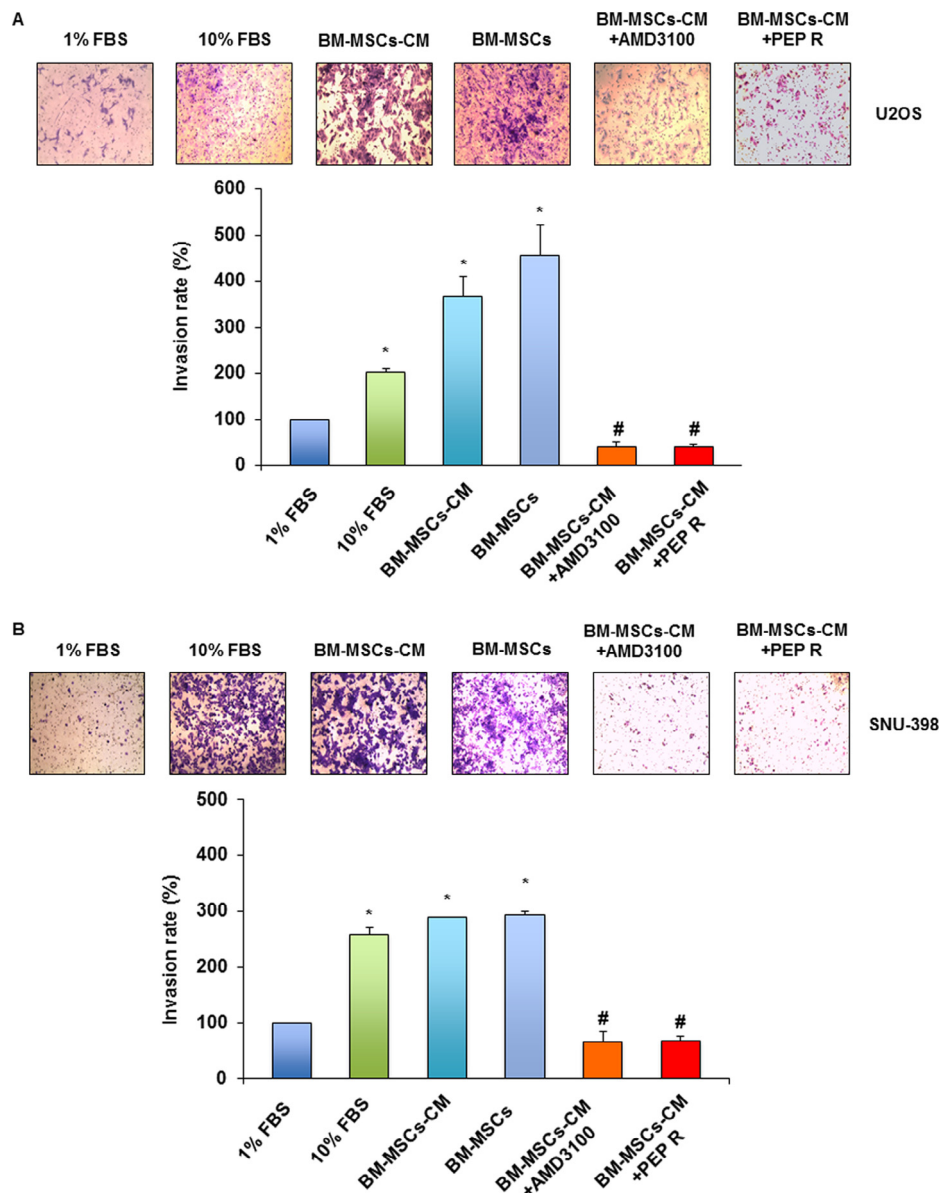


Fig. 4. CXCR4 antagonists prevent BM-MSC-mediated U2OS and SNU-398 tumor cell invasion. Tumor cells were seeded into upper chambers containing 8 μ m pore-size filters that were coated with Matrigel basement membrane matrix in the presence or absence of the CXCR4 antagonists AMD3100 (10 μ M) or Peptide R (10 μ M). Medium containing 1% FBS or 10% FBS, conditioned medium obtained from cultured BM-MSCs (BM-MSC-CM) or BM-MSCs were added to the lower chamber as a chemoattractant. The invasiveness of U2OS cells and SNU-398 cells is described in panels A and B, respectively. All experiments were performed at least three times. * $P < 0.001$ compared to the control (medium with 1% FBS); # $P < 0.001$ compared to BM-MSCs.

IL6/STAT3, CCL5 and CXCR4/VEGF [21–24], whereas few studies have reported on the crosstalk between MSCs and hepatocellular carcinoma cells [21–24]. The paracrine molecules secreted by MSCs can act as ligands for receptors that are expressed on tumor cells, thereby inducing the activation of the PI3K/Akt and Ras/ERK pathways, which are involved in tumor cell progression [34]. We have shown that conditioned medium obtained from BM-MSCs caused parallel increases in osteosarcoma and hepatocellular carcinoma cell growth and P-Akt/P-ERK levels, suggesting the activation of the PI3K/Akt as well as the Ras/ERK intracellular cascades. Recently, it was shown that MSCs are recruited into prostate tumors through CXCL16 and that they are then converted in to cancer-associated fibroblasts (CAFs) [10]. In turn, CAFs secrete CXCL12, which binds to CXCR4 on tumor cells to induce EMT, which ultimately promotes metastasis to secondary tumor sites [10]. Furthermore, it has been reported that BM-MSCs may accelerate human breast tumor growth and metastasis

by regulating the cancer stem cell population through cytokine networks, the up-regulation of miR-199a and the repression of FOXP2 [6,41].

In summary, our findings indicate that BM-MSCs recruited into the tumor stroma may promote osteosarcoma and hepatocellular carcinoma growth by activating the PI3K/Akt and Ras/Erk pathways. Furthermore, we show that BM-MSCs may cause tumor cell migration and invasion and the EMT phenotype through a process that involves CXCR4 signaling. These mechanisms were impaired by peptide R, a new CXCR4 antagonist. Future studies in animal models will help to determine whether this is a viable strategy for OS and HCC treatment.

In conclusion, this is the first report to describe a new molecule targeting CXCR4 for use as a potential therapeutic agent to prevent the cancer progression and spreading that is regulated by cross-talk between BM-MSCs and tumor cells.

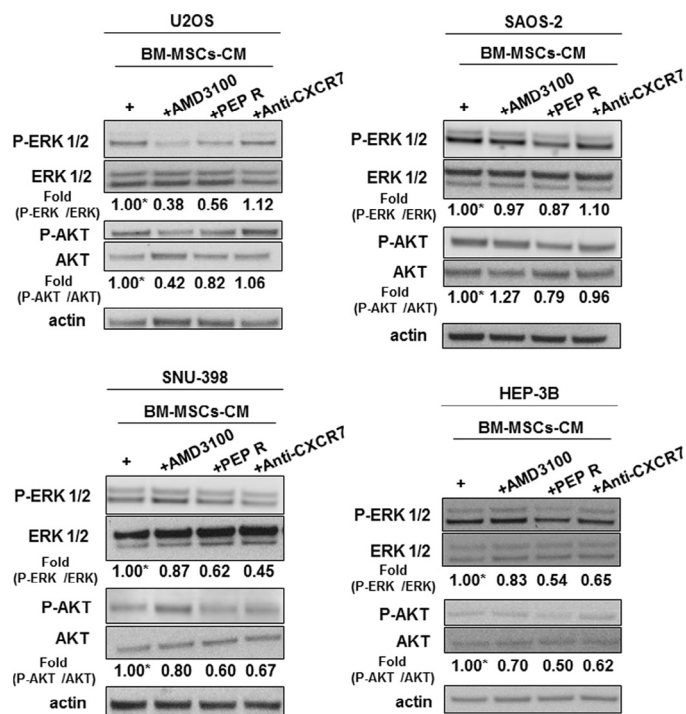


Fig. 5. CXCR4 inhibitors prevent BM-MSC-dependent activation of the ERK and AKT signaling pathways in OS and HCC cell lines. Tumor cell lines grown in the presence of BM-MSC-CM were treated with CXCR4 antagonists (AMD3100 and peptide R) or an anti-CXCR7 monoclonal antibody (10 µg/ml; 11G8, R&D Systems) for 24 h and then analyzed for P-ERK, ERK, P-AKT, and AKT levels. Actin was used as an equal loading control. Values below the blot indicate signal levels relative to the controls (BM-MSC-CM), which were arbitrarily set to 1 (labeled with an asterisk). Representative data from one of three experiments are shown.

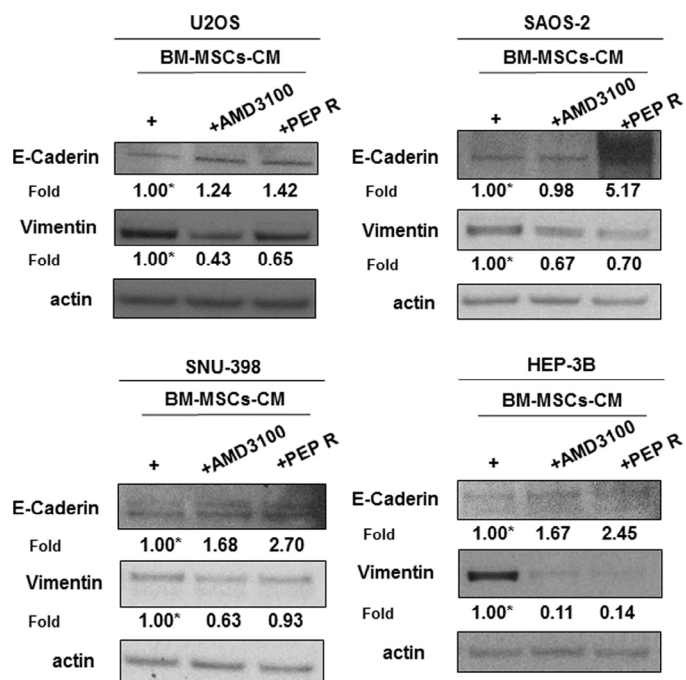


Fig. 6. CXCR4 inhibitors prevent BM-MSC-dependent EMT in OS and HCC cell lines. Tumor cell lines grown in the presence BM-MSC-CM were treated with CXCR4 antagonists (AMD3100 and peptide R) and analyzed for E-cadherin and vimentin levels. Actin was used as an equal loading control. Values below the blot indicate signal levels relative to the controls (BM-MSC-CM), which were arbitrarily set to 1 (labeled with an asterisk). Representative data from one of three experiments are shown.

Acknowledgements

We thank Prof. Rosa Marina Melillo for generously providing the CXCR4 siRNA and Dr. Rosanna Palumbo for generously providing the Saos-2 cell line. The IG Associazione Italiana per la Ricerca sul Cancro no. 13192 supported this work.

Conflict of interest

The authors declare that they have no competing interests.

Appendix: Supplementary material

Supplementary data to this article can be found online at doi:10.1016/j.canlet.2015.10.018.

References

- [1] D.F. Quail, J.A. Joyce, Microenvironmental regulation of tumor progression and metastasis, *Nat. Med.* 19 (2013) 1423–1437.
- [2] M. Quante, S.P. Tu, H. Tomita, T. Gonda, S.S. Wang, S. Takashi, et al., Bone marrow-derived myofibroblasts contribute to the mesenchymal stem cell niche and promote tumor growth, *Cancer Cell* 19 (2011) 257–272.
- [3] P. Barcellos-de-Souza, V. Gori, F. Bambi, P. Chiarugi, Tumor microenvironment: bone marrow-mesenchymal stem cells as key players, *Biochim. Biophys. Acta* 2013 (1836) 321–335.
- [4] D. Hanahan, R.A. Weinberg, Hallmarks of cancer: the next generation, *Cell* 144 (2011) 646–674.
- [5] D.L. Worthley, Y. Si, M. Quante, M. Churchill, S. Mukherjee, T.C. Wang, Bone marrow cells as precursors of the tumor stroma, *Exp. Cell Res.* 319 (2013) 1650–1656.
- [6] S. Liu, C. Ginestier, S.J. Ou, S.G. Clouthier, S.H. Patel, F. Monville, et al., Breast cancer stem cells are regulated by mesenchymal stem cells through cytokine networks, *Cancer Res.* 15 (2011) 614–624.
- [7] J. Luo, S. Ok Lee, L. Liang, C.K. Huang, L. Li, S. Wen, et al., Infiltrating bone marrow mesenchymal stem cells increase prostate cancer stem cell population and metastatic ability via secreting cytokines to suppress androgen receptor signaling, *Oncogene* 22 (2014) 2768–2778.
- [8] P. Chaturvedi, D.M. Gilkes, C.C. Wong, W. Luo, H. Zhang, et al., Hypoxia-inducible factor-dependent breast cancer-mesenchymal stem cell bidirectional signaling promotes metastasis, *J. Clin. Invest.* 123 (2013) 189–205.
- [9] K. Suzuki, R. Sun, M. Origuchi, M. Kanehira, T. Takahata, J. Itoh, et al., Mesenchymal stromal cells promote tumor growth through the enhancement of neovascularization, *Mol. Med.* 17 (2011) 579–587.
- [10] Y. Jung, J.K. Kim, Y. Shiozawa, J. Wang, A. Mishra, J. Joseph, et al., Recruitment of mesenchymal stem cells into prostate tumours promotes metastasis, *Nat. Commun.* 4 (2013) 1795.
- [11] K. Shinagawa, Y. Kitadai, M. Tanaka, T. Sumida, M. Kodama, Y. Higashi, et al., Mesenchymal stem cells enhance growth and metastasis of colon cancer, *Int. J. Cancer* 127 (2010) 2323–2333.
- [12] J.L. Halpern, A. Kilbarger, C.C. Lynch, Mesenchymal stem cells promote mammary cancer cell migration in vitro via the CXCR2 receptor, *Cancer Lett.* 308 (2011) 91–99.
- [13] B.A. Teicher, S.P. Fricker, CXCL12 (SDF-1)/CXCR4 pathway in cancer, *Clin. Cancer Res.* 16 (2010) 2927–2931.
- [14] A. Müller, B. Homey, H. Soto, N. Ge, D. Catron, M.E. Buchanan, et al., Involvement of chemokine receptors in breast cancer metastasis, *Nature* 410 (2001) 50–56.
- [15] S. Scala, A. Ottaiano, P.A. Ascierto, M. Cavalli, E. Simeone, P. Giuliano, et al., Expression of CXCR4 predicts poor prognosis in patients with malignant melanoma, *Clin. Cancer Res.* 11 (2005) 1835–1841.
- [16] J.M. Vose, A.D. Ho, B. Coiffier, P. Corradini, I. Khouri, A. Sureda, et al., Advance in mobilization for the optimization of autologous stem cell transplantation, *Leuk. Lymphoma* 50 (2009) 1412–1421.
- [17] M. Kucia, R. Reca, K. Miekus, J. Wanzeck, W. Wojakowski, A. Janowska-Wieczorek, et al., Trafficking of normal stem cells and metastasis of cancer stem cells involve similar mechanisms: pivotal role of the SDF-1-CXCR4 axis, *Stem Cells* 23 (2005) 879–894.
- [18] E. De Clercq, The AMD3100 story: the path to the discovery of a stem cell mobilizer (Mozobil), *Biochem. Pharmacol.* 77 (2009) 1655–1664.
- [19] C.W. Hendrix, A.C. Collier, M.M. Lederman, D. Schols, R.B. Pollard, S. Brown, et al., Safety, pharmacokinetics, and antiviral activity of AMD3100, a selective CXCR4 receptor inhibitor, in HIV-1 infection, *J. Acquir. Immune Defic. Syndr.* 37 (2004) 1253–1262.
- [20] L. Portella, R. Vitale, S. De Luca, C. D'Alterio, C. Ierandò, M. Napolitano, et al., Preclinical development of a novel class of CXCR4 antagonist impairing solid tumors growth and metastases, *PLoS ONE* 8 (2013) 9.
- [21] B. Tu, L. Du, Q.M. Fan, Z. Tang, T.T. Tang, STAT3 activation by IL-6 from mesenchymal stem cells promotes the proliferation and metastasis of osteosarcoma, *Cancer Lett.* 325 (2012) 80–88.

- [22] W.T. Xu, Z.Y. Bian, Q.M. Fan, G. Li, T.T. Tang, Human mesenchymal stem cells (hMSCs) target osteosarcoma and promote its growth and pulmonary metastasis, *Cancer Lett.* 281 (2009) 32–41.
- [23] P. Zhang, L. Dong, K. Yan, H. Long, T.T. Yang, M.Q. Dong, et al., CXCR4-mediated osteosarcoma growth and pulmonary metastasis is promoted by mesenchymal stem cells through VEGF, *Oncol. Rep.* 30 (2013) 1753–1761.
- [24] F.X. Yu, W.J. Hu, B. He, Y.H. Zheng, Q.Y. Zhang, L. Chen, Bone marrow mesenchymal stem cells promote osteosarcoma cell proliferation and invasion, *World J. Surg. Oncol.* 13 (2015) 52.
- [25] X. Li, Q. Luo, J. Sun, G. Song, Conditioned medium from mesenchymal stem cells enhances the migration of hepatoma cells through CXCR4 up-regulation and F-actin remodeling, *Biotechnol. Lett.* 37 (2015) 511–521.
- [26] T. Li, S. Zhao, B. Song, Z. Wei, G. Lu, J. Zhou, et al., Effects of transforming growth factor β -1 infected human bone marrow mesenchymal stem cells on high- and low-metastatic potential hepatocellular carcinoma, *Eur. J. Med. Res.* 20 (2015) 56.
- [27] J.C. Clark, C.R. Dass, P.F. Choong, A review of clinical and molecular prognostic factors in osteosarcoma, *J. Cancer Res. Clin. Oncol.* 134 (2008) 281–297.
- [28] I. Ghanem, M.E. Riveiro, V. Paradis, S. Faivre, P.M. de Parga, E. Raymond, Insights on the CXCL12-CXCR4 axis in hepatocellular carcinoma carcinogenesis, *Am. J. Transl. Res.* 6 (2014) 340–352.
- [29] M. Pierini, B. Dozza, E. Lucarelli, P.L. Tazzari, F. Ricci, D. Remondini, et al., Efficient isolation and enrichment of mesenchymal stem cells from bone marrow, *Cytotherapy* 14 (2012) 686–693.
- [30] A. Zannetti, F. Iommelli, R. Fonti, A. Papaccioli, J. Sommella, A. Lettieri, et al., Gefitinib induction of in vivo detectable signals by Bcl-2/Bcl-xL modulation of inositol trisphosphate receptor type 3, *Clin. Cancer Res.* 15 (2008) 5209–5219.
- [31] A. Zannetti, S. Del Vecchio, M.W. Carriero, R. Fonti, P. Franco, G. Botti, et al., Coordinate up-regulation of Sp1 DNA-binding activity and urokinase receptor expression in breast carcinoma, *Cancer Res.* 15 (2000) 1546–1551.
- [32] S. Scala, Molecular pathways: targeting the CXCR4-CXCL12 axis-untapped potential in the tumor microenvironment, *Clin. Cancer Res.* 21 (2015) 4278–4285.
- [33] C. Ieranò, S. Santagata, M. Napolitano, F. Guardia, A. Grimaldi, E. Antignani, et al., CXCR4 and CXCR7 transduce through mTOR in human renal cancer cells, *Cell Death Dis.* 5 (2014) e1310.
- [34] B.I. Koh, Y. Kang, The pro-metastatic role of bone marrow-derived cells: a focus on MSCs and regulatory T cells, *EMBO Rep.* 13 (2012) 412–422.
- [35] S.A. Bergfeld, Y.A. DeClerck, Bone marrow-derived mesenchymal stem cells and the tumor microenvironment, *Cancer Metastasis Rev.* 29 (2010) 249–261.
- [36] T. Zhang, Y.W. Lee, Y.F. Rui, T.Y. Cheng, X.H. Jiang, G. Li, Bone marrow-derived mesenchymal stem cells promote growth and angiogenesis of breast and prostate tumors, *Stem Cell Res. Ther.* 13 (2013) 70.
- [37] A.E. Karnoub, A.B. Dash, A.P. Vo, A. Sullivan, M.W. Brooks, G.W. Bell, et al., Mesenchymal stem cells within tumour stroma promote breast cancer metastasis, *Nature* 4 (2007) 557–563.
- [38] Y. Liu, Z.P. Han, S.S. Zhang, Y.Y. Jing, X.X. Bu, C.Y. Wang, et al., Effects of inflammatory factors on mesenchymal stem cells and their role in the promotion of tumor angiogenesis in colon cancer, *J. Biol. Chem.* 15 (2011) 25007–25015.
- [39] N.M. Hogan, M.R. Joyce, J.M. Murphy, F.P. Barry, T. O'Brien, M.J. Kerin, et al., Impact of mesenchymal stem cell secreted PAI-1 on colon cancer cell migration and proliferation, *Biochem. Biophys. Res. Commun.* 14 (2013) 574–579.
- [40] I.A. Ho, H.C. Toh, W.H. Ng, Y.L. Teo, C.M. Guo, K.M. Hui, et al., Human bone marrow-derived mesenchymal stem cells suppress human glioma growth through inhibition of angiogenesis, *Stem Cells* 31 (2013) 146–1455.
- [41] B.G. Cuiffo, A. Campagne, G.W. Bell, A. Lembo, F. Orso, E.C. Lien, et al., MSC-regulated microRNAs converge on the transcription factor FOXP2 and promote breast cancer metastasis, *Cell Stem Cell* 15 (2014) 762–774.

Aptamer-miRNA-212 Conjugate Sensitizes NSCLC Cells to TRAIL

Margherita Iaboni¹, Valentina Russo¹, Raffaella Fontanella², Giuseppina Roscigno³, Danilo Fiore¹, Elvira Donnarumma⁴, Carla Lucia Esposito³, Cristina Quintavalle¹, Paloma H Giangrande⁵, Vittorio de Franciscis³ and Gerolama Condorelli^{1,3}

TNF-related apoptosis-inducing ligand (TRAIL) is a promising antitumor agent for its remarkable ability to selectively induce apoptosis in cancer cells, without affecting the viability of healthy bystander cells. The TRAIL tumor suppressor pathway is deregulated in many human malignancies including lung cancer. In human non-small cell lung cancer (NSCLC) cells, sensitization to TRAIL therapy can be restored by increasing the expression levels of the tumor suppressor microRNA-212 (miR-212) leading to inhibition of the anti-apoptotic protein PED/PEA-15 implicated in treatment resistance. In this study, we exploited a previously described RNA aptamer inhibitor of the tyrosine kinase receptor Axl (GL21.T) expressed on lung cancer cells, as a means to deliver miR-212 into human NSCLC cells expressing Axl. We demonstrate efficient delivery of miR-212 following conjugation of the miR to GL21.T (GL21.T-miR212 chimera). We show that the chimera downregulates PED and restores TRAIL-mediated cytotoxicity in cancer cells. Importantly, treatment of Axl+ lung cancer cells with the chimera resulted in (i) an increase in caspase activation and (ii) a reduction of cell viability in combination with TRAIL therapy. In conclusion, we demonstrate that the GL21.T-miR212 chimera can be employed as an adjuvant to TRAIL therapy for the treatment of lung cancer.

Molecular Therapy—Nucleic Acids (2016) 5, e289 ; doi:10.1038/mtna.2016.5; published online 8 March 2016

Introduction

Members of the tumor necrosis factor (TNF) superfamily of cytokines bind to cognate receptors, called death receptors, on the surface of cells. Since their first discovery, more than 20 human TNF ligands and more than 30 corresponding receptors have been identified.¹ Members of this superfamily have a wide tissue distribution and regulate broad physiological processes such as immune responses, hematopoiesis, morphogenesis, and cell death, thus playing a key role in homeostasis, up to their role in tumorigenesis.² Key members of this family include TNF, CD95L (FasL), and TNF-related apoptosis-inducing ligand (TRAIL).

The clinical application of TNF ligands as cytotoxic agents for cancer is limited due to their toxicity. For example, TNF induces systemic toxicity.³ *In vivo* use of CD95L is also limited by its lethal hepatotoxicity resulting from massive hepatocyte apoptosis.^{4,5} TRAIL, instead, has been developed as a promising antitumor agent because it induces apoptosis in several tumor-derived cell types, but not in normal cells.^{6,7} However, tumors often develop resistance to TRAIL monotherapy. Resistance to drug treatment is mainly due to deregulation of apoptosis-related proteins such as PED, a death effector domain (DED) family member of 15 kDa having a variety of effects on cell growth and metabolism.⁸ PED has a broad anti-apoptotic function, being able to inhibit both the intrinsic and the extrinsic apoptotic pathways. In the extrinsic pathway, its interaction with Fas-associated protein with death domain (FADD) and pro-caspase-8 acts as competitive inhibitor of these pro-apoptotic molecules during the assembly of the

death-inducing signaling complex (DISC).^{9–13} PED has been shown to be overexpressed in TRAIL-resistant human non-small cell lung cancer (NSCLC) cells.¹⁴ An important mechanism of protein expression regulation involves microRNAs (miRNAs).^{15,16} Toward this end, we found that miR-212 negatively modulates PED expression and sensitizes NSCLC cells to TRAIL-induced apoptosis. In fact, miR-212 levels in resistant cell lines of NSCLC were downregulated and inversely correlated with PED levels.¹⁷ Consistently, transfection of a miR-212 mimic resulted in sensitization of resistant cancer cells to TRAIL-induced apoptosis. This occurred, at least in part, through PED downregulation.¹⁷

A major obstacle to the translation of RNAi drugs (e.g., miRNA mimics) into the clinic is the absence of an effective targeted delivery system. In addition to their ability to inhibit the function of their targets, in the past decade much attention has been focused on aptamers as delivery vehicles for targeted therapy.^{18–20} Aptamers are highly structured single-stranded RNA molecules that bind to their cognate molecular targets (including transmembrane receptors) with high affinity and selectivity.^{21,22} Aptamers have been successfully adapted for the targeted delivery of active molecules both *in vitro* and *in vivo*, including anticancer drugs, toxins, radionuclides, siRNAs, and, more recently, miRNAs.^{23–25} Aptamer-siRNA or aptamer-miRNA chimeras are characterized by low immunogenicity, easy chemical synthesis and modification, and superior target selectivity.^{23,26–28}

In previous studies, an internalizing RNA aptamer (GL21.T)²⁹ has been identified, through a cell-SELEX (systematic evolution of ligands by exponential enrichment)

¹Department of Molecular Medicine and Medical Biotechnology, “Federico II” University of Naples, Naples, Italy; ²IBB, CNR, Naples, Italy; ³IEOS, CNR, Naples, Italy; ⁴IRCCS-SDN, Naples, Italy; ⁵Department of Internal Medicine, University of Iowa, Iowa City, Iowa, USA. Correspondence: Gerolama Condorelli, Department of Molecular Medicine and Medical Biotechnology, “Federico II” University of Naples, Via Pansini, 5-80131 Naples, Italy. E-mail: gecondor@unina.it

Keywords: aptamer; microRNA; non-small cell lung cancer; TNF-related apoptosis-inducing ligand

Received 1 September 2015; accepted 29 December 2015; published online 8 March 2016. doi:10.1038/mtna.2016.5

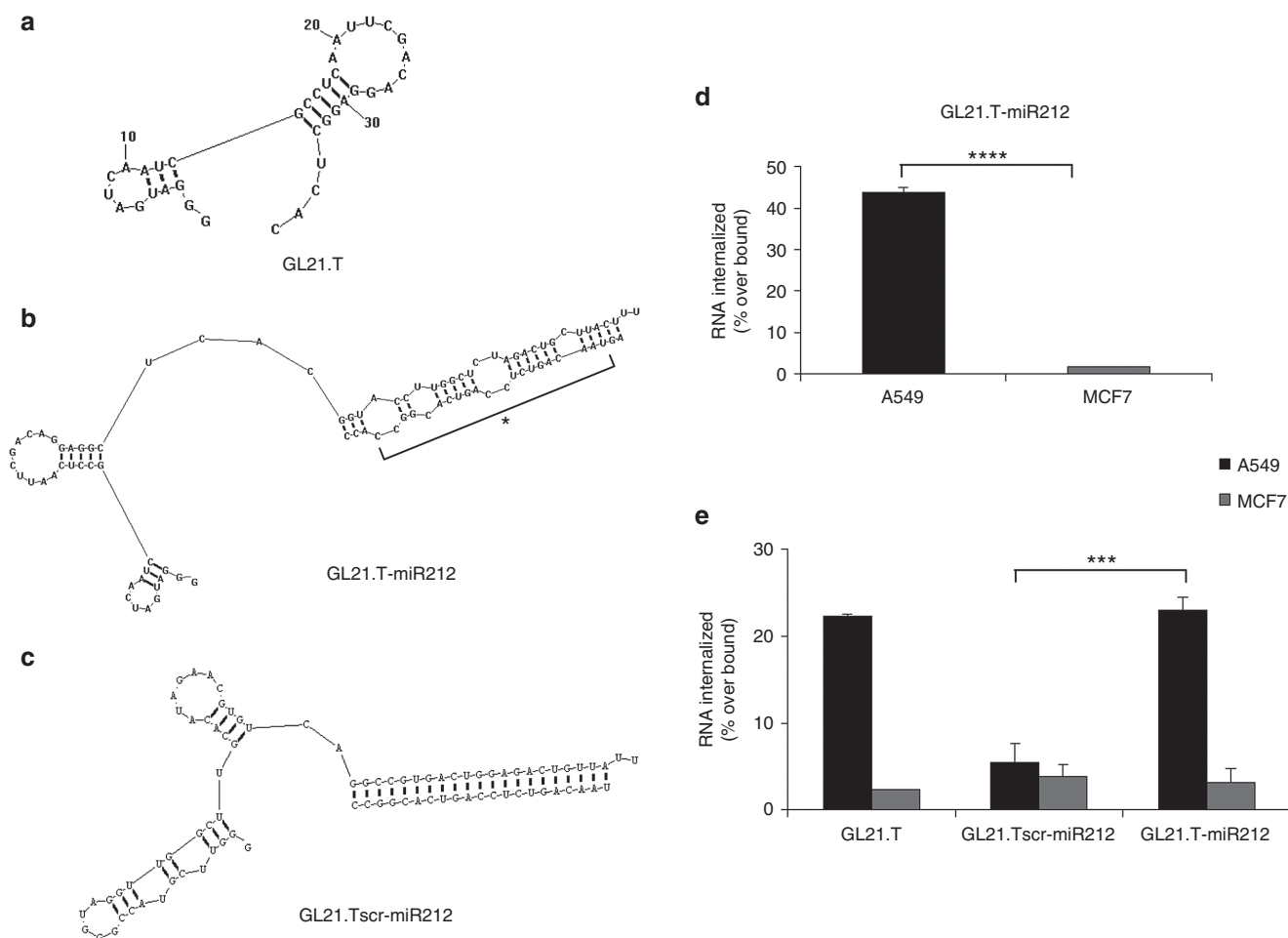


Figure 1 Chimera structure prediction and binding and internalization analysis. Secondary structure prediction of chimeras using RNA structure 5.3 program. (a) GL21.T aptamer; (b) GL21.T-miR212; (c) GL21.Tscr-miR212. MiR mature sequence is indicated with an asterisk. (d) Internalization assay for the 5'-[³²P]-labeled GL21.Tscr-miR212 and GL21.T-miR212 chimeras performed on A549 (Axl+) and MCF7 (Axl-) cells. The percentage of the RNA internalized over bound was obtained subtracting the counts relative to the scrambled chimera GL21.Tscr-miR212 used as negative control. Each bar shows the mean \pm SD values from three wells. (e) Internalization analysis of GL21.T, GL21.Tscr-miR212, and GL21.T-miR212 was monitored using quantitative RT-PCR (qRT-PCR) and normalizing to an internal RNA reference control for the PCR. The percentage of internalization has been expressed as the amount of internalized RNA relative to total bound RNA. Statistics were calculated using Student's *t*-test, **** $p < 0.0001$; *** $p < 0.001$. Each bar shows the mean \pm SEM values from three wells.

methodology.³⁰ GL21.T aptamer is able to bind and inhibit the signaling of Axl receptor, belonging to the TAM family of tyrosine kinase receptors. Axl family members are activated by growth-arrest-specific gene 6 (GAS6), a member of the vitamin K-dependent protein family, that resembles blood coagulation factors rather than typical growth factors.³¹ Axl overexpression has been reported in many human cancers and is associated with invasiveness and/or metastasis in lung,³² prostate,³³ breast,³⁴ gastric,³⁵ and pancreatic cancers,³⁶ renal cell carcinoma,³⁷ as well as glioblastoma.³⁸ Importantly, we have recently described the combinatorial potential of a chimera composed of GL21.T aptamer and a miRNA combining the clinical benefits of both moieties.²⁴ Here, we demonstrate selective delivery of miR-212 to Axl+ lung cancer cells with GL21.T resulting in restoration of TRAIL-mediated sensitivity in NSCLC cells. Treatment of Axl+ cells with the GL21.T-miR212 chimera resulted in caspase activation and in a concomitant reduction of cancer cell viability. In conclusion,

we describe a novel aptamer-miRNA chimera as a means to sensitize lung cancers to TRAIL therapy.

Results

Chimera design

To conjugate GL21.T aptamer and miR-212, a molecular chimera (termed GL21.T-miR212) was designed using the RNA structure 5.3 program. GL21.T is a 34-mer truncated version of the original GL21 aptamer, corresponding to the functional portion of the aptamer able to bind to and to antagonize Axl receptor.²⁹ GL21.T was used as a delivery carrier of human miR-212. For this purpose, the GL21.T sequence was elongated at its 3' end, by a covalent bond, with the sequence of the passenger strand of miR-212, and annealed to the guide strand. Even if full complementary miRNA sequences have been shown to be sufficient for targeted gene silencing,^{27,28} several recent reports on the use of molecular

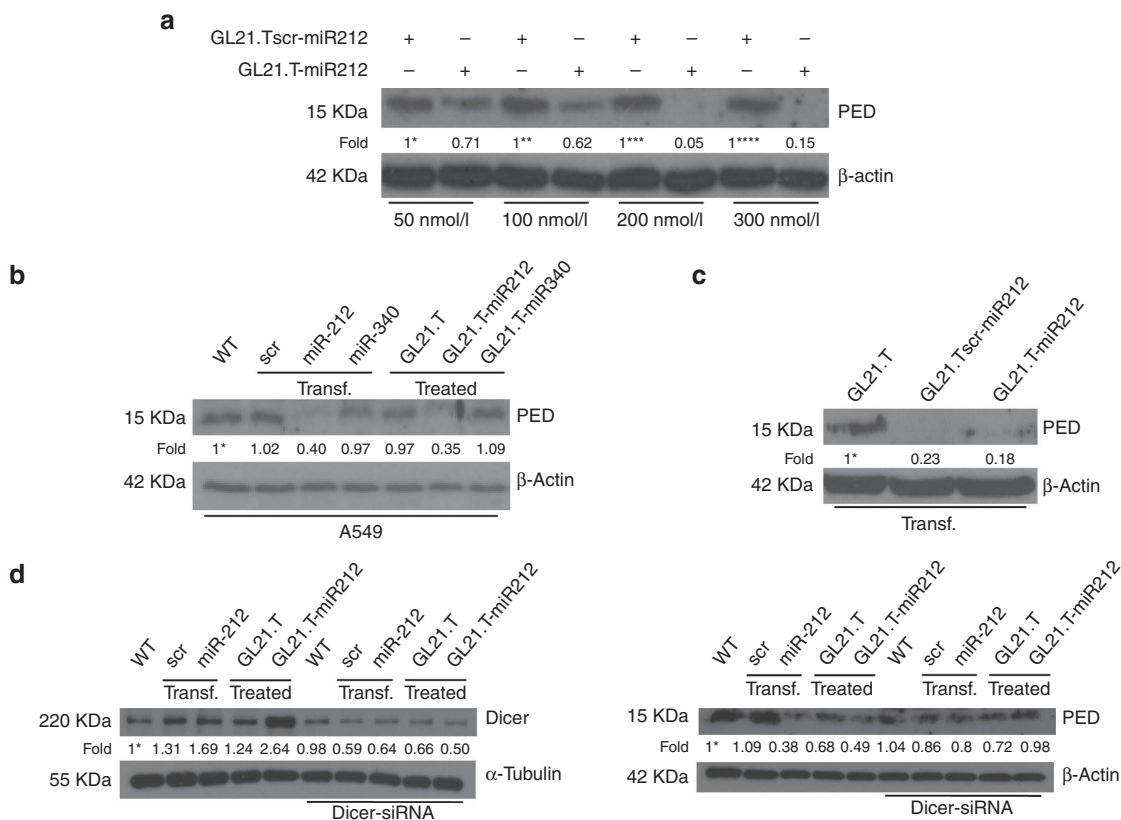


Figure 2 MiR-212 effect, aptamer-mediated specific delivery, and Dicer processing of GL21.T-miR212 chimera. (a) A549 cells were treated with different final concentrations (50, 100, 200, and 300 nM) of chimera and scrambled chimera for 48 hours. (b) A549 cells were incubated with GL21.T-miR340, GL21.T, and GL21.T-miR212 or alternatively were transfected with pre-miR-212 and pre-miR-340. (c) A549 cells were transfected with the aptamer alone, GL21.T:scr-miR212 and GL21.T-miR212. (d) A549 cells were transfected with control scrambled or pre-miR-212 or treated with the aptamer alone or GL21.T-miR212 in presence or absence of Dicer-siRNA. After 48 hours, the efficiency of si-Dicer transfection (left panel) was controlled by immunoblotting using anti-Dicer and anti- α -tubulin antibodies. The effect on the downregulation of target protein (right panel) was analyzed by immunoblotting with anti-PED and anti- β actin antibodies. Values below the blots indicate signal levels relative to (a) scrambled chimera-treated cells, arbitrarily set to 1 (with a different number of asterisks for each dose), or (b,d) to untreated cells (indicated as “WT”), and (c) to GL21.T-treated cells arbitrarily set to 1 (with asterisk). Intensity of bands was calculated using ImageJ (v1.46r). For a, b, and c, cell lysates were immunoblotted with anti-PED and anti- β actin antibodies.

aptamer-siRNA chimeras have shown that silencing efficacy and specificity can be improved by introducing internal partial complementarities and increased length extension with respect to the mature sequence in order to obtain a more effective Dicer substrate.^{26,39,40} Therefore, in order to encourage correct strand selection and thereby encourage target specificity, passenger and guide strands presented an imperfect pairing, consisting in a portion of stem-loop structure making the double strand similar to the pre-miR. A scrambled chimera, GL21.T:scr-miR212, was also designed, with the GL21.T sequence substituted by an unrelated sequence of the same length elongated with the miR-212 mimic passenger strand and annealed to the full complementary miR-212 guide strand. In both types of chimera, the antisense strand presented two overhanging bases (UU) at 3' end necessary for Dicer processing (Figure 1). Since, based on its predicted structure, the folding of GL21.T appears to be preserved also in the context of the chimera, we experimentally assessed the selective binding and the internalization potential of GL21.T-miR212 on Axl-expressing cells. Binding and internalization assays were performed using A549 (Axl+) cells, while MCF7 cells were used as negative control since they

do not express Axl. As shown in Figure 1, GL21.T-miR212 was able to bind to and internalize into A549 respect to the scrambled chimera used as control, but not in MCF7 cells, as assessed by two different methods (Figure 1d,e). Noteworthy, a similar percentage of internalization was obtained comparing GL21.T-miR212 and GL21.T alone (Figure 1e). These results indicate that, as previously reported for the GL21.T aptamer,²⁹ in the GL21.T-miR212 conjugate, the binding specificity of the GL21.T aptamer moiety is preserved and the conjugate is internalized into target cells in a receptor-dependent manner.

Dose-response effects and dicer processing of GL21.T-miR212 chimera

In order to characterize the effects of the chimera treatment on the miR-212 target, PED protein, A549 cells were treated with increasing amounts of GL21.T-miR212 and of control, GL21.T:scr-miR212, for 48 hours (Figure 2a). By western blot, we observed that PED levels were reduced in a dose-response manner by a concentration of 200 nM.

To test the specificity of the GL21.T-miR212 chimera and simultaneously evaluate the broad applicability of our delivery

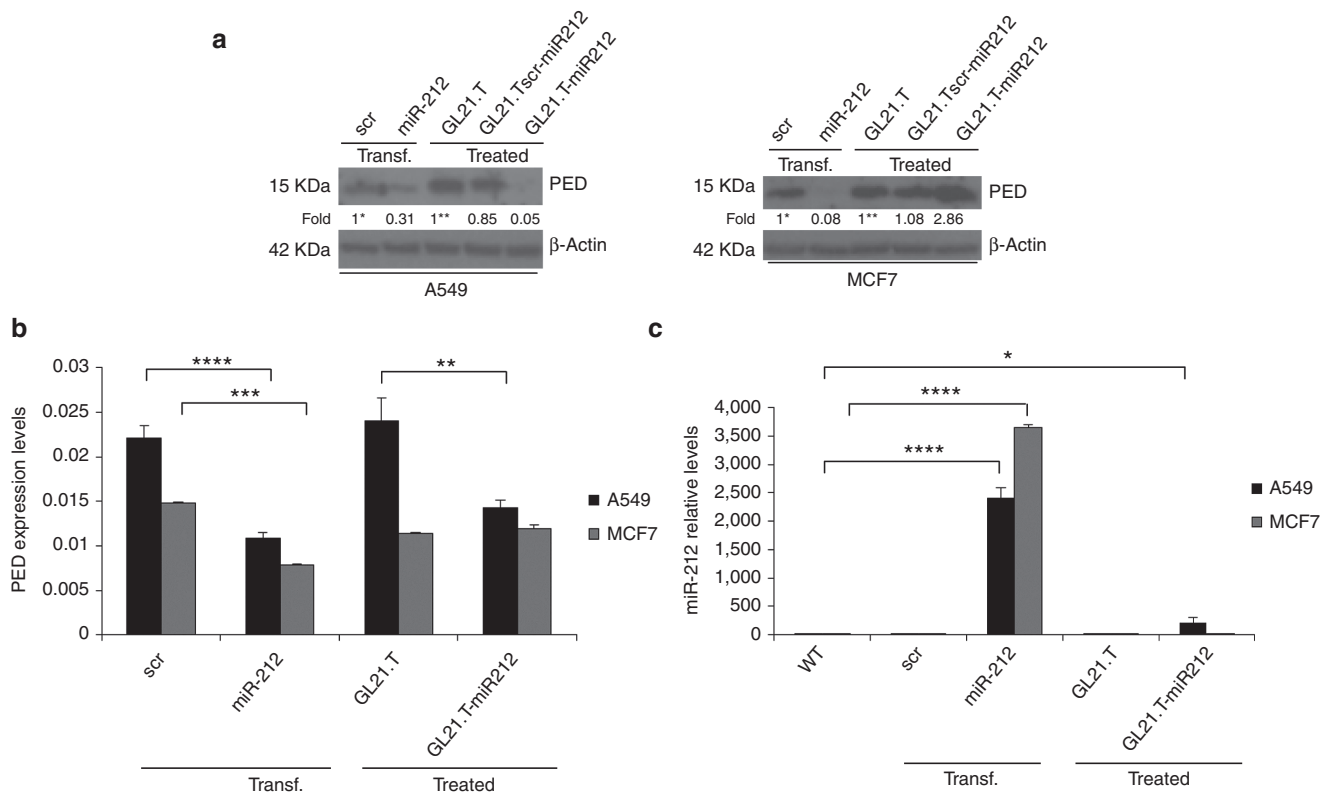


Figure 3 Cell-type specificity of chimera treatment. (a) A549 and MCF7 cells were treated with 300 nM of GL21.T-miR212 for 48 hours. GL21.T-scr-miR212 and GL21.T aptamer were used as negative controls, whereas transfection with 100 nM of pre-miR-212 was used as positive control. Control scrambled was used to assure transfection efficiency. Cell lysates were immunoblotted with anti-PED and anti- β actin antibodies for PED protein levels while (b) PED expression levels were analyzed by qRT-PCR. (c) The same samples were subjected to qRT-PCR for miR-212 expression levels analysis. Bands' intensity has been calculated as in Figure 2. In b and c each bar shows the mean \pm SD values from three wells. Statistics were calculated using Student's *t*-test, **** p < 0.0001; *** p < 0.001; ** p < 0.01; * p < 0.05.

platform, we conjugated the Axl aptamer to a different miR, miR-340. We have recently described that miR-340 has an onco-suppressive role in NSCLC by targeting *PUM1*, *PUM2*, and *SKP2*. The downregulation of these three genes was inversely correlated to *p27* expression.⁴¹ Treatment of A549 cells with GL21.T-miR340 resulted in an increase in miR-340 expression levels suggesting the proper internalization of the chimera. The effect on *SKP2* downregulation, as well as on the increase of *p27* levels, confirmed the effectiveness of the conjugate (Supplementary Figure S1). This effect was similar to that observed with transfection of A549 cells with miR-340 (used as positive control). In contrast, as anticipated, the aptamer alone and the aptamer conjugated to miR-340 (GL21.T-miR340) did not reduce PED protein levels under the same experimental conditions. By western blot, results showed that GL21.T-miR340 was not able to modify PED levels, thus indicating that PED downregulation was merely dependent on miR-212 moiety (Figure 2b).

To demonstrate that GL21.T-scr-miR212 was not functional due to the aptamer portion and not to inactivation of the miR sequence, A549 cells were transfected with the aptamer alone, GL21.T-scr-miR212 and GL21.T-miR212. As shown, following transfection, the scrambled chimera was as effective as the GL21.T-miR212 at downregulating PED protein levels (Figure 2c).

In order to investigate the mechanism by which the chimera was functional, A549 cells were transfected with a Dicer-specific siRNA and, then, treated with GL21.T-miR212. The co-transfection of pre-miR-212 was used as positive control. The efficiency of si-*Dicer* transfection and the effect on the downregulation of target protein were determined by immunoblotting (Figure 2d). As shown, in the presence of a Dicer-specific siRNA, GL21.T-miR212 was not able to reduce PED protein level, suggesting that Dicer was necessary for chimera processing.

Cell-type specificity of chimera treatment

To test whether PED downregulation was cell-type specific, A549 (Axl+) and MCF7 (Axl-) cells were treated with GL21.T-miR212 and GL21.T-scr-miR212. Transfection of pre-miR-212 and treatment with GL21.T aptamer were used as positive and negative controls, respectively. In A549 cells, GL21.T-miR212 downregulated PED both at mRNA level (measured using qRT-PCR) and protein level (assessed by immunoblotting with specific antibodies). As expected, no effect of the chimeras on PED expression was observed in MCF7 (Axl-negative) cells (Figure 3a,b). To confirm that the effects on PED protein levels were mediated by miR-212 upregulation, the same samples were evaluated by qRT-PCR to analyze miR-212 expression (Figure 3c). GL21.T delivered miR-212 inside the target cells, resulting in miR-212

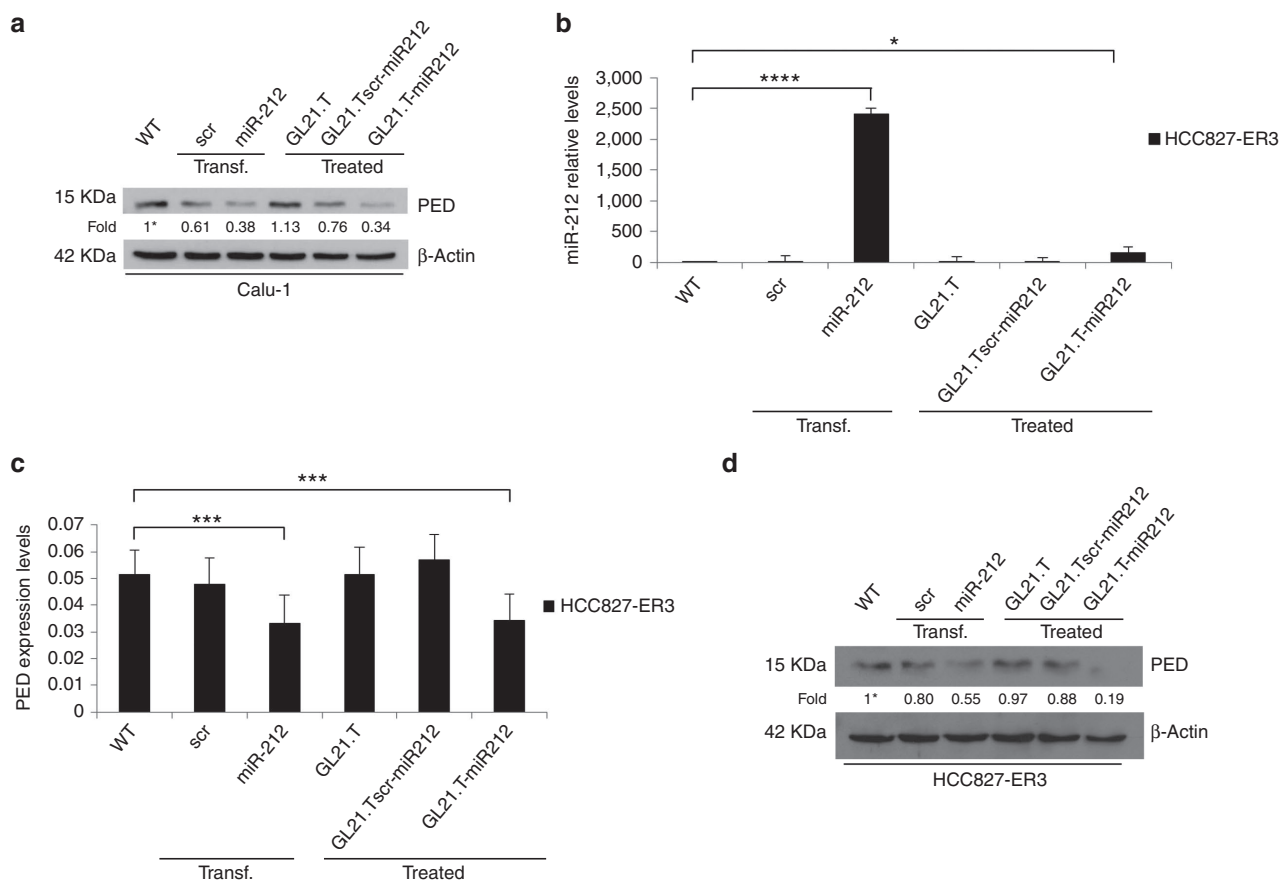


Figure 4 Effects of GL21.T-miR212 on additional Axl+ non-small cell lung cancer (NSCLC) cell lines. (a,d) Calu-1 and HCC827-ER3 cells were treated with 300 nM of GL21.T-miR212, GL21.T.Tscr-miR212, and GL21.T aptamer or, alternatively, transfected with 100 nM of pre-miR-212. After 72 hours for Calu-1 or 48 hours for HCC827-ER3, cells were collected and cell lysates were immunoblotted with anti-PED and anti- β actin antibodies for PED protein levels. (b) The same samples of HCC827-ER3 were subjected to qRT-PCR for miR-212 and (c) for PED expression levels analysis. In a,d values below the blots indicate signal levels relative to untreated cells (indicated as “WT”), arbitrarily set to 1 (with asterisk). Bands’ intensity has been calculated as in Figure 2. In b and c each bar shows the mean \pm SD values from three wells. Statistics were calculated using Student’s *t*-test, **** $p < 0.0001$; *** $p < 0.001$; * $p < 0.05$.

upregulation. Furthermore, despite the fact that the intracellular levels of miR-212 were lower in cells treated (no transfection reagent used) with GL21.T-miR212 compared with cells transfected with the pre-miR, the effects on PED downregulation were comparable. Results indicate that the efficiency of the conjugate to deliver functional miR-212 and thus modulate the expression of miRNA target genes is similar to that observed with transfection. We also validated the effect of GL21.T-miR212 on PED downregulation in other NSCLC Axl+ cell lines, Calu-1 and HCC827-ER3 (Figure 4).

Receptor-dependent internalization of GL21.T-miR212 chimera

To confirm receptor-dependent internalization of GL21.T-miR212 chimera, we silenced Axl levels in A549 cells with RNAi. Following 48 hours of si-Axl transfection, we tested the binding and internalization potential of GL21.T-miR212. As expected, we observed a statistically significant decrease in bound/internalized GL21.T aptamer and chimera in A549 (siAxl)-treated cells. In contrast, no differences in binding/internalization were observed for the

scrambled chimera (Figure 5a). The efficiency of si-Axl transfection and the effect on the downregulation of target protein were determined by immunoblotting (Figure 5b). Alternatively, Axl levels were transiently upregulated transfecting Axl cDNA. Following Axl overexpression, the treatment with GL21.T-miR212 increased miR-212 levels by twofold compared with parental A549. Simultaneously, the conjugate decreased PED levels to the same extent in parental and transfected A549 cells (Figure 5c). Thus, we conclude that the functional delivery of miR-212 is dependent on the amount of Axl on the cell surface and that the additional miR-212 delivered is not necessary to increase the effect on PED downregulation. We next assessed whether internalization of the conjugate was Axl mediated. MCF7 cells were transiently transfected with Axl cDNA and levels of miR-212 evaluated following treatment with the conjugate. As predicted, miR-212 levels were higher in cells treated with GL21.T-miR212, compared with the treatment with GL21.T.Tscr-miR212 or the aptamer alone, thus indicating that internalization of GL21.T-miR212 chimera is receptor dependent (Supplementary Figure S2).

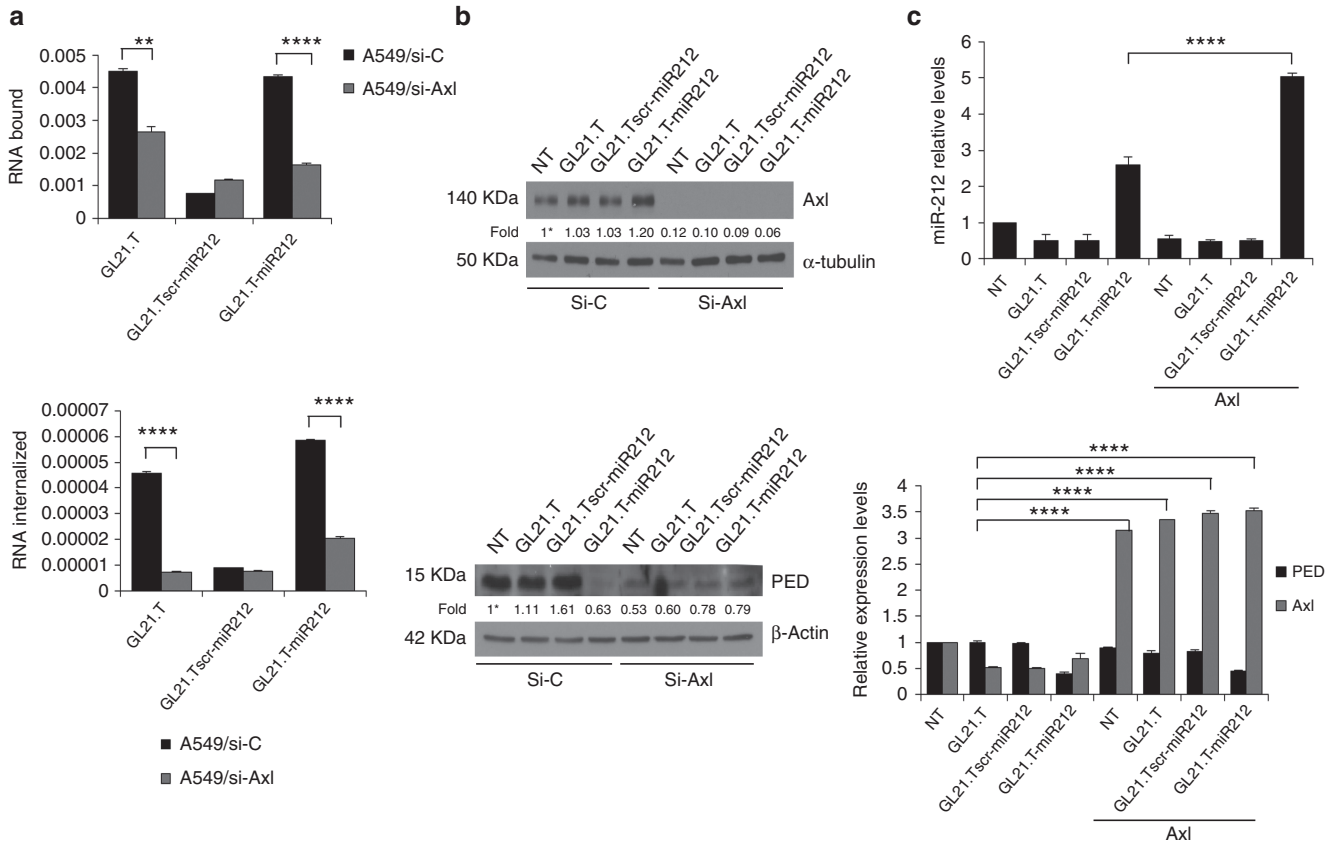


Figure 5 Receptor-dependent internalization of GL21.T-miR212 chimera. (a) A549 cells were transfected with si-Axl or siRNA control for 24 hours and, then, treated with GL21.T-miR212, the scrambled chimera or with the aptamer alone to perform the binding (upper panel) and internalization (lower panel) assays. Each bar shows the mean \pm SEM values from three wells. (b) The efficiency of si-Axl transfection and the effect on the downregulation of target protein were evaluated after 48 hours of treatment by immunoblotting with anti-Axl and anti-tubulin, in the upper panel, and with anti-PED and anti- β actin antibodies, in the lower panel. Values below the blots indicate signal levels relative to untreated cells (indicated as “WT”), arbitrarily set to 1 (with asterisk). Bands’ intensity has been calculated as in Figure 2. (c) A549 (Axl+) cells, following 24-hour transfection with Axl TruClone (Axl), were treated with 300 nM of GL21.T-miR212, GL21.T:sc-miR212, or GL21.T for additional 48 hours. miR-212 (upper panel), *PED* and *Axl* (lower panel) levels were quantified by RT-qPCR. Each bar shows the mean \pm SD values from three wells. Statistics were calculated using Student’s *t*-test, **** $p < 0.0001$; ** $p < 0.01$.

GL21.T-miR212 regulates TRAIL-induced cell death

We have previously shown that the TRAIL-resistant phenotype in NSCLC is related to aberrant elevated levels of PED. Furthermore, we showed that ectopic expression of miR-212 (achieved with a miR mimic) downregulates *PED* and re-establishes sensitivity to TRAIL.^{14,17} To investigate whether treatment with the chimera induced sensitivity to TRAIL, we treated A549 cells with GL21.T-miR212. GL21.T:sc-miR212 and transfected pre-miR-212 were included as negative and positive controls, respectively. Caspase-8 activation was evaluated following treatment with TRAIL for 3 hours by western blot (Figure 6a). As shown, cleavage of caspase-8 was evident in cells treated with GL21.T-miR212 or, alternatively, transfected with pre-miR-212, but not with the GL21.T:sc-miR212, and accompanied by the activation of caspase 3/7, assessed by Caspase-Glo® 3/7 Assay (Figure 6b). Thus, sensitization to TRAIL upon treatment with the chimera was selective for Axl-expressing cells as demonstrated by the activation of caspase 3/7. To further confirm that the chimera sensitizes cancer cells to TRAIL-induced apoptosis, we evaluated the percentage of apoptotic cells after TRAIL treatment (Figure 7a). Transfected or treated cells were labeled with

Annexin V-FITC and propidium iodide and analyzed using flow cytometry. GL21.T-miR212 increased the percentage of apoptotic (Annexin V—positive, PI—negative) cells following TRAIL treatment, as miR-212 was used as positive control. In addition, we measured cell viability using an MTT assay that showed the same results (Figure 7b). GL21.T-miR340 treatment did not produce any gain in TRAIL sensitivity (Figure 7c). In summary, the GL21.T-miR212 chimera was able to increase the activation of caspase3/7 and, consequently, TRAIL-induced cell death in A549 cells, but not in MCF7 cells. TRAIL sensitization mediated by GL21.T-miR212 treatment was also confirmed on additional NSCLC cell lines, Calu-1 and HCC827-ER3, which display a TRAIL-resistant phenotype (Figure 8).

Discussion

NSCLC represents about 80% of all lung cancers and is mostly diagnosed at an advanced stage (either locally advanced or metastatic disease). Because of resistance to therapeutic drugs, standard treatment of this tumor has

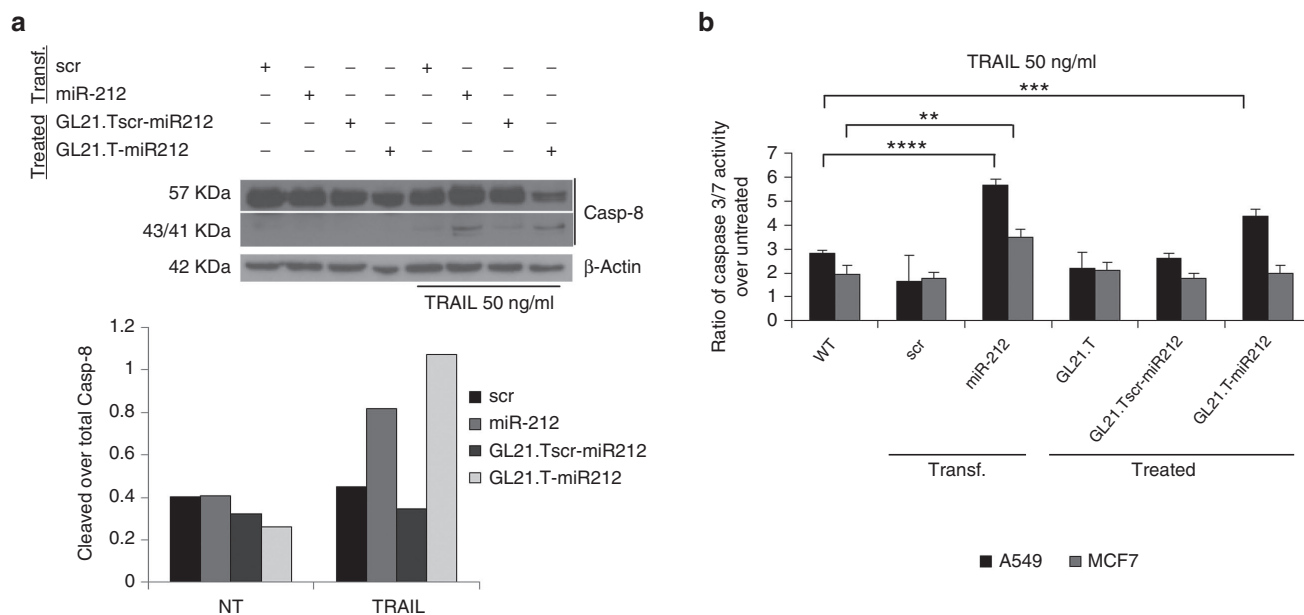


Figure 6 Caspases activation induced by GL21.T-miR212. (a) A549 cells were transfected with 100 nM of pre-miR-212 or alternatively treated with 300 nM of GL21.T-miR212 for 48 hours. Scrambled miR and scrambled chimera were used as negative controls. Cells were, then, treated for 3 hours with TNF-related apoptosis-inducing ligand (TRAIL) 50 ng/ml, and cell lysates were immunoblotted with anti-caspase-8 antibody (upper panel). Band intensity is represented in the diagram of the lower panel as a ratio of cleaved over total caspase-8, both quantization normalized over β -actin. (b) A549 and MCF7 cells were transfected with pre-miR-212 or treated with the unconjugated aptamer, the scrambled chimera and GL21.T-miR212 for 48 hours and then incubated with 50 ng/ml of TRAIL for 6 hours. The activation of caspase 3/7 was measured by Caspase-Glo® 3/7 Assay. Each bar shows the mean \pm SD values from three wells. Statistics were calculated using Student's *t*-test, *****p* < 0.0001; ****p* < 0.001; ***p* < 0.01.

only a 20% to 30% positive clinical response. Over the last years, the discovery of the pivotal of epidermal growth factor receptor (EGFR) in tumorigenesis has opened the way to a new class of targeted therapeutic agents: the EGFR tyrosine kinase inhibitors (EGFR TKIs). Since their introduction in therapy, in advanced NSCLC patients harboring EGFR mutations, the use of EGFR TKIs in first-line treatment has provided an unusually large progression-free survival benefit with a negligible toxicity when compared with cytotoxic chemotherapy. Nevertheless, resistance invariably occurs.⁴² In this setting, TRAIL emerged as a novel therapeutic agent. TRAIL (ApoL/TNF-related apoptosis-inducing ligand) is a relatively new member of the tumor necrosis factor (TNF) ligand family, which induces apoptosis in a variety of cancers.

Initial promising studies demonstrated its remarkable specificity in inducing apoptosis in tumor cell lines, but not in normal cells both *in vitro* and *in vivo*.⁷ This unique property makes TRAIL an attractive candidate for targeted cancer therapy.^{43,44} However, resistance to TRAIL-induced apoptosis poses a challenge for effective anticancer strategies. To overcome this problem, drug cocktails in combination with TRAIL therapy have been proposed in order to induce synergism or sensitize resistant cancer cells. Toward this end, a number of combinatorial treatments with chemotherapeutic agents are in phase 1/2 of clinical studies.^{45–47} More recently, aptamer-siRNA/miRNA chimeras have been proposed as novel adjuvants to standard chemotherapy.^{48,49} Unlike nontargeted drugs, the advantage of these new class of biodrugs is that they are specifically delivered into target cells where they release their therapeutic cargo, thus limiting toxicity to normal cells.

In this study, we designed a chimera composed of a RNA aptamer to Axl (GL21.T) and miR-212 as a means to deliver functional miR-212 into TRAIL-resistant Axl+ A549 cells, but not into Axl- MCF7 cells. Indeed, GL21.T-miR212 selectively sensitizes the A549 cells to TRAIL-induced apoptosis, proving to be a unique tool to synergize with TRAIL in mediating cell death.

To increase specificity and facilitate large-scale chemical synthesis,^{24,26,50} we conjugated a truncated version of the GL21 aptamer (GL21.T) to the tumor suppressor miR-212 duplex sequence. We demonstrated that in the context of the chimera, the active sequence (sequence required for binding to Axl) of GL21 is preserved, thus providing high binding affinity and the subsequent selective internalization of the conjugate into Axl+ cells. The miRNA moiety is a 25/27mer duplex having two overhanging bases (UU) at the 3' end of the passenger strand, thus adopting the conformation described as Dicer substrate for duplex siRNAs.⁵¹ By using a similar approach with miRNAs, we have recently shown that nonperfect duplex miRNAs are correctly processed by Dicer, increasing the gene target specificity of the miRNA moiety.²⁴ Indeed, the optimal loading of the guide strand into RNA-induced silencing complex (RISC) is thought to reduce off-target effects that result from inappropriate incorporation of both miRNA strands into the silencing complex.⁵²

A major limitation to the use of RNA-based drugs *in vivo* is the rapid degradation (within few minutes) of natural RNAs in serum or blood. As previously described, in order to protect the GL21.T aptamer from degradation, it was generated as a 2'-F-Py containing RNA.²⁹ Therefore, in order to increase the stability of the entire GL21.T-miR212 molecule, we substituted the

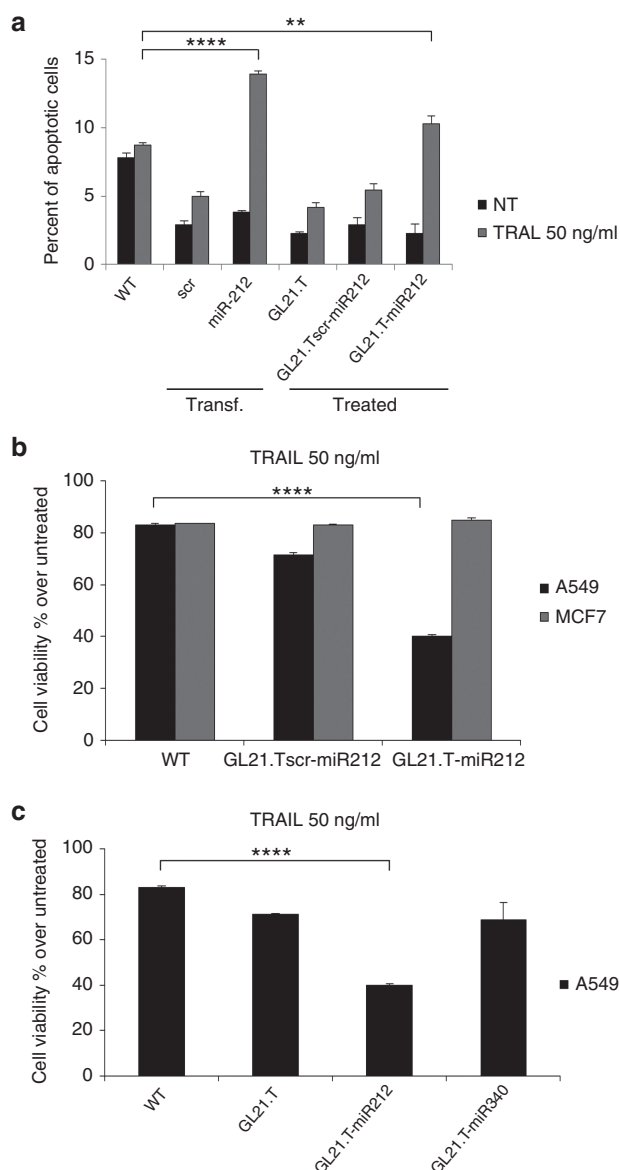


Figure 7 TNF-related apoptosis-inducing ligand (TRAIL) sensitization induced by GL21.T-miR212. (a) A549 cells were transfected with pre-miR-212 and control scrambled or treated with the chimera, the scrambled chimera and the unconjugated aptamer for 48 hours. Cells were, then, incubated with TRAIL for 24 hours, and the percentage of apoptotic cells was evaluated by flow cytometry. (b) A549 and MCF7 cells were treated with 300nM of GL21.T-miR212 and GL21.T:scr-miR for 48 hours and were exposed to TRAIL for 24 hours at 50 ng/ml as final concentration. (c) A549 cells were treated with the unconjugated aptamer, GL21.T-miR212 or GL21.T-miR340 for 48 hours and were exposed to TRAIL for 24 hours at 50 ng/ml as final concentration. For **b** and **c** cell viability was evaluated with MTT assay. In **a**, **b** and **c** each bar shows the mean \pm SD values from three wells. Statistics were calculated using Student's *t*-test, **** $p < 0.0001$; ** $p < 0.01$.

pyrimidines with 2'-F-Py at all positions. This modification is well characterized in humans and is reported to be well tolerated with little toxicity.⁵³ RNA aptamers with this modification have already been approved for their use in humans (Macugen), with many more quickly moving through the clinical pipeline.⁵⁴

Although we cannot completely rule out potential intracellular toxicity of 2'-F-Py-modified RNAs leading to nonspecific immunostimulation, experiments *in vivo* demonstrated that problematic toxicity in humans is not expected.^{24,26}

The silencing moiety of the chimera is constituted by the miR-212, a tumor suppressor miRNA that acts by negatively modulating PED expression, an onco-protein with a broad anti-apoptotic action. Indeed, the presence of elevated cellular levels of PED has been shown to contribute to resistance to TRAIL-induced cell death in several human tumors, including breast and lung cancer.^{17,55} The DED domain of PED acts as a competitive inhibitor for pro-apoptotic molecules during the assembly of a functional DISC and inhibiting the activation of caspase-8, which take place following treatment with different apoptotic cytokines (CD95/FasL, TNF- α , and TRAIL). These data demonstrate that GL21.T-miR212 is a functional molecule that upon internalization, downregulates PED in a dose-dependent manner, reaching a plateau at around 200nM. In turn, target cells become sensitive to TRAIL and upon treatment undergo apoptosis following caspase-8 and caspase-3 activation.

Based on the suppressive action of miR-212 on PED expression as a means to sensitize cancer cells to TRAIL, here we demonstrated that GL21.T-miR212 chimera can sensitize target cells in a high selective manner. Specifically, exogenous miR-212 delivered by GL21.T aptamer led to TRAIL sensitization via activation of the apoptotic cascade selectively in A549, NSCLC Axl+ cells. In conclusion, the approach presented in this work indicates an innovative tool for a combined therapy that makes use of an aptamer-based molecular chimera to selectively sensitize TRAIL-resistant target tumor cells.

Materials and methods

Cell lines and transfection. A549 and HCC827-ER3 cells were grown in RPMI 1640 while MCF7 and Calu-1 cells were grown in Dulbecco's modified Eagle's medium. A549, MCF7, and Calu cells were from American Type Culture Collection, while HCC827-ER3 were kindly provided by Dr. Balazs Halmos (Columbia University Medical Center, New York, NY). Their media were supplemented with 10% heat-inactivated fetal bovine serum, 2mM of glutamine, and 100U/ml of penicillin/streptomycin. For miRNAs transient transfection, cells were transfected with 100nM (final concentration) of miRNA stem-loop precursor hsa-miR212, hsa-miR340, or negative control 1 (Ambion, Foster City, CA) using Oligofectamine (Invitrogen, Carlsbad, CA). Also si-control and si-Axl (Santa Cruz Biotechnology, Santa Cruz, CA) were transfected using Oligofectamine (Invitrogen), according to the manufacturer's protocol. For aptamer and chimeras transient transfection, cells were transfected with 100nM (final concentration) of RNAs, using Lipofectamine 2000 (Invitrogen). Also Axl TruClone (Origene, Rockville, MD) and si-Dicer (Cell Signaling Technology, Beverly, MA) were transfected with Lipofectamine 2000, according to the manufacturer's protocol.

Aptamer-miRNA chimeras. The following sequences were used for the chimera production: GL21.T-miR212 passenger strand:

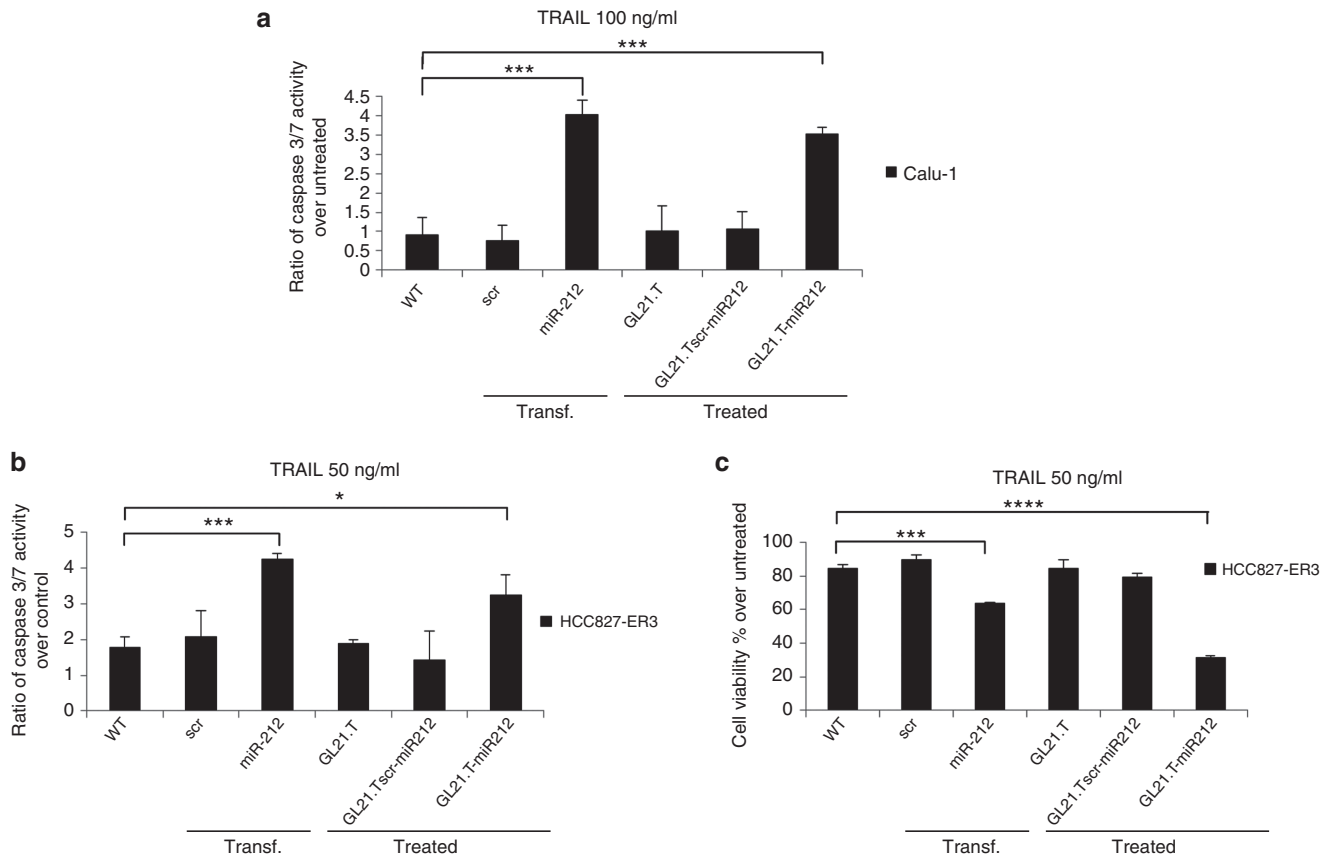


Figure 8. TNF-related apoptosis-inducing ligand (TRAIL) sensitization induced by GL21.T-miR212 in additional Axl+ non-small cell lung cancer (NSCLC) cell lines. Calu-1 and HCC827-ER3 cells were transfected with pre-miR-212 or treated with the unconjugated aptamer, the scrambled chimera and GL21.T-miR212. (a,b) After 72 hours for Calu-1 or 48 hours for HCC827-ER3 of treatment or transfection, cells were incubated with TRAIL (100 ng/ml in Calu-1 and 50 ng/ml in HCC827-ER3) for 6 hours. The activation of caspase 3/7 was measured by Caspase-Glo® 3/7 Assay. (c) The same samples of HCC827-ER3 were exposed to TRAIL for 24 hours, and cell viability was evaluated with MTT assay. Each bar shows the mean \pm SD values from three wells. Statistics were calculated using Student's *t*-test, *****p* < 0.0001; ****p* < 0.001; **p* < 0.05.

5'GGGAUGAUCAAUCGCCUCAAUUCGACAGGAGG CUCACGGUACCUUGGCUCUAGACUGCUUACUUU. miR-212 guide strand: 5' AGUACAGUCUCCAGUCACGGCC ACC. GL21.T:scr-miR212 passenger strand: 5'GGGUUCGU ACCGGUAGGUUGGCUUGCACAUAGAACGUGUCAGG CCGUGACUGGAGACUGUUAUU. miR-212 (1g) guide strand: 5' UACAGUCUCCAGUCACGGCC. GL21.T: 5' GGG AUGAUCAAUCGCCUCAAUUCGACAGGAGGCUCAC. GL21.T-miR340 passenger strand: 5'GGAUGAUCAAUCG CCUCAAUUCGACAGGAGGCUCACAAUCAGUCUCA UUGC UUAUAAUU. miR-340 guide strand: 5' UUAUAAA GCAAUGAGACUGAUU.

All RNAs were custom synthesized by TriLink Biotechnologies (San Diego, CA) as 2'-fluoropyrimidine RNAs. UU in bold are 3'-overhang. The control conjugate is composed of an unrelated aptamer sequence linked to the fully complementary miR-212 duplex. In the context of the control conjugate, it was necessary to use a fully complementary miR-212 to stabilize the functional miR duplex and prevent unwanted intramolecular interactions with the scrambled aptamer sequence.

To prepare GL21.T-miR212, GL21.T:scr-miR212, and GL21.T-miR340, 5 μ M of aptamer-passenger RNA strand

was denatured at 98 °C for 20 minutes, combined with 5 μ M of the appropriate guide strand at 55 °C for 10 minutes in binding buffer 10 \times (200 mM N-2-Hydroxyethylpiperazine-N'-2-Ethanesulfonic Acid, pH 7.4, 1.5 M NaCl, 20 mM CaCl₂) and then warmed up to 37 °C for 20 minutes.

Cell binding and internalization assays. Aptamer binding and internalization have been assessed by two different methods, by radioactivity labeling or by quantitative reverse transcription-PCR (qRT-PCR)

Radioactivity labeling. A549 and MCF7 cells were plated in 24 multiwell plates in triplicate. RNAs were 5'-[³²P]-labeled and incubated at 200 nM as final concentration on cells at 37 °C for 15 minutes. After several washings, the amount of ³²P-labeled RNA recovered in SDS 1% was determined by scintillation counting. In contrast, to check the endocytosis rate, after the incubation with radiolabeled chimeras, the cells were subjected to a stringent high-salt wash, with High Salt phosphate-buffered saline (PBS; 0.5M NaCl), to remove any unbound RNAs or RNAs bound to the cell surface. Following 5-minute treatment at 4 °C, the amount of ³²P-labeled RNA internalized was recovered in Sodium Dodecyl Sulfate 1% and determined by scintillation counting. In both assays, results were normalized for cell

number. The background values obtained with the scrambled chimera were subtracted from the values obtained with GL21.T-miR212. Finally, the resulting recovered RNAs were plotted as percent of RNA internalized over RNA bound.

qRT-PCR method. Target (A549) and nontarget (MCF7) cells were incubated with 100 nM of aptamer or chimeras for 15 minutes at 37 °C with 5% CO₂. Cells were washed with ice-cold PBS or incubated with High Salt PBS (0.5M NaCl) at 4 °C for 5 minutes, and RNA was recovered using TRIzol reagent (Invitrogen). Samples were normalized to an internal RNA reference control. Specifically, 0.5 pmol per sample CL4 aptamer⁵⁶ was added to each sample along with TRIzol as a reference control. Recovered RNAs were quantitated using Reverse Transcriptase M-MuLV (Roche Life Science, Basel, Switzerland) with SYBR Green (BioRad) with a Biorad iCycler. All reactions were done in a 25-ml volume in triplicate with specific primers (GL21.T 5': TAATACGACTCATATAGGGATGATC; 3': GTGAGCCTCCTGTcGAAT; GL21.Tscr 5': TTCGTACCGGGTAGGTT; 3': TGACACGTTCTATGTGCA) and CL4 reference control (CL4 5': TAATACGACTCACTATAGGGGCCTTA; 3': GCCTCCTGTGCAATCG).

For each cell line, the percentage of internalization has been expressed as the amount of internalized RNA relative to total bound RNA without normalizing for background. The same protocol was used for the experiment on A549 cells upon transfection with si-control and si-AXL.

Protein isolation and immunoblotting. Cells were treated with chimeras for 48 hours, or alternatively Calu-1 for 72 hours, and then were washed twice in ice-cold PBS and lysed in Lysis buffer (50 mM N-2-Hydroxyethylpiperazine-N'-2-Ethanesulfonic Acid pH 7.5 containing 150 mM NaCl, 1% GLYCEROL, 1% Triton 100x, 1.5 mM MgCl₂, 5 mM ethylene glycol tetraacetic acid, 1 mM Na₃VO₄ and 1X protease inhibitor cocktail). Protein concentration was determined by the Bradford assay (BioRad, Hercules, CA) using bovine serum albumin as the standard, and equal amounts of protein were analyzed by Sodium Dodecyl Sulfate Polyacrylamide Gel Electrophoresis (15% acrylamide). Gels were electroblotted onto nitrocellulose membrane (Merck Millipore, Billerica, MA). For immunoblot experiments, membranes were blocked for 1 hour with 5% non-fat dry milk in tris-buffered saline containing 0.1% Tween-20 and incubated at 4 °C overnight with primary antibody. Detection was performed by peroxidase-conjugated secondary antibodies using the enhanced chemiluminescence system (GE Healthcare Life Sciences, Pittsburgh, PA). Primary antibodies used were anti-PED,⁵⁷ anti-Caspase-8, anti-p27, and anti-Dicer from Cell Signaling Technology, anti- α tubulin from Santa Cruz Biotechnology, anti- β actin from Sigma-Aldrich (St. Louis, MO), and anti-Axl from R&D Systems (Minneapolis, MN).

RNA extraction and Real-time PCR. Cells were treated with 300 nM of chimeras for 48 hours, and then total RNAs (miRNA and mRNA) were extracted using TRIzol (Invitrogen) according to the manufacturer's protocol. Reverse transcription of total miRNA was performed starting from equal amounts of total RNA/sample (1 μ g) using miScript reverse Transcription Kit (Qiagen, Hilden, Germany). Quantitative analysis of miRNAs and RNU6B (as an internal reference) was performed by real-time PCR using specific primers (Qiagen) and miScript

SYBR Green PCR Kit (Qiagen). The reaction for detection of miRNAs was performed as follows: 95 °C for 15 minutes, 40 cycles of 94 °C for 15 seconds, 55 °C for 30 seconds, and 70 °C for 30 seconds. All reactions were run in triplicate. For reverse transcription of mRNA, we used SuperScript® III Reverse Transcriptase (Life Technologies). Quantitative analysis of *PED*, *AXL*, and *actin* (as an internal reference) was performed by real-time PCR using specific primers and iQ™ SYBR Green Supermix (BioRad). The threshold cycle (CT) is defined as the fractional cycle number at which the fluorescence passes the fixed threshold. For quantization has been used the 2^(- Δ CT) method, where Δ Ct is the difference between the amplification fluorescent thresholds of the miRNA of interest and the miRNA of U6 used as an internal reference. Instead, fold changes were calculated with 2^(- $\Delta\Delta$ CT) method as previously described.⁵⁸ Experiments were carried out in triplicate for each data point, and data analysis was performed by using software (Bio-Rad).

Cell death quantification. A549, MCF7, and HCC827-ER3 cells were treated with GL21.T-miR212 and GL21.Tscr-miR212 300 nM for 3 hours. Then, cells were plated in 96 multiwell plates in triplicate for 48 hours and incubated with TRAIL (Vinci-Biochem, Firenze, Italy) at a final concentration of 50 ng/ml for 24 hours. Cell viability was assessed with CellTiter 96 Aqueous One Solution Cell Proliferation Assay (Promega, Madison, WI). Metabolically active cells were detected by adding 20 μ l of 3-(4,5-dimethylthiazol-2-yl)-5-(3-carboxymethoxyphenyl)-2-(4-sulfophenyl)-2H-tetrazolium to each well, and plates were analyzed in a Multilabel Counter (BioTek, Winooski, VT).

Caspase 3/7 assay. The assay was performed with the use of Caspase-Glo® 3/7 Assay (Promega) according to the manufacturer's protocol. Briefly, A549, MCF7, and HCC827-ER3 cells were before transfected with pre-miR-212 or treated with GL21.T, GL21.Tscr-miR212, GL21.T-miR212 for 48 hours, or alternatively Calu-1 for 72 hours, and, then, incubated for 6 hours with TRAIL. An equal volume of Caspase-Glo 3/7 reagent was added to each well for 30 minutes in the dark, and luminescence was measured by luminometer (Turner BioSystems-Promega). The ratio of caspase 3/7 activity over control was calculated normalizing treated samples over untreated ones.

Flow cytometry. Apoptosis was analyzed via Annexin V-FITC Apoptosis Detection kit I (BD Biosciences, San Diego, CA). A549 cells were transfected with pre-miR-212 or treated with GL21.T, GL21.Tscr-miR212, GL21.T-miR212 for 48 hours and, then, incubated for 24 hours with TRAIL. The cells were washed in PBS, resuspended in binding buffer 10x, and labeled with Annexin V-FITC and propidium iodide according to the manufacturer's protocol. After incubation at room temperature for 15 minutes in the dark, cells were analyzed with a BD Accuri™ C6 Flow cytometry (BD Biosciences). To calculate the percent of apoptotic cells, the gate was placed on annexin V-positive, PI-negative cells, and thus double positive cells were excluded from the analysis.

Supplementary material

Figure S1. GL21.T-miR340 characterization.

Figure S2. Internalization of the GL21.T-miR212 conjugate in MCF7 exogenously expressing Axl.

Acknowledgments This work was partially supported by funds from Associazione Italiana Ricerca sul Cancro, AIRC (grant n.ro 10620) to G.C. and AIRC (grant n.ro 13345) to V.d.F.; MERIT (RBNE08E8CZ_002) to G.C., POR Campania FSE 2007–2013, Project CREME to G.C., Fondazione Ber-lucchi to G.C. This work was partially supported by grants to P.H.G. from the National Institutes of Health (R01CA138503 and R21DE019953), Mary Kay Foundation (9033-12 and 001-09), Elsa U Pardee Foundation (E2766) and the Roy J Carver Charitable Trust (RJCCT 01-224). M.I. was supported by the ‘Federazione Italiana Ricerca sul Cancro’ (FIRC) Post-Doctoral Research Fellowship. G.R. was supported by a MERIT project Fellowship. The authors declare no conflict of interest.

- Aggarwal, BB, Gupta, SC and Kim, JH (2012). Historical perspectives on tumor necrosis factor and its superfamily: 25 years later, a golden journey. *Blood* **119**: 651–665.
- Grewal, IS (2009). Overview of TNF superfamily: a chest full of potential therapeutic targets. *Adv Exp Med Biol* **647**: 1–7.
- Wielockx, B, Lannoy, K, Shapiro, SD, Itoh, T, Itoharu, S, Vandekerckhove, J et al. (2001). Inhibition of matrix metalloproteinases blocks lethal hepatitis and apoptosis induced by tumor necrosis factor and allows safe antitumor therapy. *Nat Med* **7**: 1202–1208.
- Ni, R, Tomita, Y, Matsuda, K, Ichihara, A, Ishimura, K, Ogasawara, J et al. (1994). Fas-mediated apoptosis in primary cultured mouse hepatocytes. *Exp Cell Res* **215**: 332–337.
- Galle, PR, Hofmann, WJ, Walczak, H, Schaller, H, Otto, G, Stremmel, W et al. (1995). Involvement of the CD95 (APO-1/Fas) receptor and ligand in liver damage. *J Exp Med* **182**: 1223–1230.
- Ashkenazi, A, Pai, RC, Fong, S, Leung, S, Lawrence, DA, Marsters, SA et al. (1999). Safety and antitumor activity of recombinant soluble Apo2 ligand. *J Clin Invest* **104**: 155–162.
- Walczak, H, Miller, RE, Ariail, K, Gliniak, B, Griffith, TS, Kubin, M et al. (1999). Tumoricidal activity of tumor necrosis factor-related apoptosis-inducing ligand *in vivo*. *Nat Med* **5**: 157–163.
- Fiory, F, Formisano, P, Perruolo, G and Beguinot, F (2009). Frontiers: PED/PEA-15, a multifunctional protein controlling cell survival and glucose metabolism. *Am J Physiol Endocrinol Metab* **297**: E592–E601.
- Zanca, C, Cozzolino, F, Quintavalle, C, Di Costanzo, S, Ricci-Vitiani, L, Santoriello, M et al. (2010). PED interacts with Rac1 and regulates cell migration/invasion processes in human non-small cell lung cancer cells. *J Cell Physiol* **225**: 63–72.
- Quintavalle, C, Di Costanzo, S, Zanca, C, Tasset, I, Fraldi, A, Incoronato, M et al. (2014). Phosphorylation-regulated degradation of the tumor-suppressor form of PED by chaperone-mediated autophagy in lung cancer cells. *J Cell Physiol* **229**: 1359–1368.
- Garofalo, M, Romano, G, Quintavalle, C, Romano, MF, Chiurazzi, F, Zanca, C et al. (2007). Selective inhibition of PED protein expression sensitizes B-cell chronic lymphocytic leukaemia cells to TRAIL-induced apoptosis. *Int J Cancer* **120**: 1215–1222.
- Garofalo, M, Quintavalle, C, Di Leva, G, Zanca, C, Romano, G, Taccioli, C et al. (2008). MicroRNA signatures of TRAIL resistance in human non-small cell lung cancer. *Oncogene* **27**: 3845–3855.
- Ricci-Vitiani, L, Pedini, F, Mollinari, C, Condorelli, G, Bonci, D, Bez, A et al. (2004). Absence of caspase 8 and high expression of PED protect primitive neural cells from cell death. *J Exp Med* **200**: 1257–1266.
- Zanca, C, Garofalo, M, Quintavalle, C, Romano, G, Acunzo, M, Ragno, P et al. (2008). PED is overexpressed and mediates TRAIL resistance in human non-small cell lung cancer. *J Cell Mol Med* **12**(6A): 2416–2426.
- Garofalo, M, Leva, GD and Croce, CM (2014). MicroRNAs as anti-cancer therapy. *Curr Pharm Des* **20**: 5328–5335.
- Garofalo, M, Condorelli, GL, Croce, CM and Condorelli, G (2010). MicroRNAs as regulators of death receptors signaling. *Cell Death Differ* **17**: 200–208.
- Incoronato, M, Garofalo, M, Urso, L, Romano, G, Quintavalle, C, Zanca, C et al. (2010). miR-212 increases tumor necrosis factor-related apoptosis-inducing ligand sensitivity in non-small cell lung cancer by targeting the antiapoptotic protein PED. *Cancer Res* **70**: 3638–3646.
- Yan, AC and Levy, M (2009). Aptamers and aptamer targeted delivery. *RNA Biol* **6**: 316–320.
- Farokhzad, OC, Karp, JM and Langer, R (2006). Nanoparticle-aptamer bioconjugates for cancer targeting. *Expert Opin Drug Deliv* **3**: 311–324.
- Zhou, J and Rossi, JJ (2014). Cell-type-specific, aptamer-functionalized agents for targeted disease therapy. *Mol Ther Nucleic Acids* **3**: e169.
- Wang, J and Li, G (2011). Aptamers against cell surface receptors: selection, modification and application. *Curr Med Chem* **18**: 4107–4116.
- Catuogno, S, Esposito, CL, de Franciscis, V (2016). Developing Aptamers by Cell-Based SELEX. *Methods Mol Biol* **1380**: 33–46.
- Zhou, J and Rossi, JJ (2010). Aptamer-targeted cell-specific RNA interference. *Silence* **1**: 4.
- Esposito, CL, Cerchia, L, Catuogno, S, De Vita, G, Dassi, JP, Santamaria, G et al. (2014). Multifunctional aptamer-miRNA conjugates for targeted cancer therapy. *Mol Ther* **22**: 1151–1163.
- Dai, F, Zhang, Y, Zhu, X, Shan, N and Chen, Y (2012). Anticancer role of MUC1 aptamer-miR-29b chimera in epithelial ovarian carcinoma cells through regulation of PTEN methylation. *Target Oncol* **7**: 217–225.
- Dassi, JP, Liu, XY, Thomas, GS, Whitaker, RM, Thiel, KW, Stockdale, KR et al. (2009). Systemic administration of optimized aptamer-siRNA chimeras promotes regression of PSMA-expressing tumors. *Nat Biotechnol* **27**: 839–849.
- McNamara, JO 2nd, Andrechek, ER, Wang, Y, Viles, KD, Rempel, RE, Gilboa, E et al. (2006). Cell type-specific delivery of siRNAs with aptamer-siRNA chimeras. *Nat Biotechnol* **24**: 1005–1015.
- Dai, F, Zhang, Y, Zhu, X, Shan, N and Chen, Y (2013). The anti-chemoresistant effect and mechanism of MUC1 aptamer-miR-29b chimera in ovarian cancer. *Gynecol Oncol* **131**: 451–459.
- Cerchia, L, Esposito, CL, Camorani, S, Rienzo, A, Stasio, L, Insabato, L et al. (2012). Targeting Axl with an high-affinity inhibitory aptamer. *Mol Ther* **20**: 2291–2303.
- Ellington, AD and Szostak, JW (1990). *In vitro* selection of RNA molecules that bind specific ligands. *Nature* **346**: 818–822.
- Stitt, TN, Conn, G, Gore, M, Lai, C, Bruno, J, Radziejewski, C et al. (1995). The anticarcinogenic factor protein S and its relative, Gas6, are ligands for the Tyro 3/Axl family of receptor tyrosine kinases. *Cell* **80**: 661–670.
- Shieh, YS, Lai, CY, Kao, YR, Shieh, SG, Chu, YW, Lee, HS et al. (2005). Expression of axl in lung adenocarcinoma and correlation with tumor progression. *Neoplasia* **7**: 1058–1064.
- Sainaghi, PP, Castello, L, Bergamasco, L, Galletti, M, Bellosta, P and Avanzi, GC (2005). Gas6 induces proliferation in prostate carcinoma cell lines expressing the Axl receptor. *J Cell Physiol* **204**: 36–44.
- Zhang, YX, Knyazev, PG, Cheburkin, YV, Sharma, K, Knyazev, YP, Orfi, L et al. (2008). AXL is a potential target for therapeutic intervention in breast cancer progression. *Cancer Res* **68**: 1905–1915.
- Wu, CW, Li, AF, Chi, CW, Lai, CH, Huang, CL, Lo, SS et al. (2002). Clinical significance of AXL kinase family in gastric cancer. *Anticancer Res* **22**(2B): 1071–1078.
- Koorstra, JB, Karikari, CA, Feldmann, G, Bisht, S, Rojas, PL, Offerhaus, GJ et al. (2009). The Axl receptor tyrosine kinase confers an adverse prognostic influence in pancreatic cancer and represents a new therapeutic target. *Cancer Biol Ther* **8**: 618–626.
- Chung, BI, Malkowicz, SB, Nguyen, TB, Libertino, JA and McGarvey, TW (2003). Expression of the proto-oncogene Axl in renal cell carcinoma. *DNA Cell Biol* **22**: 533–540.
- Hutterer, M, Knyazev, P, Abate, A, Reschke, M, Maier, H, Stefanova, N et al. (2008). Axl and growth arrest-specific gene 6 are frequently overexpressed in human gliomas and predict poor prognosis in patients with glioblastoma multiforme. *Clin Cancer Res* **14**: 130–138.
- Wu, X, Ding, B, Gao, J, Wang, H, Fan, W, Wang, X et al. (2011). Second-generation aptamer-conjugated PSMA-targeted delivery system for prostate cancer therapy. *Int J Nanomedicine* **6**: 1747–1756.
- Amarzguoui, M, Lundberg, P, Cantin, E, Hagstrom, J, Behlke, MA and Rossi, JJ (2006). Rational design and *in vitro* and *in vivo* delivery of Dicer substrate siRNA. *Nat Protoc* **1**: 508–517.
- Fernandez, S, Risolino, M, Mandia, N, Talotta, F, Soini, Y, Incoronato, M et al. (2014). miR-340 inhibits tumor cell proliferation and induces apoptosis by targeting multiple negative regulators of p27 in non-small cell lung cancer. *Oncogene* **34**: 3240–3250.
- Sgambato, A, Casaluce, F, Maione, P, Rossi, A, Rossi, E, Napolitano, A et al. (2012). The role of EGFR tyrosine kinase inhibitors in the first-line treatment of advanced non small cell lung cancer patients harboring EGFR mutation. *Curr Med Chem* **19**: 3337–3352.
- Stuckey, DW and Shah, K (2013). TRAIL on trial: preclinical advances in cancer therapy. *Trends Mol Med* **19**: 685–694.
- Herbst, RS, Eckhardt, SG, Kurzrock, R, Ebbinghaus, S, O’Dwyer, PJ, Gordon, MS et al. (2010). Phase I dose-escalation study of recombinant human Apo2L/TRAIL, a dual proapoptotic receptor agonist, in patients with advanced cancer. *J Clin Oncol* **28**: 2839–2846.
- Falschlehner, C, Ganten, TM, Koschny, R, Schaefer, U and Walczak, H (2009). TRAIL and other TRAIL receptor agonists as novel cancer therapeutics. *Adv Exp Med Biol* **647**: 195–206.
- Soria, JC, Smit, E, Khayat, D, Besse, B, Yang, X, Hsu, CP et al. (2010). Phase 1b study of dulanerin (recombinant human Apo2L/TRAIL) in combination with paclitaxel, carboplatin, and bevacizumab in patients with advanced non-squamous non-small-cell lung cancer. *J Clin Oncol* **28**: 1527–1533.
- Hotte, SJ, Hirte, HW, Chen, EX, Siu, LL, Le, LH, Corey, A et al. (2008). A phase 1 study of mapatumumab (fully human monoclonal antibody to TRAIL-R1) in patients with advanced solid malignancies. *Clin Cancer Res* **14**: 3450–3455.
- Thiel, KW, Hernandez, LI, Dassi, JP, Thiel, WH, Liu, X, Stockdale, KR et al. (2012). Delivery of chemo-sensitizing siRNAs to HER2+ breast cancer cells using RNA aptamers. *Nucleic Acids Res* **40**: 6319–6337.
- Liu, N, Zhou, C, Zhao, J and Chen, Y (2012). Reversal of paclitaxel resistance in epithelial ovarian carcinoma cells by a MUC1 aptamer-let-7i chimera. *Cancer Invest* **30**: 577–582.

50. Esposito, CL, Catuogno, S and de Franciscis, V (2014). Aptamer-mediated selective delivery of short RNA therapeutics in cancer cells. *J RNAi Gene Silencing* **10**: 500–506.
51. Ma, JB, Ye, K and Patel, DJ (2004). Structural basis for overhang-specific small interfering RNA recognition by the PAZ domain. *Nature* **429**: 318–322.
52. Sledz, CA, Holko, M, de Veer, MJ, Silverman, RH and Williams, BR (2003). Activation of the interferon system by short-interfering RNAs. *Nat Cell Biol* **5**: 834–839.
53. Behlke, MA (2008). Chemical modification of siRNAs for *in vivo* use. *Oligonucleotides* **18**: 305–319.
54. Keefe, AD, Pai, S and Ellington, A (2010). Aptamers as therapeutics. *Nat Rev Drug Discov* **9**: 537–550.
55. Stassi, G, Garofalo, M, Zerilli, M, Ricci-Vitiani, L, Zanca, C, Todaro, M et al. (2005). PED mediates AKT-dependent chemoresistance in human breast cancer cells. *Cancer Res* **65**: 6668–6675.
56. Esposito, CL, Passaro, D, Longobardo, I, Condorelli, G, Marotta, P, Affuso, A et al. (2011). A neutralizing RNA aptamer against EGFR causes selective apoptotic cell death. *PLoS One* **6**: e24071.
57. Condorelli, G, Vigiotta, G, Iavarone, C, Caruso, M, Tocchetti, CG, Androzzzi, F et al. (1998). PED/PEA-15 gene controls glucose transport and is overexpressed in type 2 diabetes mellitus. *EMBO J* **17**: 3858–3866.
58. Livak, KJ and Schmittgen, TD (2001). Analysis of relative gene expression data using real-time quantitative PCR and the 2(-Delta Delta C(T)) Method. *Methods* **25**: 402–408.



This work is licensed under a Creative Commons Attribution-NonCommercial-NoDerivs 4.0 International License. The images or other third party material in this article are included in the article's Creative Commons license, unless indicated otherwise in the credit line; if the material is not included under the Creative Commons license, users will need to obtain permission from the license holder to reproduce the material. To view a copy of this license, visit <http://creativecommons.org/licenses/by-nc-nd/4.0/>